DEVELOPMENT OF DYNAMIC SEATING SYSTEM FOR HIGH-TONE EXTENSOR THRUST

A Thesis
Presented to
The Academic Faculty

by

Vlad P. Patrangenaru

In Partial Fulfillment
of the Requirements for the Degree
Master of Science in the
School of Mechanical Engineering

Georgia Institute of Technology
May 2006

DEVELOPMENT OF DYNAMIC SEATING SYSTEM FOR HIGH-TONE EXTENSOR THRUST

Approved by:

Dr. William Singhose, Advisor
School of Mechanical Engineering
Georgia Institute of Technology

Dr. David Sanborn, Committee Member
School of Mechanical Engineering
Georgia Institute of Technology

Dr. Stephen Sprigle, Committee Member
School of Applied Physiology
Georgia Institute of Technology

Date Approved: January 5th, 2006

ACKNOWLEDGEMENTS

I would like to thank my advisor, Dr. William Singhose, and Dr. S.W. Hong for their guidance and assistance throughout the entire research process. Their experience and dedication to the project made the research presented in this thesis possible. I would also like to acknowledge the significant contributions made by Dr. Stephen Sprigle, who provided valuable expertise and the necessary support to sustain the project as needed. Additionally, I would like to thank Dr. David Sanborn for his mentorship and assistance throughout my time at Georgia Tech. Another well-deserved thank you goes out to Jim Kitchen, who has been a great project partner and a good friend. The efforts made by Joel Fortang, the ME Machine Shop, the ME Electronics Shop, as well as other groups/individuals who have supported me along the way should also be recognized.

Finally I would like to mention my family, who has always been there for me. Specifically, I would like to thank my parents, Adriana and Victor, for their unconditional love and dedication, and my girlfriend, Ginna, who has brought great joy to my life.

TABLE OF CONTENTS

LIST OF FIGURES

Page

SUMMARY

High-tone extensor thrusts, or involuntary muscle contractions experienced by many children with cerebral palsy, can cause problems that are not addressed by current seating systems. This thesis is concerned with the development of a dynamic seating system to better accommodate individuals who exhibit high-tone extensor thrusts.

The first part of the thesis is focused on obtaining a general understanding of extensor thrusts from a mechanical perspective. To achieve this goal, an analytical dynamic model of a human subject undergoing an extensor thrust on a rigid chair is created. This model is validated experimentally, and inferences about the nature of extensor thrusts are made from the simulation and experimental results.

A Dynamic-Hingeback Seating System which allows the occupant to lean back during an uncontrolled extensor thrust is developed. This system is capable of maintaining seatback rigidity during an intentionally-induced episode, thereby enabling the occupant to communicate or interact with his/her environment. The design of this system is influenced by the results obtained from the rigid seat study, as well as by numerical simulation results gathered with a commercial dynamic simulation software package (Working Model 2D). The improved seatback performance is characterized through experimentation.

Alternative dynamic seating systems are considered. The important features of each of these systems are identified, and the desired motion of the system occupant during an extensor thrust is verified through Working Model simulations.

CHAPTER 1

INTRODUCTION

Many people spend a good portion of their day sitting, and thus a large effort has been made over the years to continuously improve seating systems. As technology has advanced, seating systems have been modified to provide maximum safety and comfort for task-specific applications. In some automobiles, for example, the seats have been designed to move during the impact of an accident to cradle the passengers and reduce their forward motion [23]. Many tractors and other pieces of heavy machinery are equipped with an active seat suspension that senses ground disturbances and automatically adjusts the position of the seat such that the driver is exposed to less harmful vibration [24]. Some seating systems can even heat, cool, and massage their occupant.

Wheelchair occupants are one important seating-system demographic that are sometimes overlooked. Disabled individuals with restricted mobility have limited seating options available to them. This deficiency has been reduced over the last few decades, yet much work remains to be done for some subsets of this population. One such subset of individuals includes those who experience high-tone extensor thrusts. The work described in this thesis aims to improve the comfort and safety of people who experience high-tone extensor thrusts, as well as to increase the lifetime of their wheelchairs.

1.1 Background and Motivation

Extensor thrusts occur when the brain erroneously sends out signals to nearly every muscle group in the body, causing them to contract. During a high-tone extensor thrust many muscle groups are affected by involuntary high-intensity muscle contractions.

Typically, extensor muscles which straighten human joints are more powerful than the flexor muscles which bend them. Because of this, the net effect is an overall straightening of the body dictated by the extensor muscles. Figure 1 depicts the progression of an unconstrained thrust.

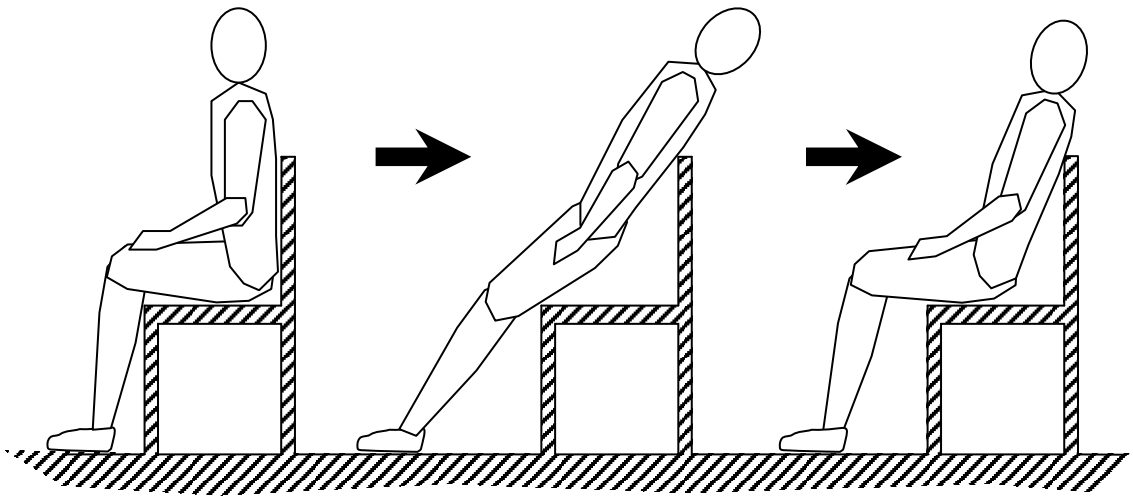

Figure 1: Progression of a high-tone extensor thrust in a standard fixed chair

High-tone extensor thrusts are exhibited by many who suffer from cerebral palsy, or other deteriorating neurological conditions, as well as by head trauma victims. Such a neurological condition can be incapacitating, leaving one with very little volitional control over his or her muscles. Most of the time the affected muscle groups are in a relaxed state, leaving the individual in a slouched configuration, yet at times the muscles groups rapidly fire and extend the individual. Such an extensor thrust can vary in intensity depending on the individual and on the affected muscle groups.

Frequent extensor thrusts can cause a host of problems for the person, as well as for the seating system. First, there is the issue of safety. Since most existing chairs are rigid, the occupant must be constrained in the seat, usually by the means of seatbelts, such that

he or she will not fall out of the chair during an extensor thrust. Once strapped down, however, the occupant is able to exert very large forces on the seatback and footrest of the seating system. If the seat surfaces are not properly padded, then the occupant can obtain significant injuries during the course of an extensor thrust. Even if the seatback is well padded, however the occupant can suffer from a condition known as skin breakdown. Skin breakdown is a complex problem caused by normal and shear (frictional) loading on human tissue. Tissue ability to withstand load is reduced by moisture, or transpiration, which also increases the contact friction between the seating components and the occupant.

Poor circulation caused by the pinching of the seatbelt and improper posture can lead to circulation-related problems. The caretakers in charge of the affected individuals must constantly reposition them because the relaxation process at the end of a thrust causes the individuals to slouch under the belt and slide forward, as shown in Figure 1. Finally, the seating hardware itself is also affected, as the cyclical loading and unloading of mechanical components significantly shortens their lifespan.

Presently, there are very few companies that are seriously addressing the needs of this population. Up to this point, there have been few published studies done to better understand high-tone extensor thrusts from a mechanical perspective, or to propose a means by which to design and evaluate seating systems that can better accommodate affected individuals [2,5-8].

1.2 Research Objectives

This thesis is one part of a larger study at Georgia Tech that aims to develop a seating system to improve wheelchair designs for children and others who experience

high-tone extensor thrusts. Because extensor thrusts have gone largely unstudied, at least from a mechanical perspective, there is much that can be done to improve the knowledge in the medical and engineering communities on this subject.

The scope of this thesis is twofold. The first goal is to lay the groundwork for current and future, in-depth, studies regarding extensor thrusts. This can be done by addressing many of the pertinent questions and providing the tools that will lead others to the best seating system designs for this niche population. A second research objective is to create a functional dynamic seating system that can be optimized through computer simulation and verifiably shown to improve the conditions of the occupant and wheelchair during an extensor thrust. These goals are to be met while also ensuring the occupant will not experience reduced functionality as a result of being seated in a dynamic seat. Many individuals with cerebral palsy are able to communicate and increase their functionality through controlled extensor thrusts by pushing against the seatback of the chair. This ability is preserved by the system developed in this thesis. This, as well as other useful information regarding extensor thrusts, is found in the Dynamic Seating System (DSS) Focus Group Survey provided in Appendix C.

1.3 Literature Review

Providing greater personal freedom to wheelchair users with high-tone extensor thrust while preventing secondary injuries is a challenging problem. Recently, the concept of a dynamic seat, which allows movement with respect to the wheelchair frame during an extensor thrust events, has been suggested as a potential solution [2]. Some products based on the dynamic seat concept are commercially available [3,4]. However,

most of the products appear to be empirically designed only to prevent wheelchair breakage without addressing the needs of the wheelchair occupant.

1.3.1 Previous Studies

In order to properly design a seating system for occupants with high extensor tone, the forces generated during an event must be well understood. Attempts at measuring the forces caused by extensor thrusts have been made, for example, by measuring the spasticity at the elbow [5], by developing a passive dynamic model of the knee joint affected by spastic paresis [6], and by developing a quantitative measurement of muscle spasticity with the pendulum knee drop test [7]. However, there is little publicly available knowledge regarding the motion and forces during unconstrained extensor thrust events. Since it is very hard to directly measure the human-generated forces, this thesis proposes an inverse dynamic approach to indirectly identify the human-generated forces using limited measurements of forces and motion of the occupants.

Inverse dynamic analysis has played an important role in estimating the forces on the human body. The inverse dynamic analysis extracts the internal and external forces or moments from measured kinematic responses of the human body segments and some limited set of force measurements. With the help of the inverse dynamic analysis procedure, many researchers have been able to obtain joint forces and moments during biomechanical studies of locomotion such as those relating to, sit-to-stand, jumping, gait and running. Among these, the study on sit-to-stand movement is most relevant to this thesis. Hutchinson, et al., calculated the net forces and torques on human joints using inverse dynamics with measured ground reaction forces and motions during sit-to-stand motions [8]. Biomechanical analysis of sit-to-stand movement through the use of an

inverse dynamic approach has often been performed from a medical point of view, such as for a comparison between normal and obese subjects in the joint torques of hip and knee joints [9] and for a comparison between healthy subjects and people with Parkinson's disease [10,11].

1.3.2 Existing Commercial Products

There are less than a handful of commercial products currently on the market that are specifically designed to address extensor thrusts. The most complete seating system currently being sold is the Activeline Traveling Seat [21], sketched in Figure 2.

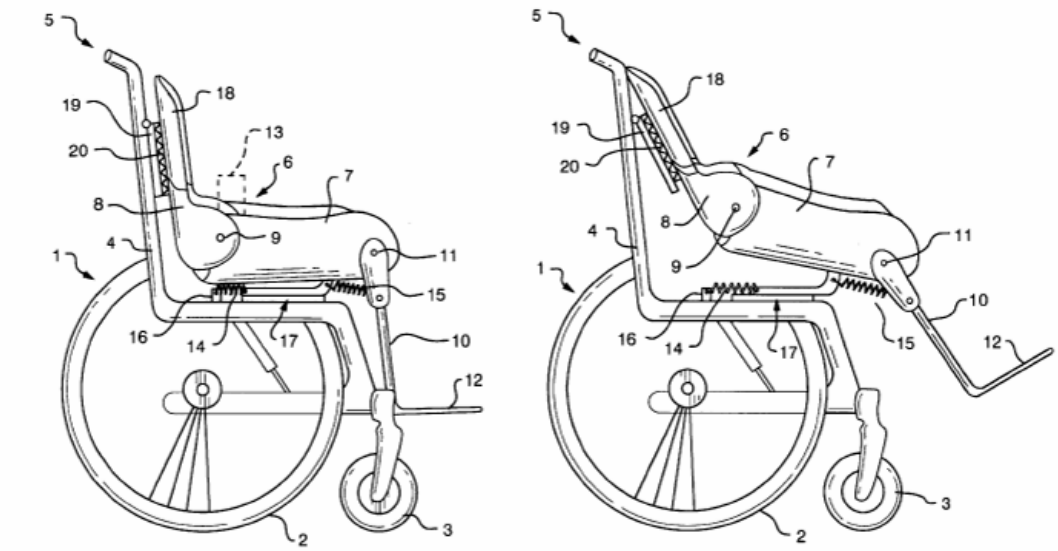

Figure 2: Design Schematic of Traveling Seat (US Patent 6,488,332)

This system is designed specifically for smaller children who exhibit high-tone extensor thrusts, and is the only product that combines significant seatback and footrest actuation. Moreover, the Activeline product makes use of an anatomical hip joint and energy dissipation technology to improve the seat response during an extensor thrust.

Another dynamic seat is the "Ergonomically Designed Seat Assembly for a Portable Wheelchair." This design [22], while not fully dynamic, does contain some dynamic components and is fully adjustable, as shown in Figure 3.

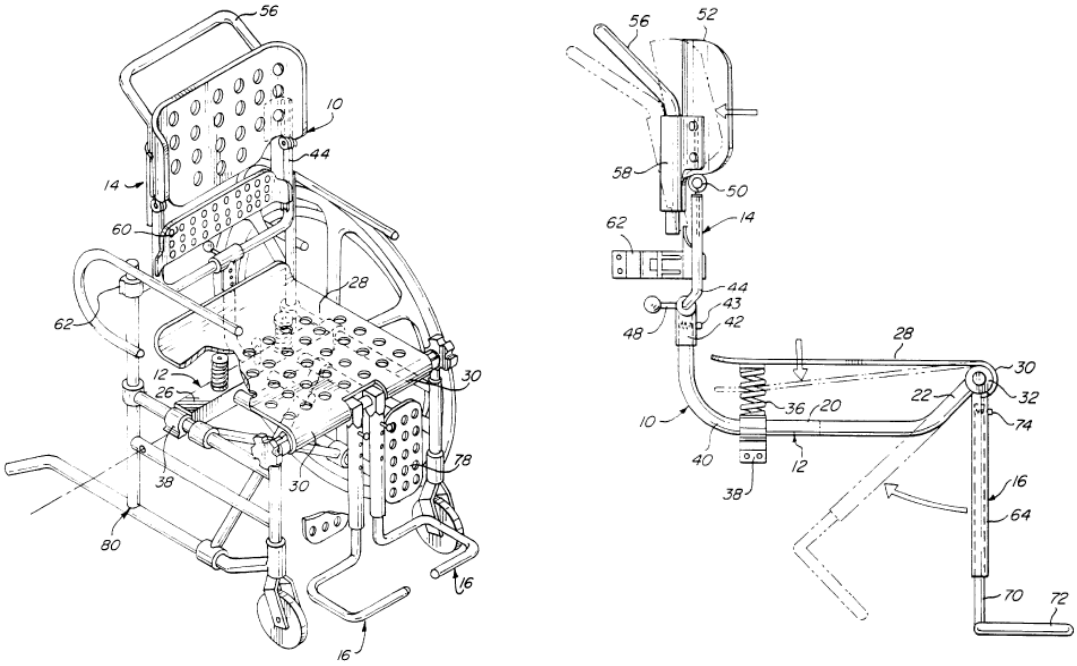

Figure 3: Ergonomically Designed Seat Assembly for a Portable Wheelchair (US Patent Number 5,904,398)

The adjustability of the seating system is especially noteworthy, as the length and angles of the footrest can be fixed to conform to the occupant of the seat. Also, this seating system has a few passive-dynamic components that could be used to dissipate energy during a high-tone extensor thrust.

1.4 Thesis Structure

The first part of this research work, presented in Chapter 2, is primarily concerned with understanding the basic mechanical properties of extensor thrusts in terms of internal human forces and torques in the joints of the body. This knowledge can be

obtained by studying an unconstrained extensor thrust motion in a rigid chair with the help of analytical dynamic model and an experimental system. From this study it is possible to determine what the internal torque profiles look like during an extensor thrust, and thus use that information in the design of subsequent dynamic seating systems. Additionally, this part of the study reveals the parameters that are important for this investigation and those that can be largely ignored.

Once typical thrust profiles are known, they can be used for improving the design of a dynamic seating system, as shown in Chapter 3. This chapter introduces the development of a simple dynamic seatback design. The design process is outlined, and a detailed design is documented. A Seatback Rigidizer is integrated into the seating system to keep the seat in a rigid configuration while the occupant undergoes normal motions. The entire system is simulated with a commercial dynamic modeling package called Working Model 2D. By using this software it is possible to perform numerous simulations iteratively where the critical design parameters are varied over a specified parameter range. This technique can be used for tuning the seat parameters to improve the system response for the individual who will be seated in the system. To demonstrate the validity of parameter tuning with Working Model, the results of an investigation with the experimental system are compared to an extensor thrust simulation.

The final contribution of this thesis work is the introduction of a number of seating system design concepts, that while more complex, could provide significant improvements over any seating systems that is currently available on the market. The potential benefits of each design concept are addressed in Chapter 4.

CHAPTER 2

ANALYTICAL EXTENSOR THRUSTS MODELING IN RIGID SEAT

2.1 Rigid Chair Model

The first step to designing an effective seating system for occupants who experience high-tone extensor thrusts is to understand these thrusts from a mechanical perspective. Many important questions must be answered, including: How hard is the occupant pushing on the seatback and the footrest? Does the duration of the thrust have a great influence on thrust characteristics? What are the critical parameters, geometric and otherwise, that affect the thrust behavior, and conversely what parameters can be ignored? Without this basic knowledge it is very difficult to proceed with designing and tuning appropriate seating systems.

As a first attempt to answer some of these questions, a simple two-segment model of a human body was generated, as shown in Figure 4.

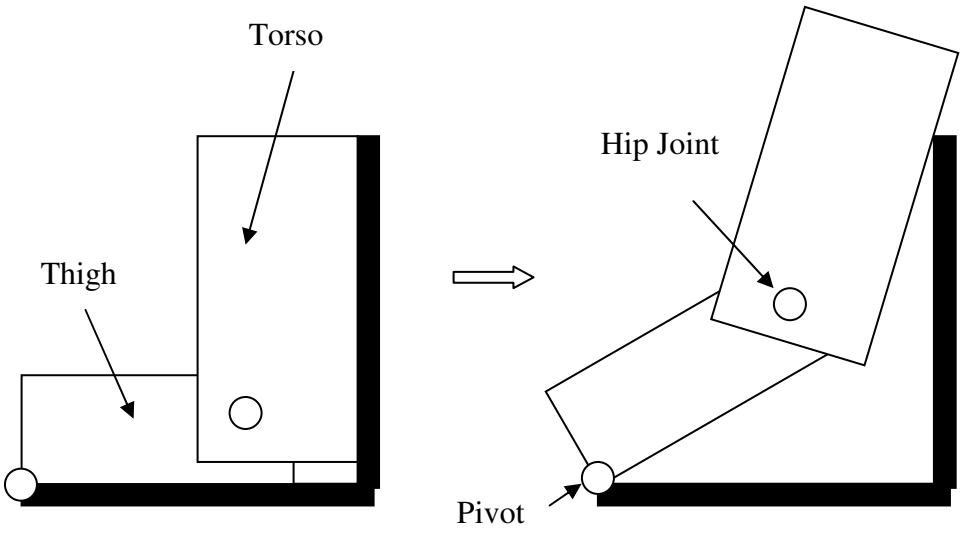

Figure 4: Two-segment body model of extensor thrust in rigid chair

This one degree of freedom (DOF) model incorporates the thigh and torso of the individual, and thus provided a good starting block for the modeling. Ultimately, however, this model proved to be overly simplified, as it neglects the forces at the footrest of the seating system, which are known to be critical.

A three-segment, one DOF model was developed to more accurately represent the extensor thrust dynamics. This model includes the calf, the thigh, and the upper body (i.e. torso, head and upper extremities). A graphical model representation can be seen in Figure 5.

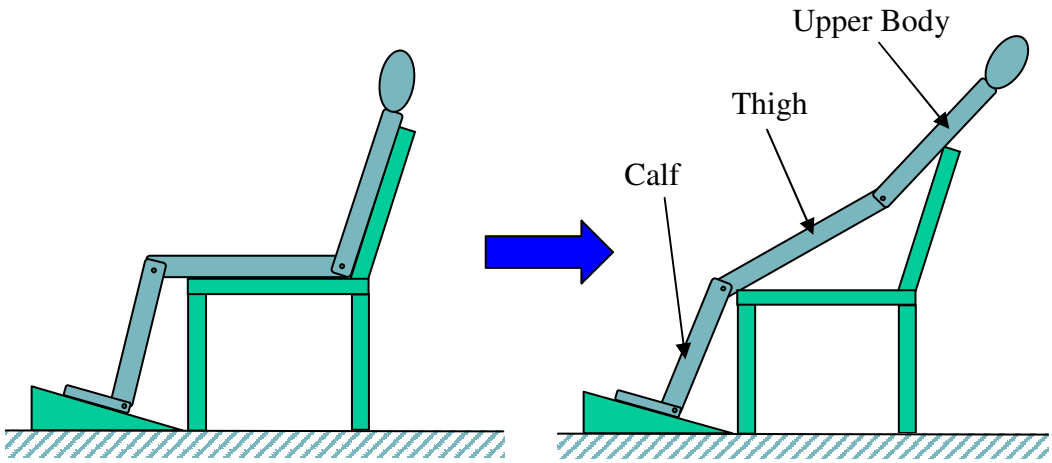

Figure 5: Three-segment body model of extensor thrust in rigid chair

2.1.1 Basic Assumptions

The first assumption used to develop this model is that sagittal-plane motion dominates extensor thrust dynamics. By limiting the study to sagittal-plane motion, three out of the six degrees of freedom for each unconstrained body segment are eliminated, leaving a total 9 DOF that have yet to be fixed for the free-floating segments. Assuming sliding does not occur at the interface between the foot and the footrest, the ankle joint

can be fixed to the ground and the calf pinned to pivot around it. Additionally, if the thigh and torso are considered to be joined serially at the knee and hip joints respectively, the spatial configuration of the body can be fully defined by providing the angle each body segment makes with the horizontal axis, as shown in Figure 6. The resulting 3 DOF system can be further constrained by enforcing contact between the upper body and seatback, as well as between the thigh and the seat bottom. After adding these final two constraints, the resulting model has only the one DOF remaining. All of the geometric parameters of the model are also shown in Figure 6. The lengths of each segment are given by L_i, λ_i locates each center of mass, and θ_i gives each angle with the horizontal.

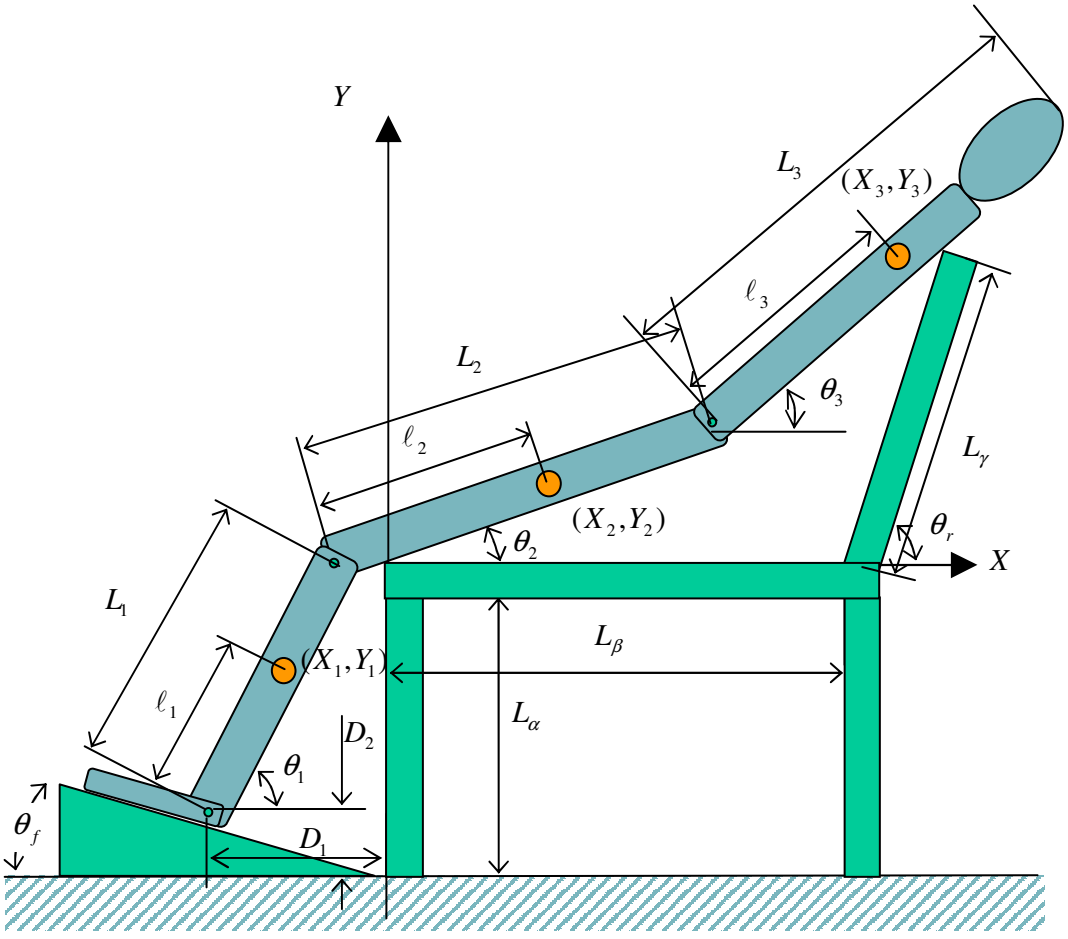

Figure 6: Three-Segment detailed schematic model of human body on rigid chair

The chair is assumed to be completely rigid and thus modeled as ground, and the occupant is assumed to be composed of fully rigid segments. Such a model ignores the compressibility of the individual, as well as other body details such as the curvature of the back and thighs. Finally, the ankle torque is assumed to be equal to zero so that an inverse dynamic approach can be implemented. This assumption can be made because the location of the ankle would only vary slightly if the actual ankle torque was high enough to cause the heel of the occupant to lift off the ground during a thrust, and also because there are breakaway mechanisms available that can eliminate effect of the ankle torque on the occupant configuration all together.

2.1.1 Equations of Motion

Figure 7 shows the external forces applied to the body. The developed model accounts for gravitational forces and friction forces.

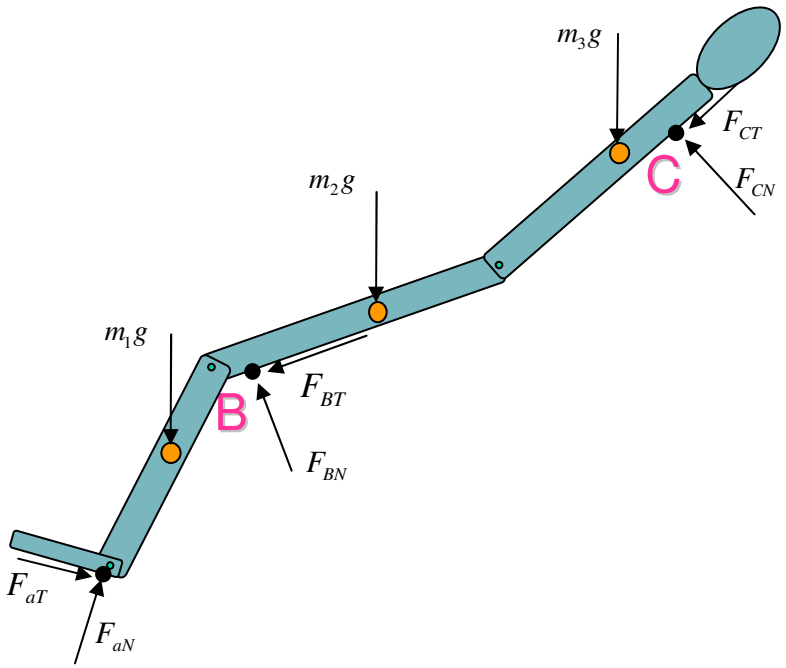

Figure 7: External forces acting on the human body

Upon applying Newton's law of motion to each segment, the equations of motion can be obtained as follows*:

$$m_1\ddot{X}_1 = F_{aX} - F_{kX}$$

$$m_1\ddot{Y}_1 = F_{aY} - F_{kY} - m_1 g \tag{1a}$$

$$I_1^G\ddot{\theta}_1 = \{F_{aX}\ell_1 + F_{kX}(L_1 - \ell_1)\}\sin\theta_1 - \{F_{aY}\ell_1 + F_{kY}(L_1 - \ell_1)\}\cos\theta_1 - \tau_k$$

$$m_2\ddot{X}_2 = -F_{BT}\cos\theta_2 - F_{BN}\sin\theta_2 + F_{bX} - F_{cX}$$

$$m_2\ddot{Y}_2 = -F_{BT}\sin\theta_2 + F_{BN}\cos\theta_2 + F_{bY} - F_{cY} - m_2 g \tag{1b}$$

$$I_2^G\ddot{\theta}_2 = -sign(X_2)F_{BN}\sqrt{X_2^{\,2} + Y_2^{\,2}} + F_{bX}\ell_2\sin\theta_2 - F_{bY}\ell_2\cos\theta_2 + \tau_b - \tau_c + F_{cX}(L_2 - \ell_2)\sin\theta_2 - F_{cY}(L_2 - \ell_2)\cos\theta_2$$

$$m_3\ddot{X}_3 = -F_{CT}\cos\theta_3 - F_{CN}\sin\theta_3 + F_{hX}$$

$$m_3\ddot{Y}_3 = -F_{CT}\sin\theta_3 + F_{CN}\cos\theta_3 + F_{hY} - m_3 g \tag{1c}$$

$$I_3^G\ddot{\theta}_3 = sign(L_\gamma\sin\theta_r - Y_3)F_{CN}\sqrt{(L_\beta + L_\gamma\cos\theta_r - X_3)^2 + (L_\gamma\sin\theta_r - Y_3)^2} + F_{hX}\ell_3\sin\theta_3 - F_{hY}\ell_3\cos\theta_3 + \tau_h$$

where m_i and $I_i^G, i = 1,2,3$, are the mass and mass moment of inertia for the ith segment, respectively. The lower case subscripts *a, k* and *h* on the forces, *F*, and torques, τ, denote the ankle, knee and hip joints, respectively. The capital subscripts *B* and *C* denote the corresponding contact points as indicated in Figure 7. The subscripts *T* and *N*

* Dr. S.W. Hong from Kumoh National Institute of Technology, Kumi, South Korea, was invaluable in the development of the mathematical model presented in this section.

represent tangential and normal forces, respectively. All the other parameters which appear in (1) were indicated in Figure 6. The tangential forces at the edges of the seat bottom and seatback are friction forces proportional to the corresponding normal forces:

$$F_{BT} = u_B F_{BN} \tag{2a}$$

$$F_{CT} = u_C F_{CN} \tag{2b}$$

where u_B and u_C are the friction coefficients at the corresponding contact point, i.e., between the human subject and seat bottom, and between the human subject and seatback, respectively. This friction model assumes the human segments are sliding relative to the seat. Therefore, this model is only valid for the dynamic motion, and not for static cases. The nine equations in (1) contain ten unknown forces and moments, implying that the system is mathematically indeterminate. One of the possible ways to avoid the indeterminacy is to make measurements of one of the unknown variables. In this thesis, one unknown force component is measured based on the experimental procedure that will be described in detail in the next section.

2.2 Force Identification Method Using Inverse Dynamic Analysis

Based on the system geometry, kinematic relations can be derived as follows:

$$\begin{aligned}
&X_1 = \ell_1 \cos\theta_1 - D_1,\ Y_1 = \ell_1 \sin\theta_1 - (L_\alpha - D_2) \\
&X_2 = L_1 \cos\theta_1 + \ell_2 \cos\theta_2 - D_1,\ Y_2 = L_1 \sin\theta_1 + \ell_2 \sin\theta_2 - (L_\alpha - D_2) \\
&X_3 = X_2 + (L_2 - \ell_2)\cos\theta_2 + \ell_3 \cos\theta_3,\ Y_3 = Y_2 + (L_2 - \ell_2)\sin\theta_2 + \ell_3 \sin\theta_3 \\
&\theta_2 = \tan^{-1}\frac{Y_2}{X_2},\ \theta_3 = \tan^{-1}\frac{L_\gamma \sin\theta_r - L_2 \sin\theta_2 + (L_\alpha - D_2 - L_1 \sin\theta_1)}{L_\beta + L_\gamma \cos\theta_r - L_2 \cos\theta_2 + (D_1 - L_1 \cos\theta_1)}
\end{aligned} \tag{3}$$

As can be seen in (3), there are eight kinematic constraints but nine coordinates. This leaves only one independent degree of freedom, implying that measurement of one coordinate provides all other coordinates based on the kinematic relations. With the position information, one can obtain the velocity and acceleration data by analytical differentiation of the kinematic relations given in (3). These expressions are listed in Appendix A. The kinematic relations are nonlinear, requiring a nonlinear solver. The kinematic relations, as described in (3) and in Appendix A, are very useful for estimating accelerations that are necessary for inverse dynamic analysis.

2.2.1 Inverse Dynamics Equations

There are three sets of inverse dynamic equations used in this study. The first set of equations is that of the generic equations used for a typical extensor thrust simulation where the body is making contact with both the seat bottom and the seatback. The second set is a simplification of the first set of equations that is used specifically for model validation where the body is only making contact with the seatback. Finally, the last set introduced is a modification that allows for force identification during an extensor thrust.

2.2.1.1 Generic Equations for Inverse Dynamic Analysis

Consider the normal and tangential force components at the foot rest, F_{aN} and F_{aT}. The force components at the foot rest can be expressed as follows:

$$F_{aX} = F_{aN}\sin\theta_f + F_{aT}\cos\theta_f$$
$$F_{aY} = F_{aN}\cos\theta_f - F_{aT}\sin\theta_f \qquad (4)$$

In this case, (1) can be rearranged to give:

$$\underset{9\text{x}10}{[G_0]}\,\underset{10\text{x}1}{\{F_0\}} = \underset{9\text{x}1}{\{Q_0\}} \tag{5}$$

where

$$\{F_0\} = \{F_{aN}\ \ F_{aT}\ \ F_{kX}\ \ F_{kY}\ \ F_{BN}\ \ F_{hX}\ \ F_{hY}\ \ F_{CN}\ \ \tau_k\ \ \tau_h\ \}^T,$$

$$\{Q_0\} = \{(m_1\ddot{X}_1)\ (m_1 g + m_1\ddot{Y}_1)\ (I_1^G\ddot{\theta}_1)\ (m_2\ddot{X}_2)\ (m_2 g + m_2\ddot{Y}_2)\ * \\ *(I_2^G\ddot{\theta}_2)\ (m_3\ddot{X}_3)\ (m_3 g + m_3\ddot{Y}_3)\ (I_3^G\ddot{\theta}_3)\}^T$$

$$[G_0] = \begin{bmatrix}
\sin\theta_f & \cos\theta_f & -1 & 0 & 0 & 0 & 0 & 0 & 0 & 0 \\
\cos\theta_f & -\sin\theta_f & 0 & -1 & 0 & 0 & 0 & 0 & 0 & 0 \\
-\ell_1\cos(\theta_1+\theta_f) & \ell_1\sin(\theta_1+\theta_f) & (L_1-\ell_1)\sin\theta_1 & -(L_1-\ell_1)\cos\theta_1 & 0 & 0 & 0 & 0 & -1 & 0 \\
0 & 0 & 1 & 0 & -D_{BEX} & -1 & 0 & 0 & 0 & 0 \\
0 & 0 & 0 & 1 & -D_{BEY} & 0 & -1 & 0 & 0 & 0 \\
0 & 0 & \ell_2\sin\theta_2 & -\ell_2\cos\theta_2 & -sign(X_2)\sqrt{X_2^2+Y_2^2} & (L_2-\ell_2)\sin\theta_2 & -(L_2-\ell_2)\cos\theta_2 & 0 & 1 & -1 \\
0 & 0 & 0 & 0 & 0 & 1 & 0 & -D_{CEX} & 0 & 0 \\
0 & 0 & 0 & 0 & 0 & 0 & 1 & -D_{CEY} & 0 & 0 \\
0 & 0 & 0 & 0 & 0 & \ell_3\sin\theta_3 & -\ell_3\cos\theta_3 & L_\delta(\theta_r, X_3, Y_3) & 0 & 1
\end{bmatrix}$$

and

$$D_{BEX} = u_B\cos\theta_2 + \sin\theta_2,\ \ D_{BEY} = u_B\sin\theta_2 - \cos\theta_2,$$

$$D_{CEX} = u_C\cos\theta_3 + \sin\theta_3,\ D_{CEY} = u_C\sin\theta_3 - \cos\theta_3,$$

$$L_\delta(\theta_r, X_3, Y_3) = sign(L_\gamma\sin\theta_r - Y_3)\sqrt{(L_\beta + L_\gamma\cos\theta_r - X_3)^2 + (L_\gamma\sin\theta_r - Y_3)^2}\ .$$

Equation (5) shows that the system is mathematically indeterminate, i.e. the number of unknown forces and moments is greater than the number of equations. Thus, a special

condition such as measurement or removal of one unknown variable must be accomplished to directly solve the equation.

2.2.1.2 Equations for Model Validation

If there is no contact between the human subject and the seat bottom, then F_{BN} vanishes. In this case, the equations of motion can be rearranged to provide a mathematically determinate equation, which does not require any measurement of the unknown forces to solve: i.e., equation (5) can be rearranged to give

$$\underset{9x9}{[G_1]}\ \underset{9x1}{\{F_1\}} = \underset{9x1}{\{Q_1\}} \tag{6}$$

where

$$\{F_1\} = \{F_{aN}\ \ F_{aT}\ \ F_{kX}\ \ F_{kY}\ \ F_{hX}\ \ F_{hY}\ \ F_{CN}\ \ \tau_k\ \ \tau_h\ \}^T$$

$$\{Q_1\} = \{(m_1\ddot{X}_1)\ (m_1 g + m_1\ddot{Y}_1)\ (I_1^G\ddot{\theta}_1)\ (m_2\ddot{X}_2)\ (m_2 g + m_2\ddot{Y}_2)* \\ *(I_2^G\ddot{\theta}_2)\ (m_3\ddot{X}_3)\ (m_3 g + m_3\ddot{Y}_3)\ (I_3^G\ddot{\theta}_3)\}^T$$

$$[G_1] = \begin{bmatrix} \sin\theta_f & \cos\theta_f & -1 & 0 & 0 & 0 & 0 & 0 & 0 \\ \cos\theta_f & -\sin\theta_f & 0 & -1 & 0 & 0 & 0 & 0 & 0 \\ -\ell_1\cos(\theta_1+\theta_f) & \ell_1\sin(\theta_1+\theta_f) & (L_1-\ell_1)\sin\theta_1 & -(L_1-\ell_1)\cos\theta & 0 & 0 & 0 & -1 & 0 \\ 0 & 0 & 1 & 0 & -1 & 0 & 0 & 0 & 0 \\ 0 & 0 & 0 & 1 & 0 & -1 & 0 & 0 & 0 \\ 0 & 0 & \ell_2\sin\theta_2 & -\ell_2\cos\theta_2 & (L_2-\ell_2)\sin\theta_2 & -(L_2-\ell_2)\cos\theta_2 & 0 & 1 & -1 \\ 0 & 0 & 0 & 0 & 1 & 0 & -D_{CEX} & 0 & 0 \\ 0 & 0 & 0 & 0 & 0 & 1 & -D_{CEY} & 0 & 0 \\ 0 & 0 & 0 & 0 & \ell_3\sin\theta_3 & -\ell_3\cos\theta_3 & L_\delta(\theta_r, X_3, Y_3) & 0 & 1 \end{bmatrix}$$

The adequacy of the model in the proposed force identification method may be validated with equation (6) by comparing the estimated and measured normal force F_{aN}.

2.2.1.3 Equations for Extensor Thrust Force Identification

In the case of the indeterminate system, among the unknown forces and moments, the normal force at the foot rest, F_{aN}, is the easiest force component to measure. Therefore, F_{aN} is measured, and together with the experimental position data, is used to estimate the other forces and moments. If F_{aN} is measurable, equation (5) can be rearranged to give:

$$\underset{9x9}{[G_2]}\underset{9x1}{\{F_2\}} = \underset{9x1}{\{Q_2\}} \tag{7}$$

where

$$\{F_2\} = \{F_{aT}\ \ F_{kX}\ \ F_{kY}\ \ F_{BN}\ \ F_{hX}\ \ F_{hY}\ \ F_{CN}\ \ \tau_k\ \ \tau_h\ \}^T$$

$$\begin{aligned}\{Q_2\} = \{&(-F_{aN}\sin\theta_f + m_1\ddot{X}_1)\ (m_1 g - F_{aN}\cos\theta_f + m_1\ddot{Y}_1) * \\ &*(F_{aN}\ell_1\cos(\theta_1+\theta_f) + I_1^G\ddot{\theta}_1)(m_2\ddot{X}_2)\ (m_2 g + m_2\ddot{Y}_2) * \\ &*\ (I_2^G\ddot{\theta}_2)\ (m_3\ddot{X}_3)\ (m_3 g + m_3\ddot{Y}_3)\ (I_3^G\ddot{\theta}_3)\}^T\end{aligned}$$

$$[G_2]=\begin{bmatrix}
\cos\theta_f & -1 & 0 & 0 & 0 & 0 & 0 & 0 & 0 \\
-\sin\theta_f & 0 & -1 & 0 & 0 & 0 & 0 & 0 & 0 \\
\ell_1\sin(\theta_1+\theta_f) & (L_1-\ell_1)\sin\theta_1 & -(L_1-\ell_1)\cos\theta_1 & 0 & 0 & 0 & 0 & -1 & 0 \\
0 & 1 & 0 & -D_{BEX} & -1 & 0 & 0 & 0 & 0 \\
0 & 0 & 1 & -D_{BEY} & 0 & -1 & 0 & 0 & 0 \\
0 & \ell_2\sin\theta_2 & -\ell_2\cos\theta_2 & -sign(X_2)\sqrt{X_2^2+Y_2^2} & (L_2-\ell_2)\sin\theta_2 & -(L_2-\ell_2)\cos\theta_2 & 0 & 1 & -1 \\
0 & 0 & 0 & 0 & 1 & 0 & -D_{CEX} & 0 & 0 \\
0 & 0 & 0 & 0 & 0 & 1 & -D_{CEY} & 0 & 0 \\
0 & 0 & 0 & 0 & \ell_3\sin\theta_3 & -\ell_3\cos\theta_3 & L_\delta(\theta_r, X_3, Y_3) & 0 & 1
\end{bmatrix}$$

Now, the force vector which includes unmeasured human-generated force components can easily be obtained by solving the linear equation (7).

2.2.1.4 Parameter and Modeling Error Compensation

The parameters used to describe the human body in the model significantly affect the inverse dynamic analysis results [17,18]. Therefore, accurate parameters are essential to accurate estimation of forces. There are some existing empirical formulae based on cadaver studies and/or computer modeling techniques [17,19]. However, most inertial properties of the human body are still hard to accurately estimate due to the fact that these properties depend significantly upon gender, obesity, race and age. In this thesis, the regression formulae suggested by Zatsiorsky and Seluyanov [19, 20] have been adopted.

Since the kinematic relations are based on a simple model of the human body, errors will be introduced into the estimation of kinematic variables. Obviously, the shapes of the back and thigh of each individual human subject also affect the kinematics. Thus, it would be hard to exactly estimate the kinematic responses. Figure 8 shows a conceptual diagram of the errors associated with the thicknesses of the thigh and back.

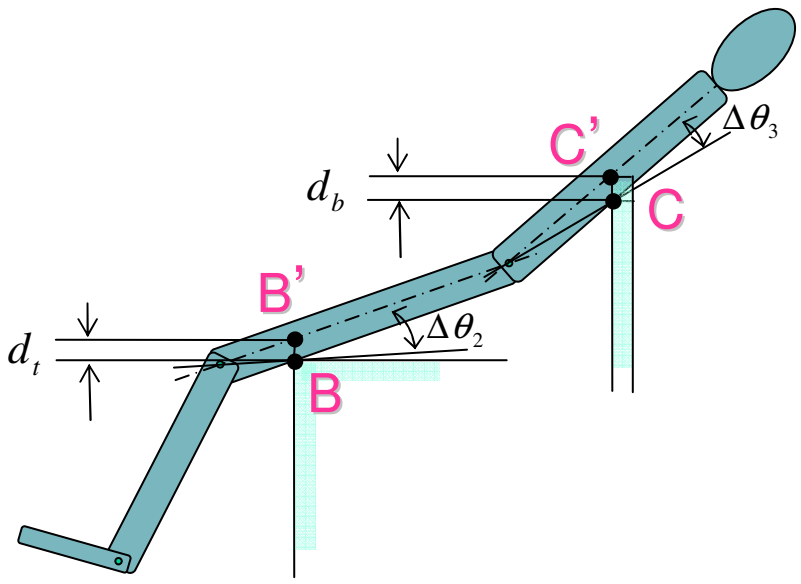

Figure 8: A conceptual plot on the geometric errors in modeling

The offset angles, d_t and d_b, make the measured angles at the joints differ from those between each segment and the seat, by $\Delta\theta_2$ for the thigh, and by $\Delta\theta_3$ for the back. Based on the proposed model, there are some differences between the theoretical and actual contact points indicated by d_t and d_b, which are variant along with the change in posture. However, since d_t is also relevant to the shape of thigh, d_t is not changing much throughout the entire extensor thrust event. Therefore, an easy way to compensate for the error in the thigh segment is by increasing the height of the seat L_α by d_t, and decreasing the seatback length L_γ by the same amount.

On the other hand, d_b changes significantly with the posture, while $\Delta\theta_3$, the difference between the measured and estimated values of θ_3 is not changing much during the extensor thrust event. Thus, an easy, approximate compensation for this error is adding $\Delta\theta_3$ to the estimated angle θ_3. The moment arm associated with the seatback reaction force is also adjusted since the contact point is not on the line between the hip joint and the mass center of the upper body. The proposed approximations will be proven effective later in this paper. However, in order to obtain very accurate estimates for kinematic variables, it would be helpful to measure and use the curvature of the occupants' thigh and back.

2.2.2 Experimental Procedure Overview

Figure 9 shows the experimental setup that is used to provide measurements of chair forces and human body motion during an extensor thrust event. The system consists of a wheelchair seat with a foot rest, a force plate, a general-purpose digital video camera, a data acquisition system and a PC. The chair has adjustable joint angles and the length of the leg rest is also adjustable.

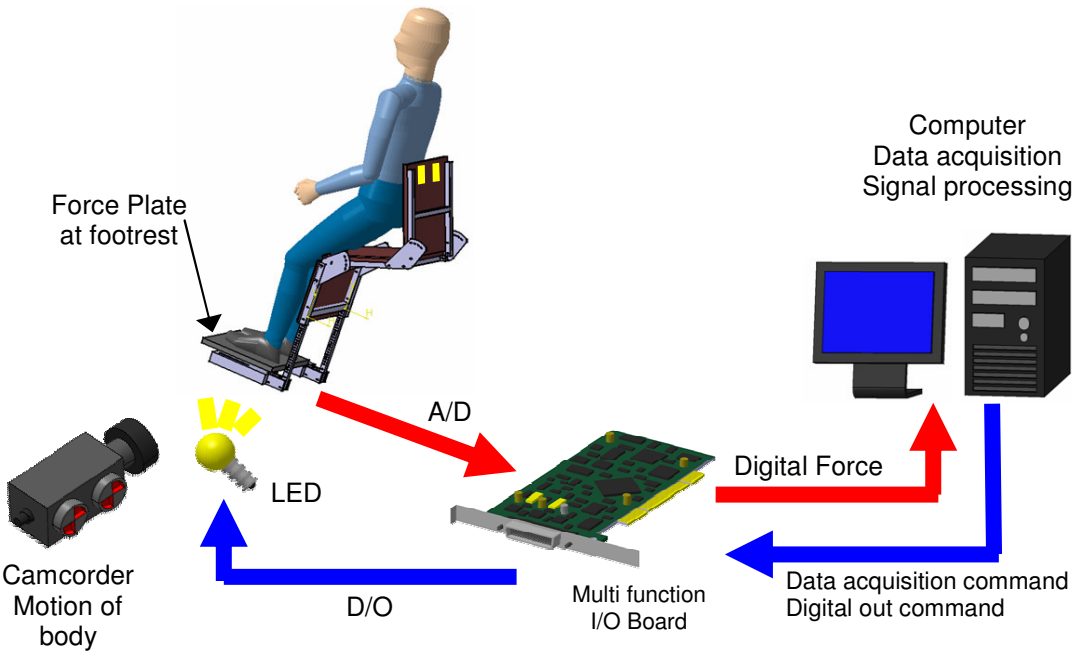

Figure 9: Schematic diagram of the experimental setup

A sequence of digital image frames taken during an extensor thrust experiment is shown in Figure 10. As shown in the figure, markers are attached to the human subject.

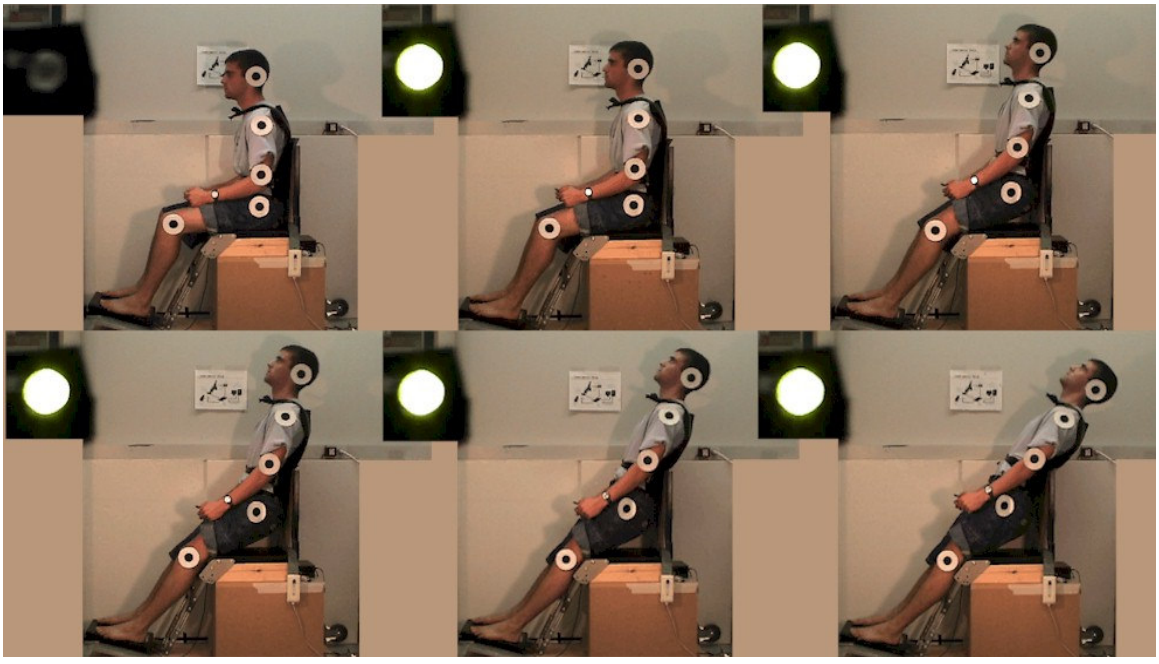

Figure 10: Progression of extensor thrust experiment

Human body motion angles are extracted by tracking the markers attached to the human subject using a digital video camera. To synchronize the video measurements with the force measurement, an LED is triggered simultaneously with the starting time of force measurement. At the upper left corner of each frame, the LED distinguishes the starting point of the experiment. There are five markers, which are attached at two joints of interest, the knee and hip joint, as well as the elbow, shoulder and head. The marker motions are automatically tracked to determine the position data of each link of the human subject. Figure 11 shows typical marker trajectories during an extensor thrust event. The approximate parameters of the human subject participating in the experiments are calculated from the formulae in [19,20] and are given in Appendix B.

Due to the scope of the project and lack of able-bodied occupants, multi-trial experiments were not conducted. All of the conclusions made in the following sections assume good experimental repeatability. Extensor thrust repeatability can be independently verified experimentally using the method that was introduced.

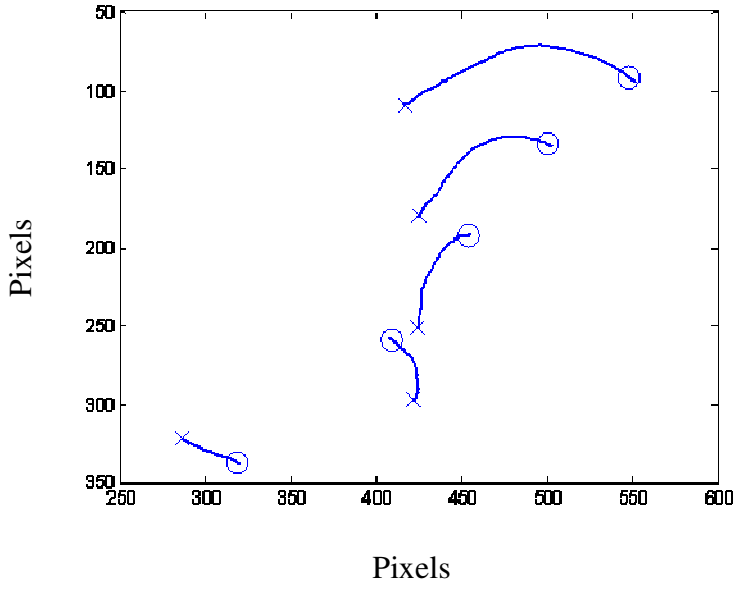

Figure 11: Typical body marker trajectories; X: starting pt, O: ending pt

2.2.3 Model Validation

The main goal of this subsection is to establish a method for testing the validity of the proposed mathematical model. To accomplish this goal, an extensor thrust experiment is performed with a motion that intentionally breaks contact between the human subject and the seat bottom such that equation (6) governs this case. As mentioned earlier, this approach eliminates the need for an additional force measurement.

The measured angular displacements for such an experiment are shown in Figure 12. Each angle is plotted against nondimensional time, meaning that the time vector is rescaled such that the beginning of the thrust is considered to be t = 0, and the end of the thrust is set to t = 1. The reason for this choice is discussed in section 2.3.2. The angles θ_1, θ_2 and θ_3 are reported relative to the horizontal, as shown in Figure 6. The angle θ_3 is computed based on the relative coordinates of the shoulder with respect to the hip joint during the extensor thrust episode. In this analysis, the angular displacements are approximated with fourth-order polynomials ensuring a close fit to the experimental data.

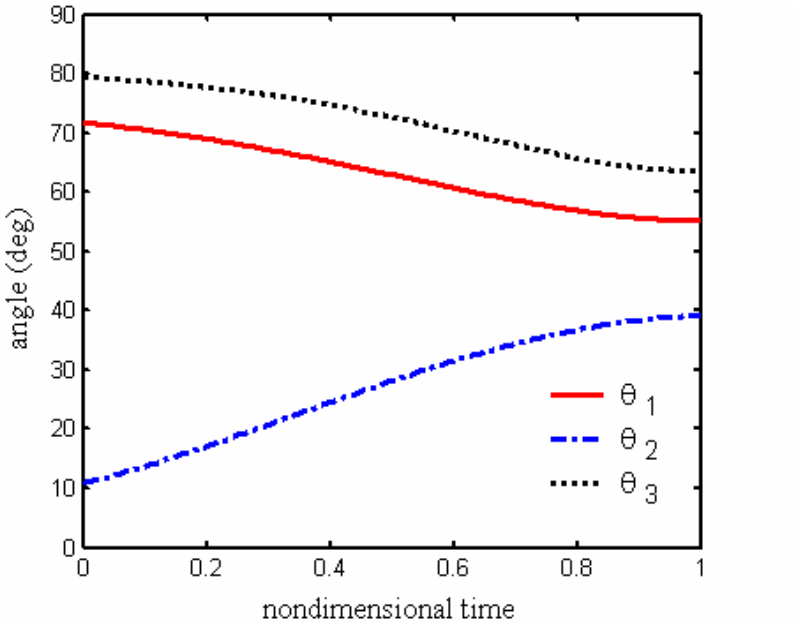

Figure 12: Measured angular displacement for model validation

For the experiment shown in Figure 12 these fourth order polynomials are: $\theta_1 = 13.6x^4 + 4.35x^3 - 15.1x^2 - 10.6x + 71.8$, $\theta_2 = 6x^4 - 40.6x^3 + 37.8x^2 + 25x + 10.9$, and $\theta_3 = 35.1x^4 - 45.2x^3 + 2.03x^2 - 7.84x + 79.5$. Linear and angular acceleration data, which are necessary for the force estimation, are obtained by analytical differentiation of the fourth-order polynomial of the angles.

2.2.3.1 Friction-Related Modeling Error

Figure 13 compares the measured and estimated normal forces at the footrest. A friction force, μ, is considered for the contact regions between the occupant and the seat. The experimental data is well bounded by the two theoretical cases of μ = 0.15 and μ = 0.45. Therefore, μ = 0.3 provides a very good estimate of the actual dynamics. The fluctuation in the measured force appears to be caused by an uneven surface and the dynamics of the chair, which rarely affect the human body motion. The friction

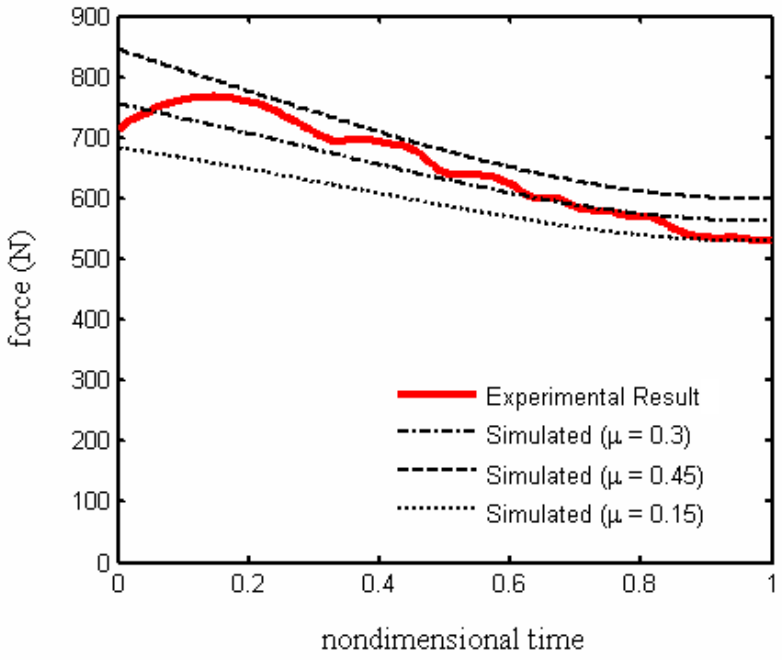

Figure 13: Comparison of measured and simulated normal foot forces for validation experiment

coefficient is one of the most difficult parameters to be identified, so it is very fortunate that such a good estimate is available. A detailed sensitivity analysis with respect to modeling errors of human parameters will be discussed in the next section.

2.2.3.2 Simulation Input Methods

Another model consideration is the relevance of the way the position inputs are devised for the inverse dynamic simulation. To address this concern, an experiment is performed where the foot rest and seatback angles are set to 15° and 90°, respectively. Figure 14 compares a set of the measured angular displacements and a set of the estimated angular displacements based on the kinematic relations and compensation scheme as discussed in the previous section. In general, only one angular displacement is required to estimate the other coordinates, and the angular displacement θ_2 is used in this case. Figure 14 shows that the estimated angles are close to the measured angles.

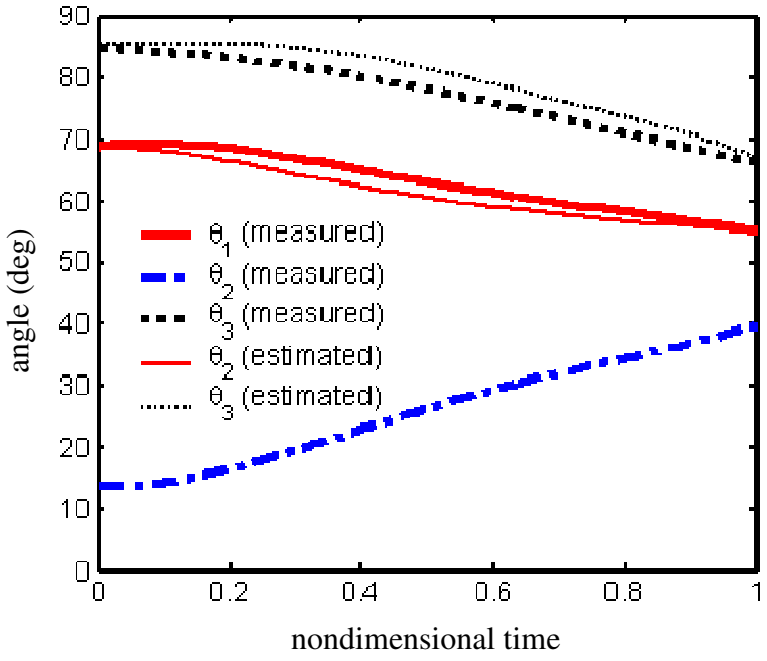

Figure 14: Measured and estimated angular displacements: foot rest angle = 15°, seatback angle = 90°

However, θ_1 and θ_3 are somewhat underestimated and overestimated, respectively. These errors probably result from the tapering shapes of the thigh and back of the human subject. Fortunately, however, these errors do not significantly affect the force identification as shown below.

Figure 15, shows two sets of identified forces, using only measured angles and using two estimated angles and one measured angle. The identified forces include the tangential force (F_{aT}) at the foot rest, and the normal forces on the seat bottom (F_{BN}) and seatback (F_{CN}). The comparison of two sets of the identified forces confirms that the forces estimated with a combination of measured and estimated angles are in a good agreement with those only using measured angles. The results imply that the derived kinematic results provide good representation of the system kinematic behavior. Figure 16, shows the identified torques at the knee (τ_b) and hip (τ_c) joints, which also illustrates

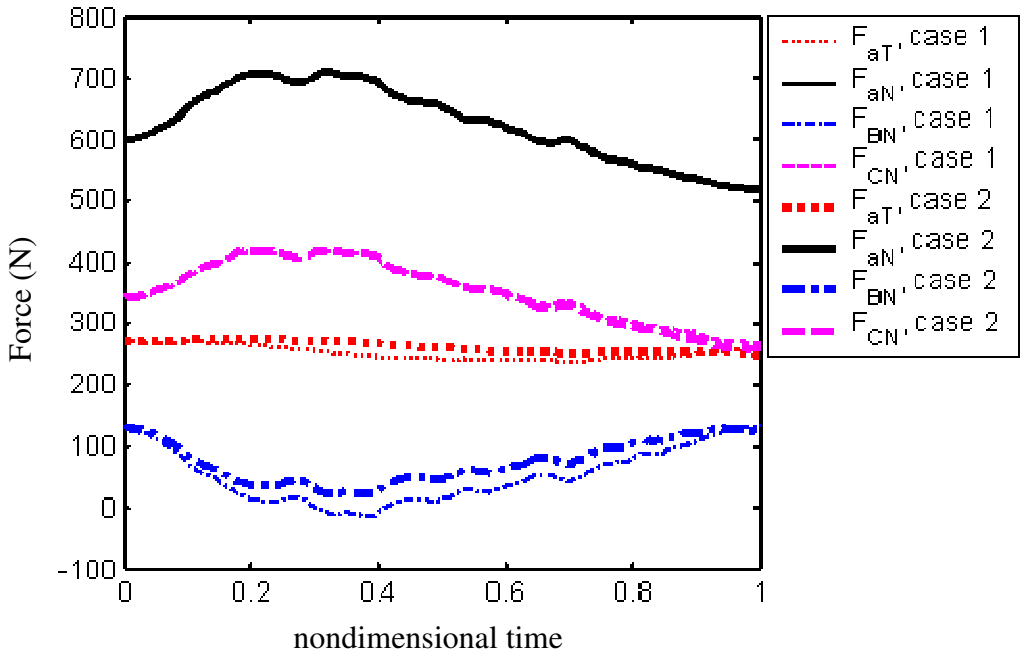

Figure 15: Forces identified with two different sets of angular displacements: case 1: using only measured angular displacements; case 2: using one measured and two estimated angular displacements; foot rest angle = 15^o, seatback angle = 90^o

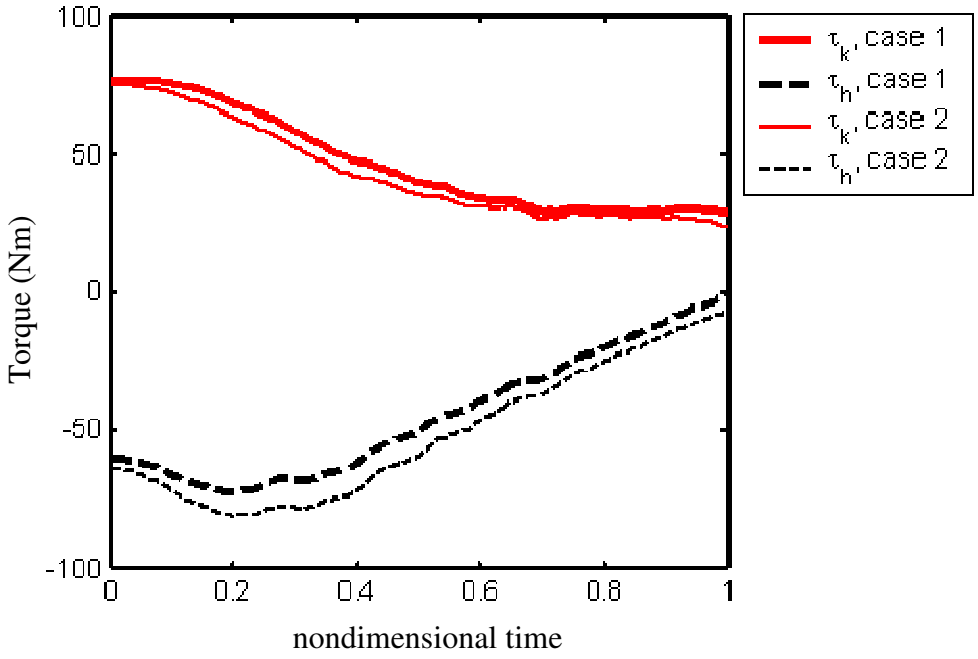

Figure 16: Torques identified with two different sets of angular displacements: case 1: using only measured angular displacements; case 2: using one measured and two estimated angular displacements; foot rest angle = 15^o, seatback angle = 90^o.

that there are only minor differences between using only measured angles and using a combination of estimated and measured angles.

2.3 Investigation of Extensor Thrusts on a Rigid Chair

Given that the rigid seat model can adequately represent a real world extensor thrust, this model can be used in multiple studies to reveal added insights into the extensor thrust phenomenon. One important study is to investigate the configuration effects of seat and occupant and the impact a configuration change may have on extensor thrusts. Additionally, the importance of the extensor thrust speed and occupant-induced disturbances are also interesting areas of study. Finally, a sensitivity analysis is performed to identify the human parameters that will have the biggest impact on thrust behavior. These findings

2.3.1 Chair and Configuration Effects

To show the effects of the chair configuration, two experiments were performed where the foot rest and seatback angles were changed. Figures 17 and 18 show identified forces and Figure 19 shows torques from these experiments. Figure 17 reveals that a change in seatback angle from 90° to 80° decreases the normal force, given the same 15° footrest angle, while slightly increasing the tangential force at the foot rest. This shift occurs because more tangential force is required to compensate for the increase in horizontal reaction force from the seatback. Additionally, it is noticeable that the thigh of the occupant carries more load if the seatback is in a reclined configuration. This observation could be largely attributed to the motion of the occupant. Specifically the added rotation in the shank combined with less thigh rotation, lead to more thigh compression. Examining Figure 18, one finds that the increase of foot rest angle makes it

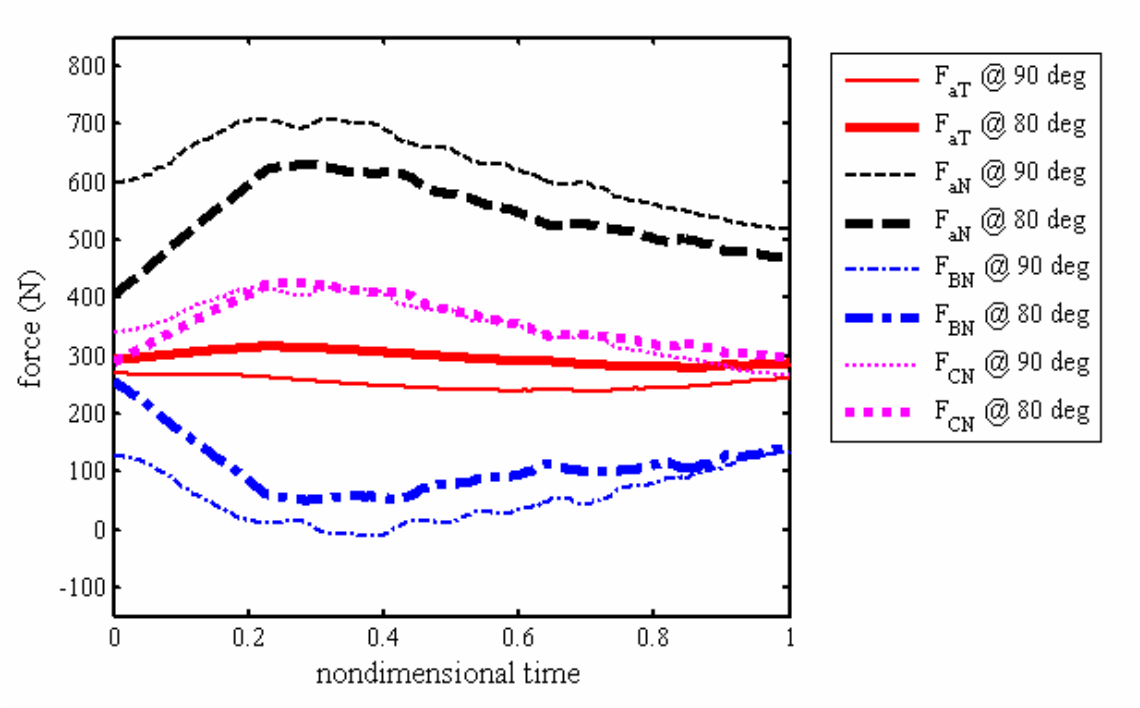

Figure 17: Forces identified with changing the seatback angle from 80° to 90°; footrest angle = 80°.

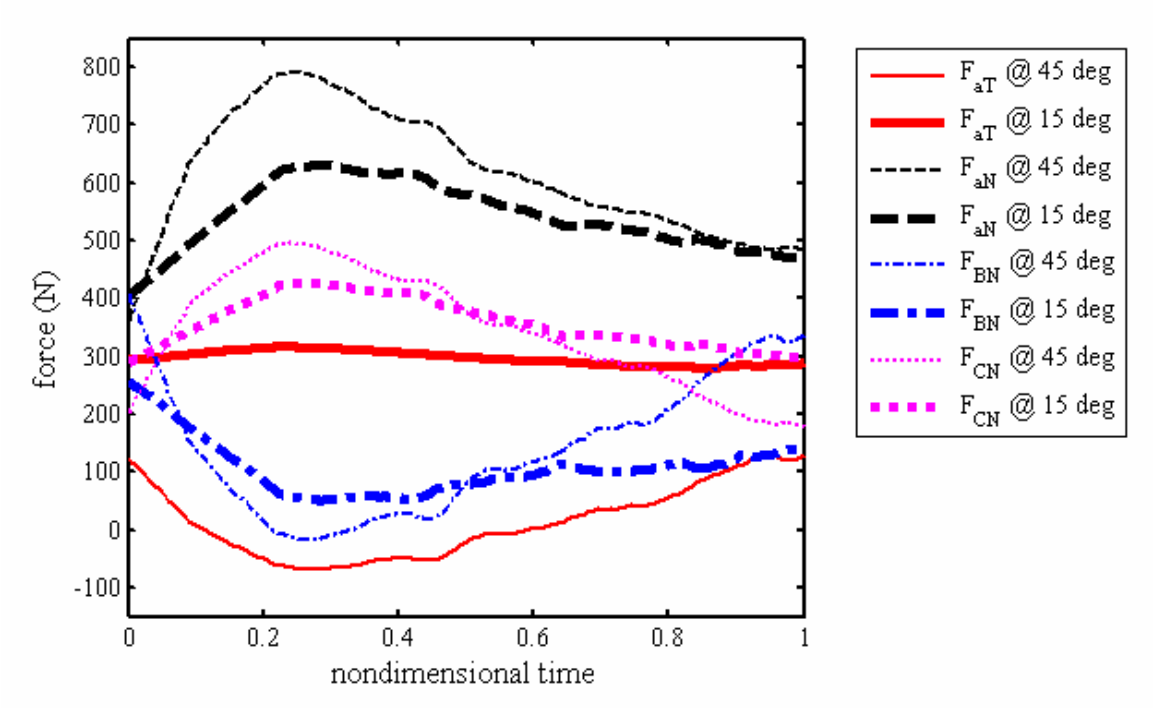

Figure 18: Forces identified with changing the foot rest angle from 15° to 45°; seatback angle = 80°.

easy to produce horizontal force by increasing the normal foot force. In this case, the tangential foot force is drastically reduced while the normal force is increased. Such an adjustment could therefore be beneficial if it is desired to restrain the occupant to the footrest primarily through the means of friction, rather than other constrictive foot restraints. Clearly, such an approach could not work as a standalone solution, but rather as a complimentary solution that would also require a secondary foot restraint mechanism to ensure that the feet of the occupant would remain over the footrest at all times. One such mechanism could be as simple as an elastic collar that would limit the motion of the occupant's feet during the relaxed state occurring before and after a thrust.

Figure 19 shows that the joint torques are also affected by the change of foot rest angle. Overall, the normal force at the foot rest is relatively significant and is the

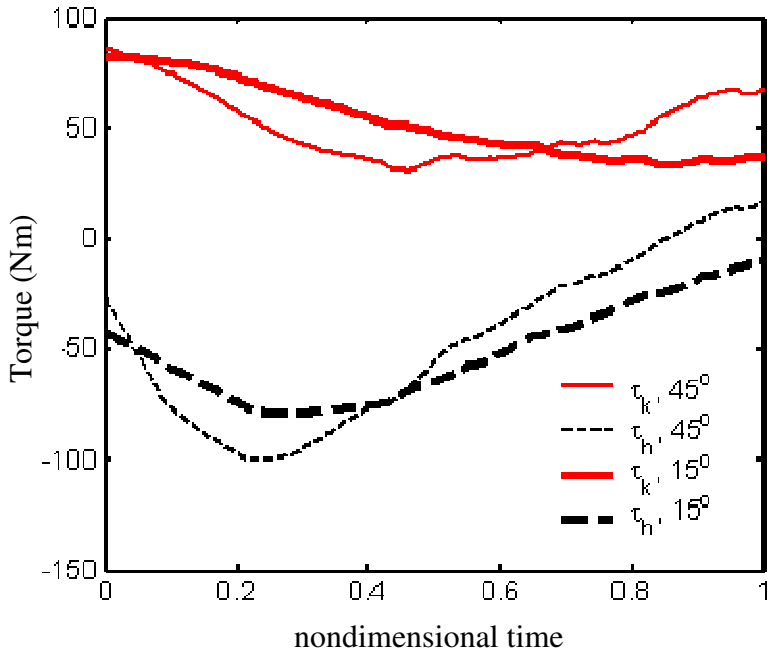

Figure 19: Torques identified with changing the foot rest angle from 15° to 45°; seatback angle = 80°.

dominant driving force for the extension motion, while the tangential force is less significant but becomes larger as the extension progresses.

2.3.2 Extensor Thrust Speed Effects

Experiments were performed to evaluate the effects of extensor thrust speed. Determining whether extensor thrust speed has a significant influence on the occupant torque profiles is crucial for further modeling work. Figures 20 and 21 show identified forces and torques during extensor thrusts that lasted approximately 0.8, 1.3 and 2.0 seconds. These values represent a fast, medium and slow thrust profile respectively. Each force and torque is plotted with the same linetype for all of the experiments performed. The overall pattern of the force and torques does not depend greatly on the speed. This implies that the gravity forces dominate throughout the event and dynamic effects from seat interactions are secondary in importance.

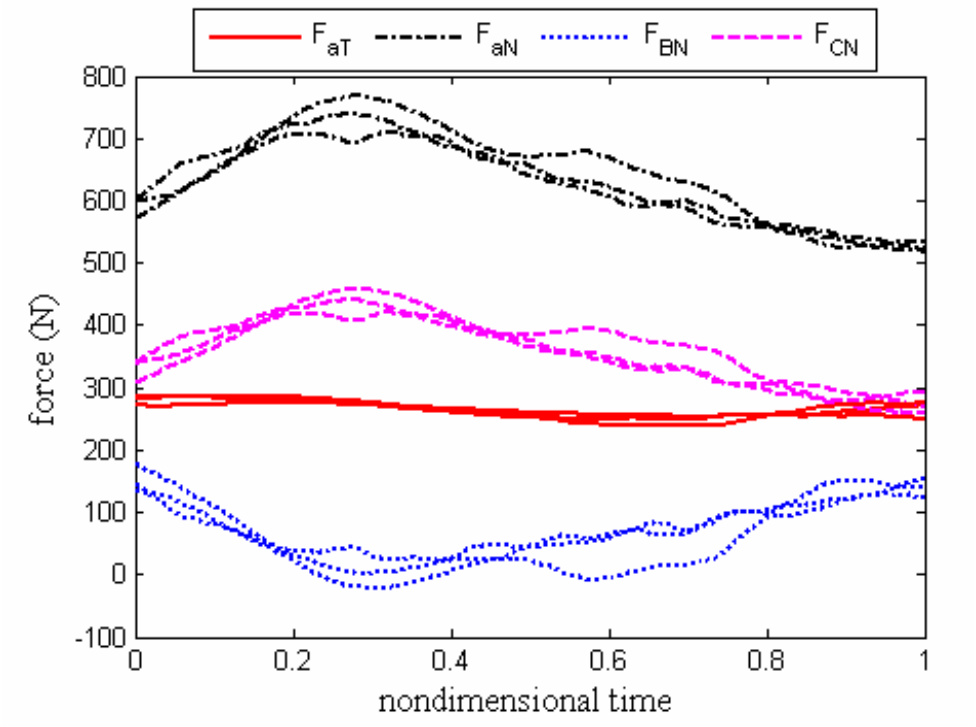

Figure 20: Identified forces with the duration of extensor thrust event varied: durations = 0.8, 1.3 and 2.0 seconds; foot rest angle = 15°, seatback angle = 80°.

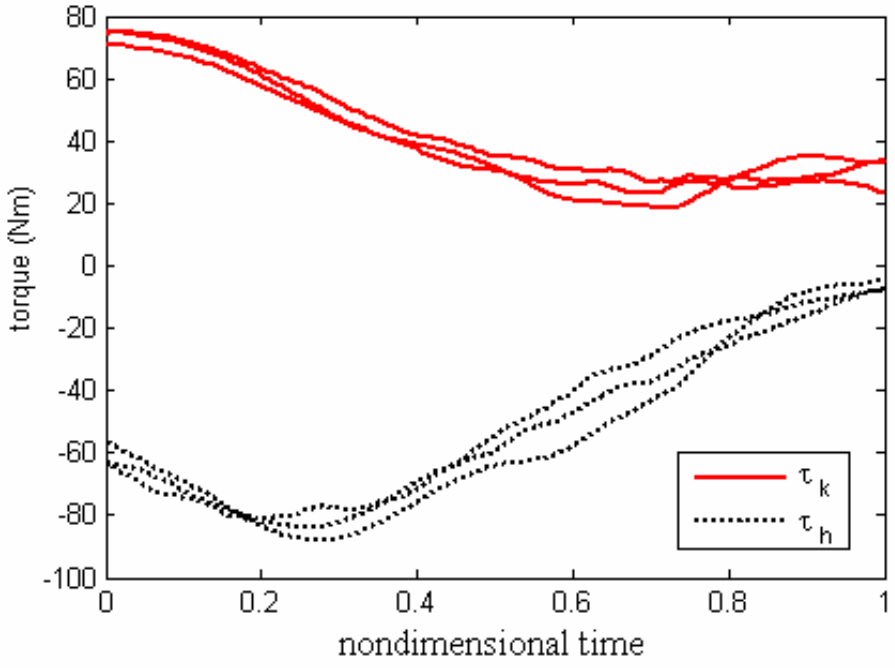

Figure 21: Identified torques with the duration of extensor thrust event varied: durations = 0.8, 1.3 and 2.0 seconds foot rest angle = 15°, seatback angle = 80°.

2.3.3 Occupant-Induced Disturbance Effects

Figure 22 shows the human-generated forces when a non-smooth extensor thrust is simulated. For this experiment the human subject rocked forward and backward during the extensor thrust event. The force and torque patterns are quite different from those from the regular experiments due to the significant change in angular displacement patterns. However, the peak values are not significantly different from others, implying that the gravitational forces are also dominant in this case.

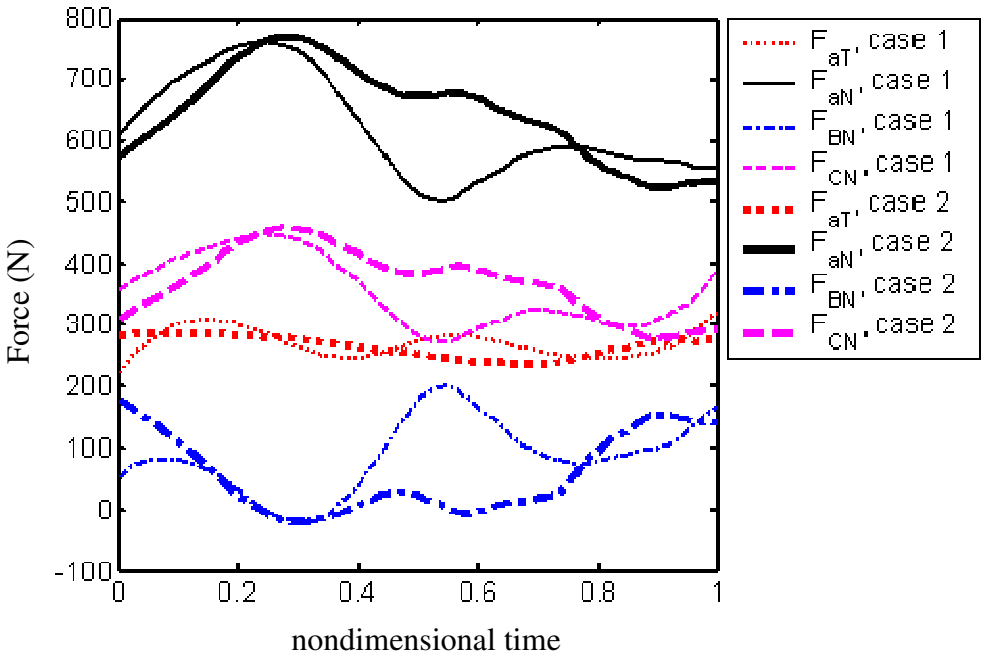

Figure 22: Comparison of identified forces with and without intentional rocking motion during the extensor thrust event

2.3.4 Sensitivity Analysis of Human Parameters

Because the proposed method utilizes human-related modeling parameters, which are subject to some amount of uncertainty, it is very important to investigate the robustness of the proposed method with respect to the modeling errors. In order to

determine this robustness, a sensitivity analysis was performed with respect to the human parameters. Among these, masses and mass center locations which are most difficult to estiate or measure were considered. Figures 23 and 24 demonstrate the variations of the identified forces and torques when the thigh mass, m_2, and the location of mass center of the thigh, l_2, are varied 10 % from their nominal values. Overall, the results show that the identified results are not very sensitive to these parameter variations. In particular, the identification error is relatively insensitive to the mass center location parameter. However, the identification error due to the thigh mass is somewhat more significant and is varying with time.

The magnitude of errors appears to be dependent on the system matrix which is relevant to the dimensions and posture of human body and other seat related parameters. The modeling error sensitivity is extremely high when the system matrix is singular. In order to correlate the system matrix singularity with the sensitivity, the following reliability index is defined:

$$I = \min_i S_i \tag{8}$$

where $S_i, i = 1,2,...,9,$ are singular values of G_2 in equation (7) and defined from the singular value decomposition formula as follows [21]:

$$[G_2] = [U]^T [S][V] \tag{9}$$

Theoretically, every matrix can be decomposed using equation (9), in which the diagonal matrix [*S*] contains non-negative singular values. If any singular values are zero, then the system matrix is singular. The reliability index in equation (8) is defined

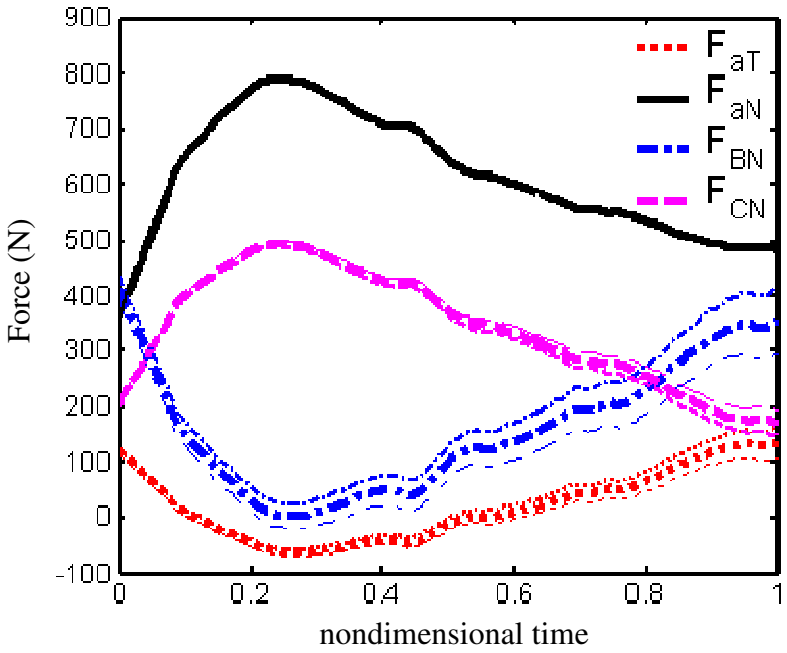

(a) forces

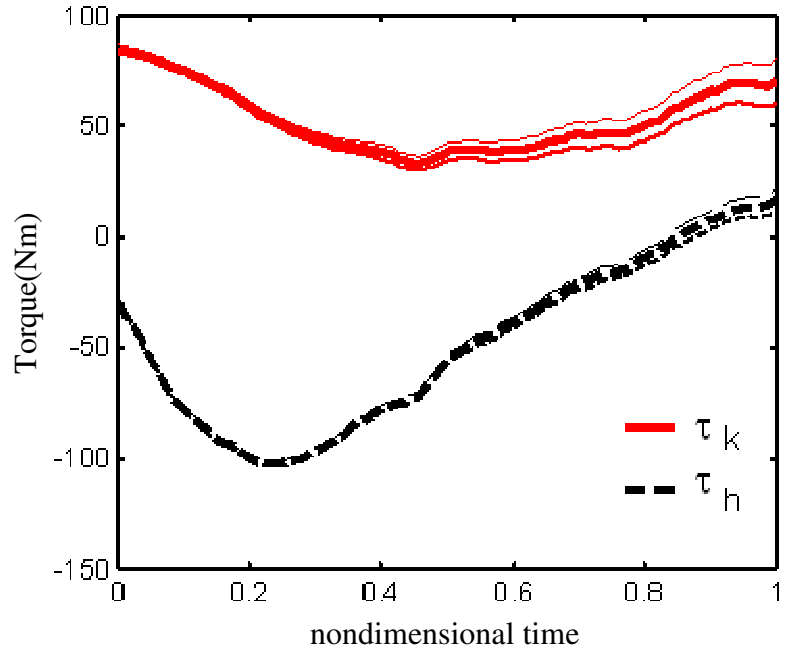

(b) torques

Figure 23: Variation of the identified forces and torques with the mass of the thigh changed by ±10% from the nominal value.

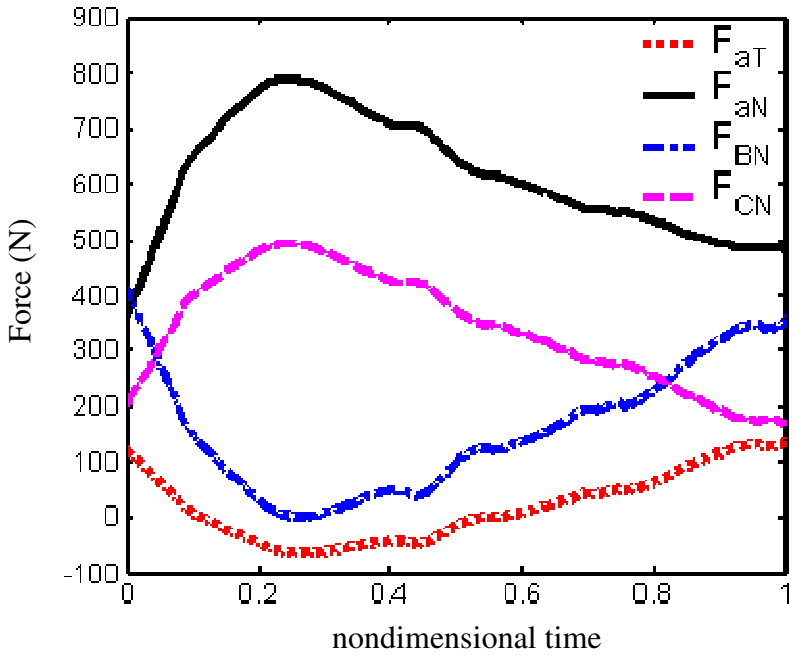

(a) forces

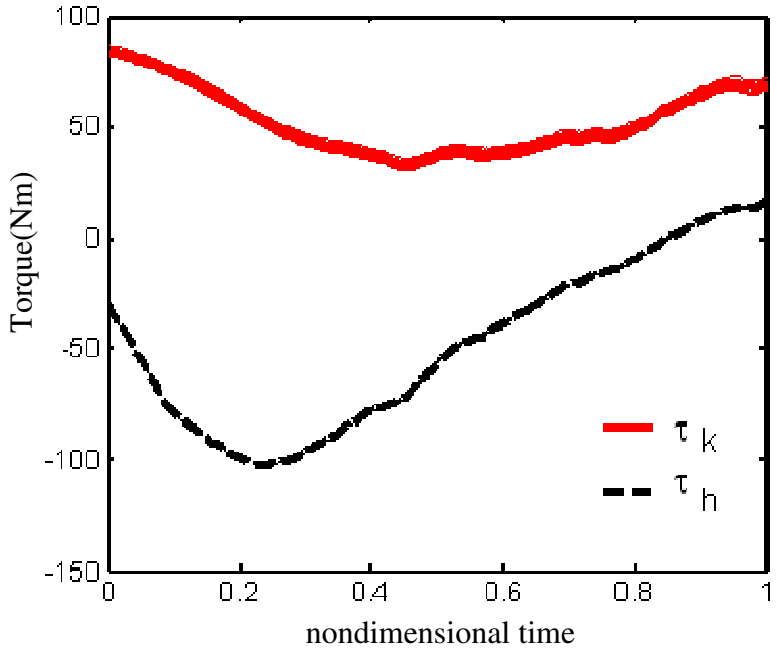

(b) torques

Figure 24: Variation of the identified forces and torques with the mass center location for the thigh changed by 10% from the nominal value:

so as to represent the degree of non-singularity of the system matrix. The smaller the index is, the more likely the system matrix becomes singular and the identification is more sensitive to modeling errors or noise. Figure 25 shows the index value for the extensor thrust event corresponding to Figures 23 and 24. Comparison of Figure 23 and Figure 25 reveals that the index becomes small in the region where the errors become larger. Therefore, this index provides useful information regarding the robustness of the method for each individual case, and the reliability of the identified results.

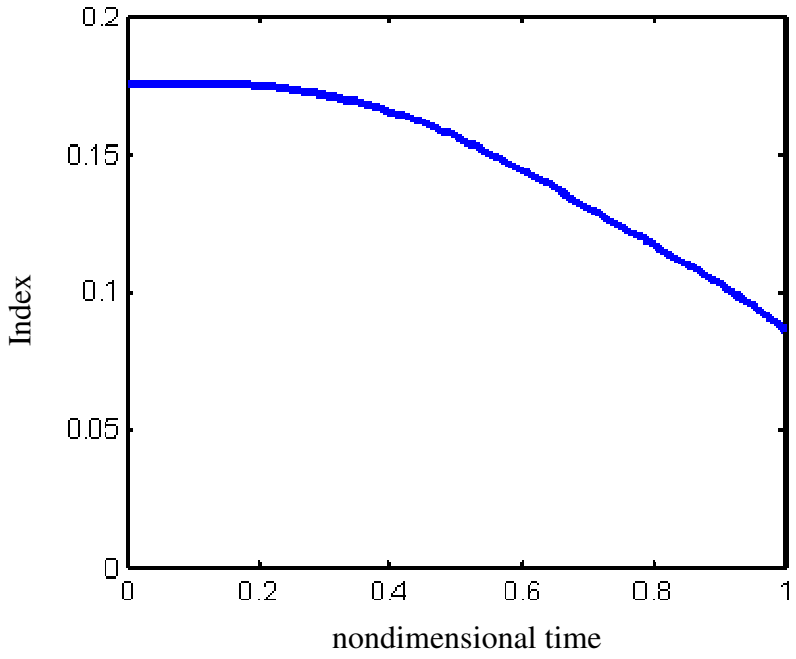

Figure 25: Identification reliability index:
(Footrest and seatback angles are set to 45^{o} and 80^{o})

CHAPTER 3

DYNAMIC SEATING SYSTEM DESIGN AND IMPLEMENTATION

After developing a basic understanding of extensor thrust characteristics, it is now possible to make use of that information to develop a functional dynamic seating system. The purpose of such a system is to improve occupant comfort and safety, as well as improve system durability. A highly-adjustable dynamic seating system is proposed to address many of the needs of those affected by high-tone extensor thrusts. These needs are identified by making use of the findings from the study in the previous chapter, as well as of input from caregivers of children with Cerebral Palsy. This seating system is designed as a standalone solution for some of the affected individuals, as well a springboard for further research in this area.

3.1 Design Overview

Acting as a proof of concept for multiple technologies that can positively impact dynamic seating system design in the future, the Hingeback design, shown in Figure 26, fulfills multiple project objectives. This system operates by allowing the seatback to pivot backwards when the seat is in a dynamic configuration while remaining rigid when the seatback rigidizer is engaged. When the seat is in a dynamic mode the occupant is able to dissipate some of the thrust energy and is met with less resistance than during a comparable thrust in a rigid seat, thus improving the thrust characteristics.

The Dynamic Hingeback seating system has been designed to allow for significant adjustability and data collection capability. Pictured in Figure 26, the dynamic seatback system is composed of a mounting platform, adjustable footrest, dynamic seatback, and a Seatback Rigidizer. Additionally, force and strain sensors are integrated with the

mechanical components to provide data needed to understand the loading of the system during a thrust event. These sensors are connected through a custom-made amplifier that enables a computer to record and process the event, as well as to control the Seatback Rigidizer by using the newly-processed strain data for triggering.

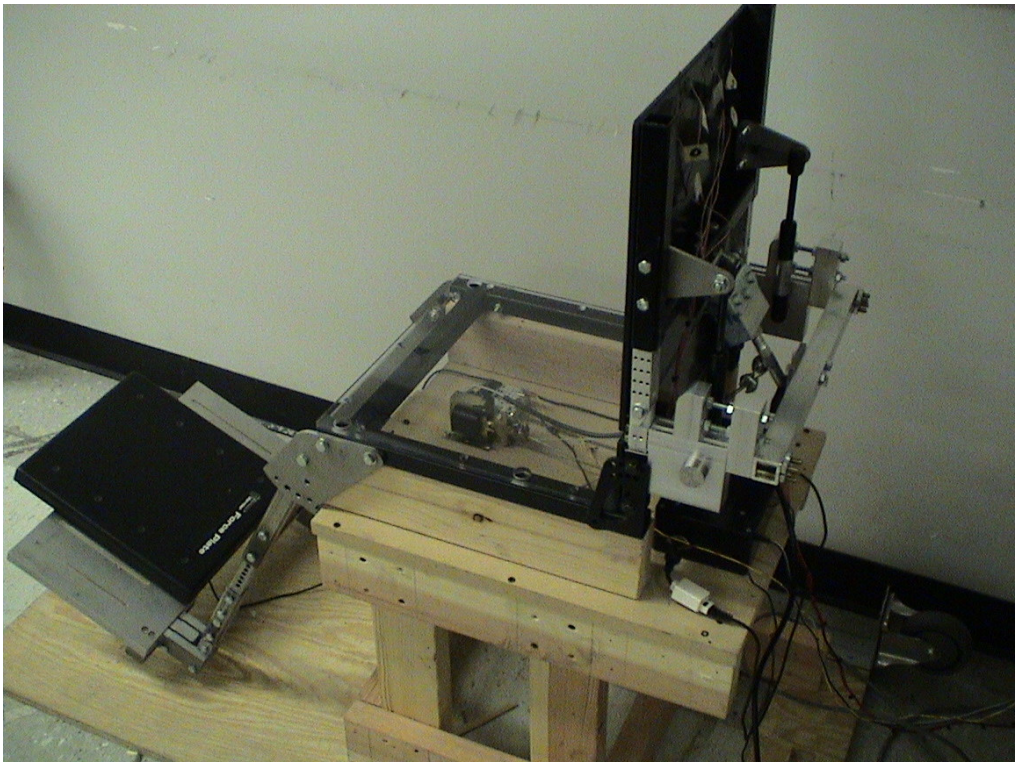

Figure 26: Picture of Dynamic Hingeback Seating System

The system can measure the critical forces which occur during the course of an extensor thrust, thereby quantifying some of the more obvious benefits of a dynamic seat. Additionally, this prototype demonstrates how seating functionality can be improved by adding active feedback control to the seat. The system is also used to validate a simulation-based design approach for dynamic seats. This approach opens the door to simplified seat customization and eliminates the need for the construction of expensive prototypes otherwise needed to explore other creative dynamic seating system solutions.

Finally, due to the highly adjustable design, the Hingeback seat can be used to perform additional studies with children affected by Cerebral Palsy or other disorders that result in high-tone extensor thrusts. Although reaching this future goal would involve an added effort to childproof the existing seat to meet all necessary Internal Review Board standards, the information that could be collected may prove invaluable.

3.1.2 Dynamic Seating System Components

The Dynamic-Hingeback Seating System (DHSS) is composed of four primary mechanical subsystems, as well as the integrated onboard electronics. The overall system schematic outlining the individual subsystems is shown in Figure 27. The DHSS is bolted onto a mobile platform for stability and portability. The adjustable frame of the seating system is designed to accommodate multiple body types without sacrificing occupant safety. By maintaining the seatback rigid whenever desired, the occupant is

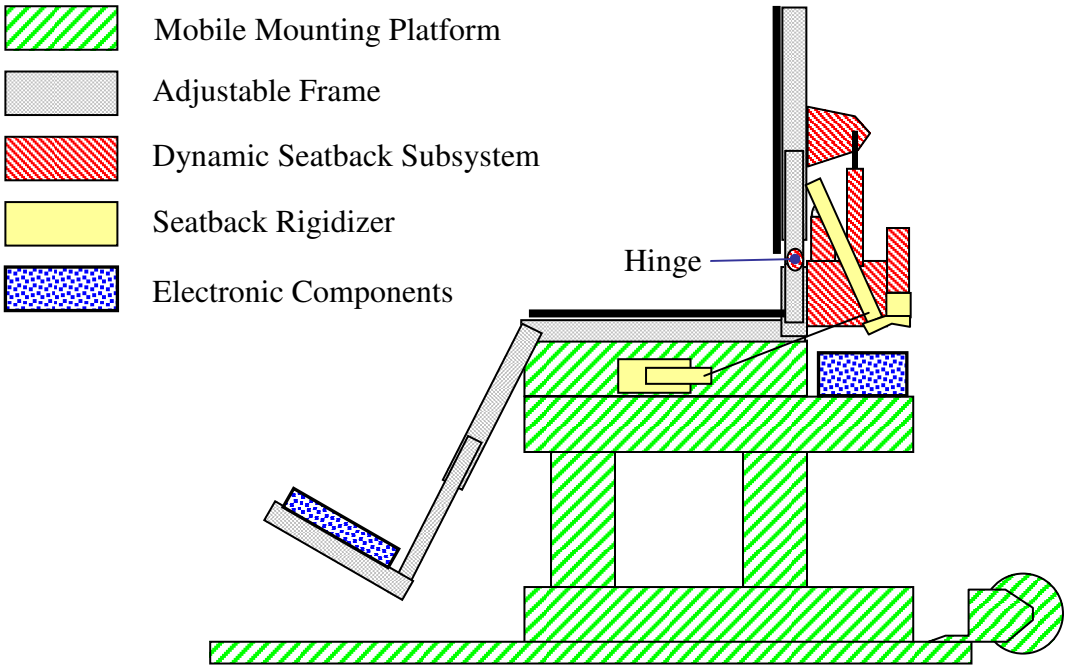

Figure 27: DHSS mechanical subsystem schematic

able to leverage off the seatback to communicate and interact with his or her environment. Each subsystem is discussed in a corresponding subsection where the key features of the subsystem are outlined in detail.

3.1.2.1 Mounting Platform

The mounting platform is designed to address two primary goals. The most important feature is ensuring the safety of the seat occupant. In meeting this critical objective it is important to consider everything that could go wrong with the mounting platform and designing the structure to avoid all of those scenarios. A sturdy frame made entirely of a solid wood 2 x 4 beams ensures the platform will not fail even under extreme loading conditions. Four 5/16" diameter self-locking bolts are used to secure the seating system onto the wooden frame. The frame is securely attached to a large solid plywood base that ensures the system will not tip over due to the large footprint provided by the base. The complete subsystem is shown in Figure 28.

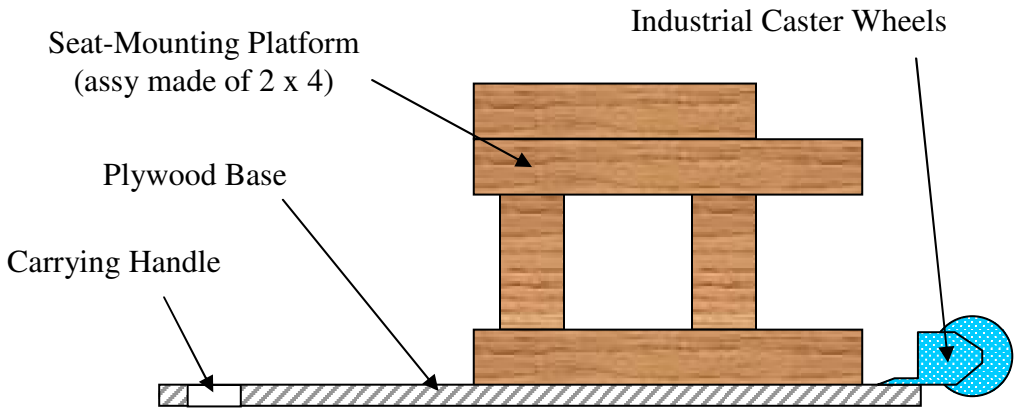

Figure 28: DHSS Mobile Mounting Platform schematic

Another consideration that drove the platform design was portability, as it may be necessary to transport the DHSS to various locations for occupant testing. To address

this need a pair of industrial casters was added to the base on the side closer to the CG of the entire system and a handle was cut out on the other side.

3.1.2.2 Adjustable Frame

One of the key features of the DHSS is providing a highly adjustable seat frame that can accommodate multiple body types. Since the system is to be used primarily for testing it must be able to handle individuals both large and small. Additionally, while seeking the optimal position for each individual it is desirable to have significant adjustability to experiment with multiple configurations, both on an individual basis and for the general affected population as a whole. Figure 29 shows the multiple seat parameters that can be adjusted in the DHSS frame.

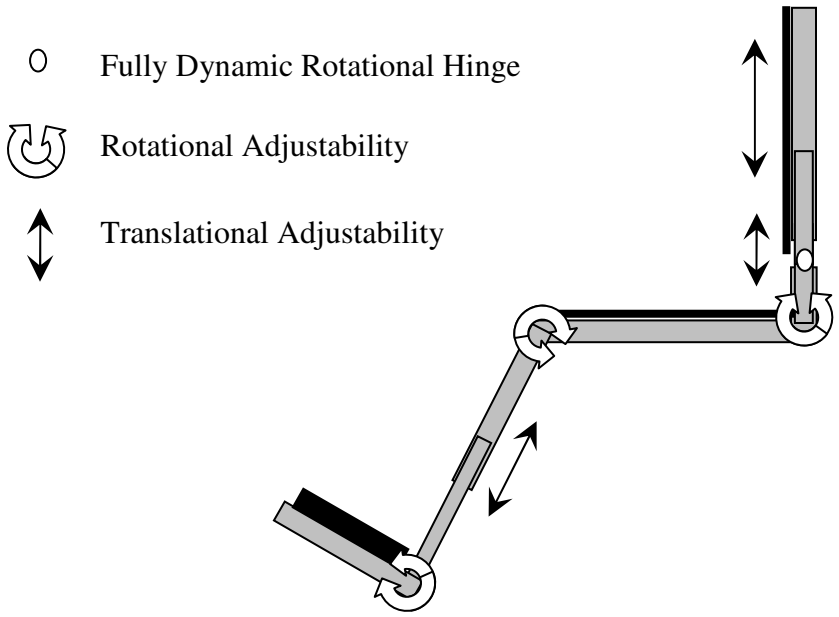

Figure 29: Schematic showing adjustability of DHSS Frame

3.1.2.3 Dynamic Seatback

The dynamic seatback concept is the central feature of the DHSS. The ability to have the seatback pivot backwards as an occupant undergoes an involuntary extensor

thrust is proposed as a way to reduce the strain on both the occupant and the seating system. The seatback is designed to become dynamic only if there is a significant force pushing on it. This behavior can be achieved by implementing a counterbalancing preload on the seatback that will keep it in a rigid configuration, unless the torque exerted by the occupant is greater than the preload torque. This concept is implemented through the use of preloaded gas shocks, as shown in Figure 30. The gas shocks can be replaced

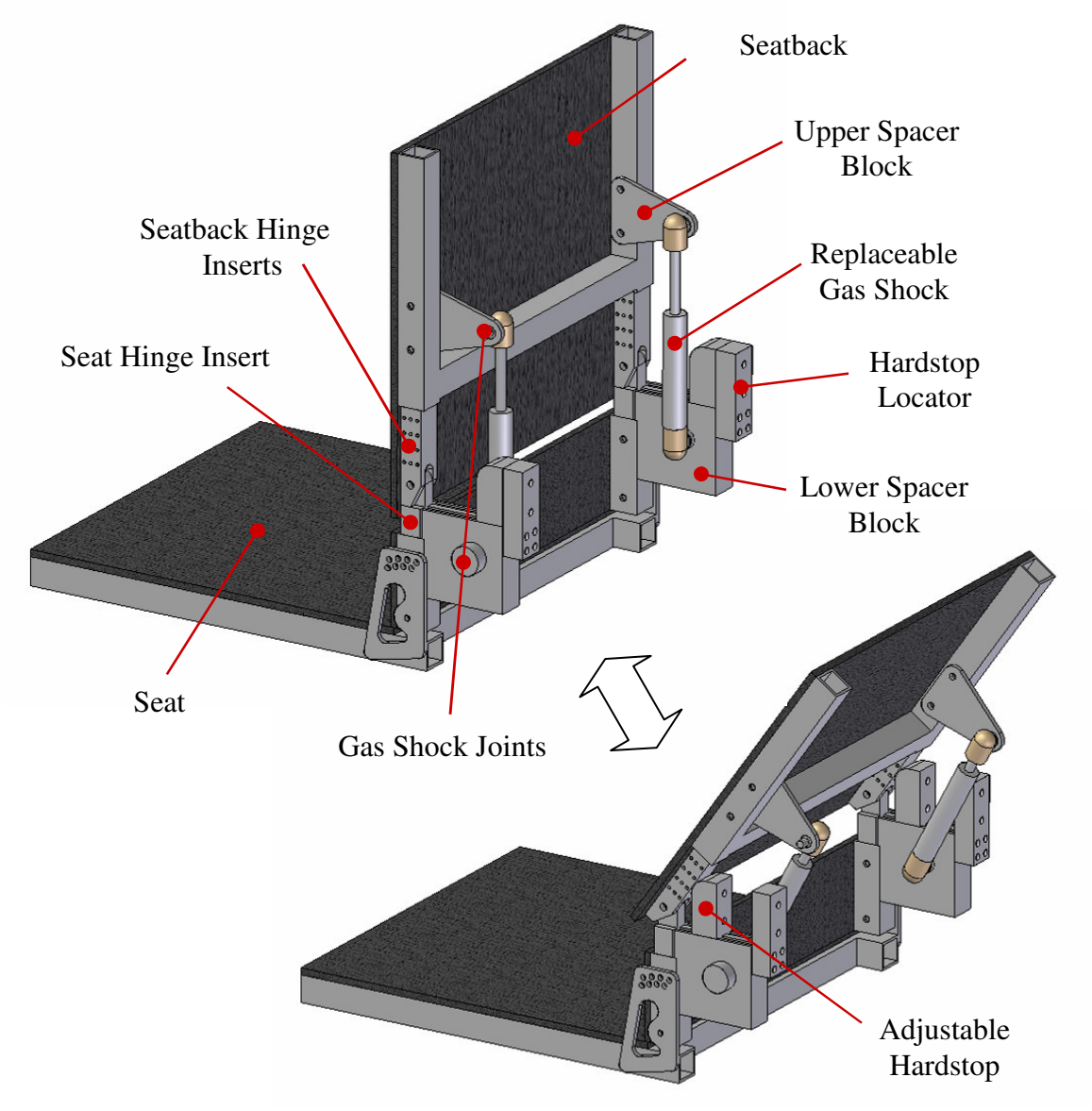

Figure 30: 3D Model of dynamic seat shown in upright and extended configurations

to adjust the preload torque that must be overcome in order to have the system enter the dynamic regime. The seatback hinge inserts are designed to prevent the back from making an acute angle. This is done by using a mechanical hardstop which prevents further rotation once the seatback and seat hinges are aligned.

Another key feature of the hingeback design is the adjustable hardstops that can be used to limit the maximum seatback deflection. This added level of mechanical control enables caretakers to personalize the system for each individual occupant, and is especially important in quantifying the benefits of a dynamic seatback through experimentation. By incrementing the allowable rotation of the seatback it is possible to experimentally find a typical thrust profile at each increment, and use that information to establish trends between maximum seatback deflection and thrust characteristics.

3.1.2.4 Seatback Rigidizer

The final mechanical subsystem to be discussed is the seatback rigidizer shown in Figure 31. This is an optional system that can be made available for occupants who have learned to use extensor thrusts in a controlled manner to communicate or perform a functional task such as pushing a button or readjusting their position in the seat. Keeping the seat in a rigid configuration during a volitional thrust has been identified as an important feature in some cases, as seen from the survey results found in Appendix C. Occupants who rely on the seatback rigidity to reach a switch would loose that functionality if the seatback were to rotate backward during every extensor thrust. The rigidizer system is able to keep the seatback upright even if the preload torque is surpassed, and only if an electronic controller has determined that the thrust is involuntary will the chair enter the dynamic domain and pivot backward.

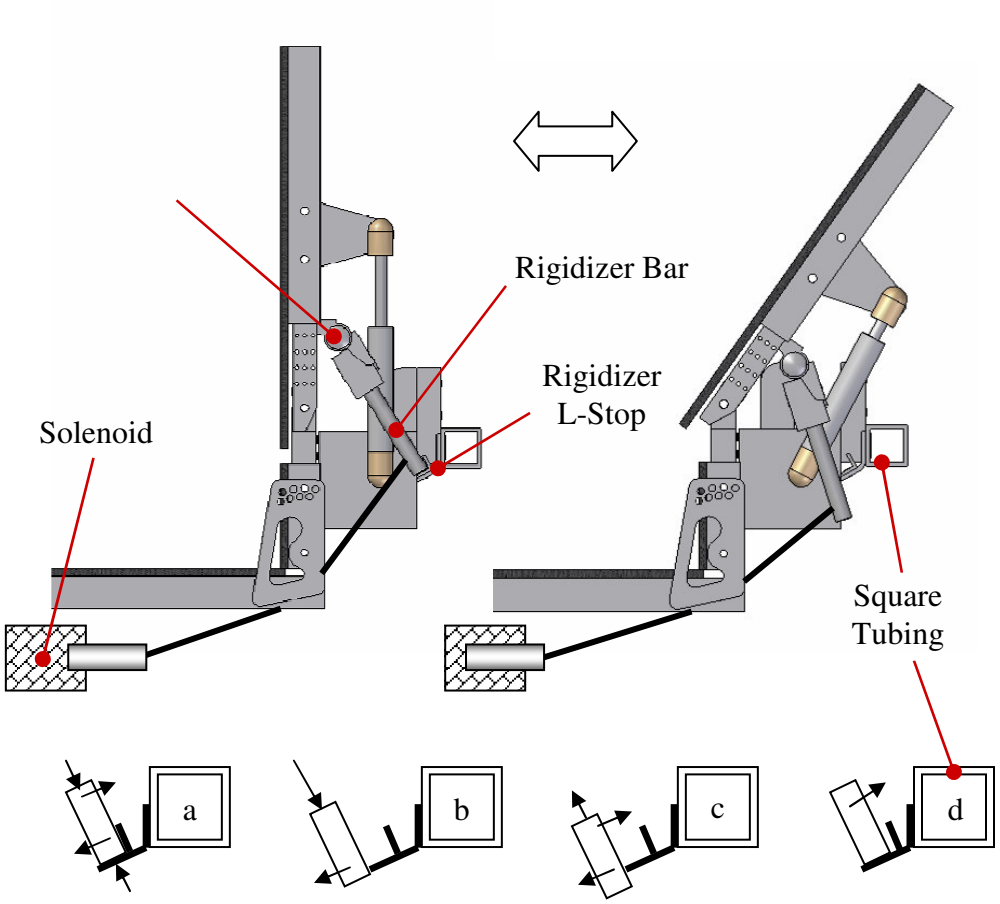

Figure 31: Detailed concept schematic of Seatback Rigidizer

Mechanically, the seatback rigidizer works by having a bar that is preloaded by a torsion spring hinge push against an L-stop. When the seatback is upright, the end of the bar tucks into the "L," which is fixed onto the rigid frame by the means of square aluminum tubing. If a compressive load is transferred through the rigidizer while it is locked in the L-stop the seatback is effectively grounded and is unable to pivot (a). A solenoid located below the seat is connected to the bar via a cable, and when activated, it is able to pull on the bar and dislodge it from the L-stop (b). Once the L-stop is no longer in the way the seatback is free to pivot about the hinge axis. While the seatback is deflected the rigidizer bar slides against the tip of the L-stop due to the preload from the torsion spring (c). Once the seat is upright again the bar locks back into place (d).

3.1.3 Measurement and Control Systems

In order to evaluate the DHSS performance, it is necessary to obtain data that can reveal the quantitative improvements provided by the dynamic seatback. This data collection process requires motion and force measurements which are discussed in the following sections. Additionally, the seatback rigidizer is an active system and requires a control algorithm to operate properly. This control algorithm is also discussed in detail.

3.1.3.1 Motion Measurement

The motion tracking system used to obtain experimental data is similar to the technique presented in Chapter 2 for the rigid seat. There are, however, a number of improvements that were made to measure this moving seat. The most significant change in hardware was the use of a high-end webcam in place of the digital camcorder. This swap eliminated the time-consuming process of digitizing the video capture, thereby streamlining the entire motion data collection process. Additionally, modifications were made to the MATLAB code to improve tracking ability and reduce processing time. Figure 32 shows motion tracking results for a rigid and a dynamic seating configuration obtained with the measurement system.

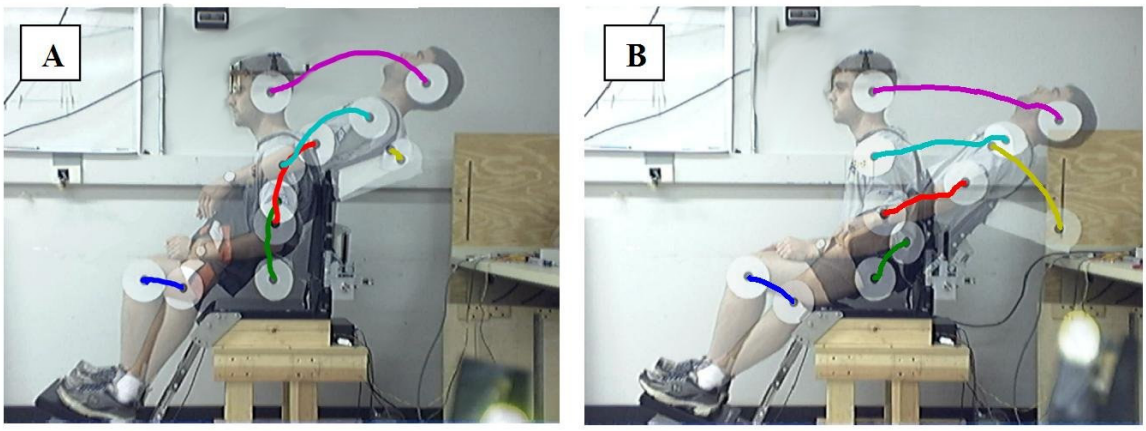

Figure 32: Motion tracking for (A) rigid and (B) dynamic seatback configurations

3.1.3.2 Force Measurement

To obtain the force and strain measurements required, uniaxial strain gages were adhered to the plastic backrest of the seatback. In total, six gages were attached, as shown in Figure 33. Three gages measure the horizontal strain of the backrest during loading, and the remaining three gages measure the vertical strain. In the case of the horizontal gages the sensors elongate during seatback loading, while the vertical gages undergo compression. Each sensor completes a wheatstone bridge and the signal goes through an adjustable amplifier in the electronics box.

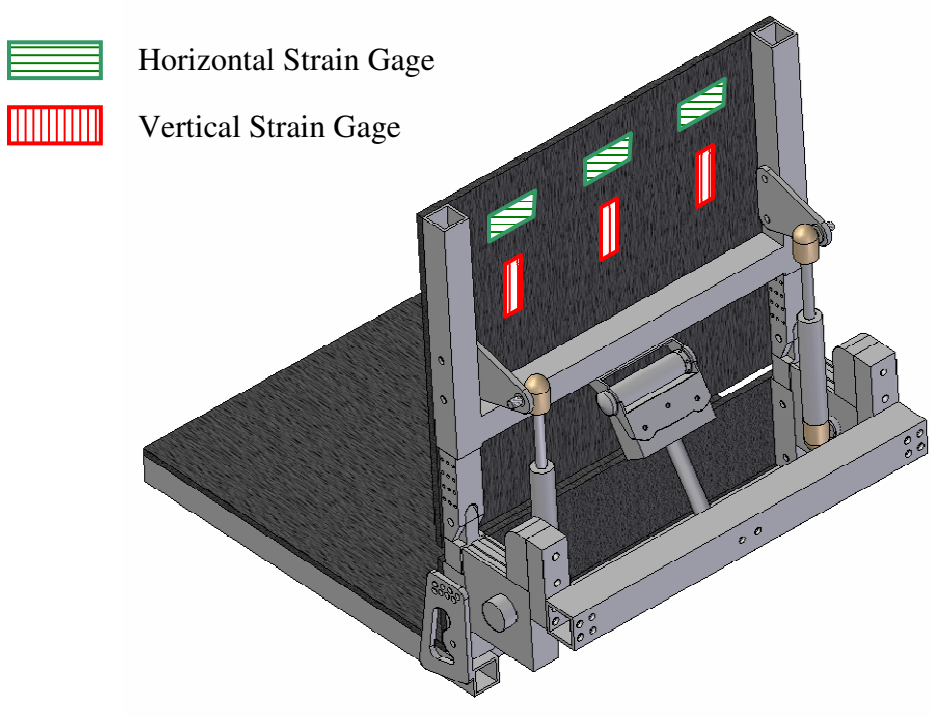

Figure 33: Isometric view of DHSS seat with seatback Strain Gages shown

The six channel box is also used to power a commercial force-plate, and thus obtains an accurate, pre-calibrated and amplified signal from the footrest. While it is difficult to calibrate the seatback strain gage signals to obtain a resulting seatback force, the footrest forceplate reading is easily converted into an equivalent load. For this reason

the forceplate signal is regarded as a more reliable singlal, while the seatback readings are used primarily to identify and verify trends in seatback loading.

All of the signals are transferred to a National Instruments (NI) contoller board that uses A/D converters to record the data. The electronics box was designed and manufactured in-house.

3.1.3.3 Seatback Rigidizer Feedback Control Algorithm

The NI board is also used to output a control signal that operates the seatback rigidizer, as previously described in section 3.1.2.4. The controller logic, shown in Figure 34, has two modes of operation that can be manually selected by the user. Three amplified strain gage signals from the backrest are used for feedback to the on-off controller. These signals are either differentiated to obtain a net change in seatback strain, or summed to measure the overall strain on the back depending on the controller mode of operation. The resulting value is compared against a modifiable threshold. If the threshold is exceeded, then an I/O port activates the solid-state relay switch for a tenth

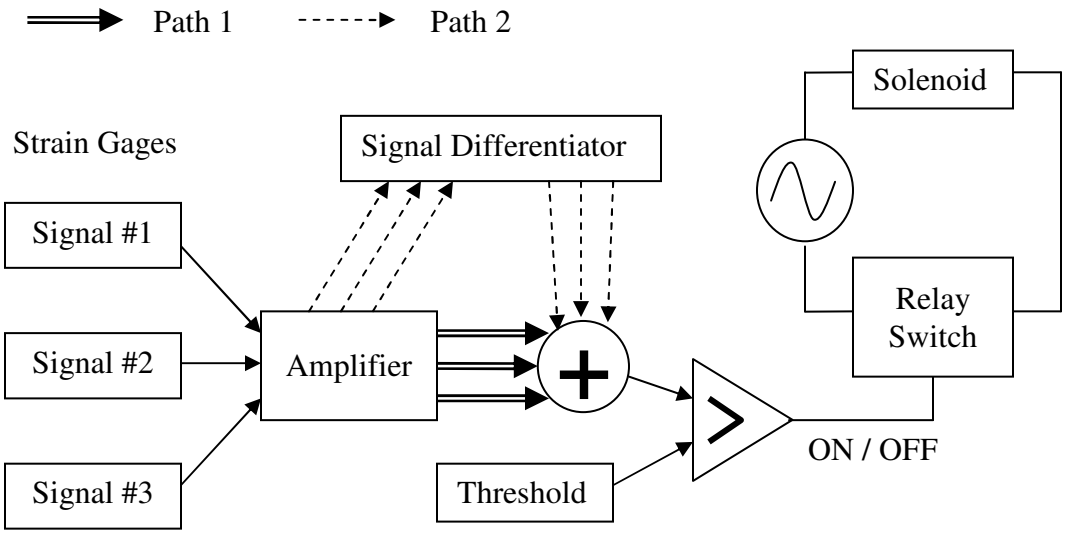

Figure 34: Seatback Rigidizer control system schematic

of a second, in turn firing the high-powered solenoid. When the solenoid fires the rigidizer bar is dislodged and the seatback can rotate backwards, as previously described.

Once the solenoid has fired, an ON command cannot be issued again for a pre-specified period of time, such that the 10% duty cycle limit of the solenoid is not exceeded. Increasing the solenoid reactivation time also ensures the occupant is not exposed to unnecessary impact noise generated whenever the solenoid is turned ON. A more advanced solenoid reactivation algorithm could also be implemented. Such an approach would call for the solenoid to become operational only after the seatback strain has fallen bellow an acceptable threshold, thus ensuring the seatback has returned to an upright position prior to reactivation.

The strain derivative controller mode is desirable when the speeds of a controlled and uncontrolled occupant thrust are different, while the strain magnitude controller mode is preferred if the distinguishing factor between the two types of thrusts is the intensity of the thrust more so than the rate of the thrusts.

3.1.3.4 Software and Hardware Implementation

Control of the NI Board used in this study is achieved through the use of a Labview program. A schematic of the program is shown in Figure 35. The sampling rate, operational mode, triggering thresholds, and output methods are easily modifiable through a GUI, shown in Figure 36. A/D and I/O port control is implemented with build-in software protocols. The principal program block operates in a conditional while loop that can also be controlled through the GUI. Finally, Data processing and Boolean operations are achieved through the use of built-in function blocks.

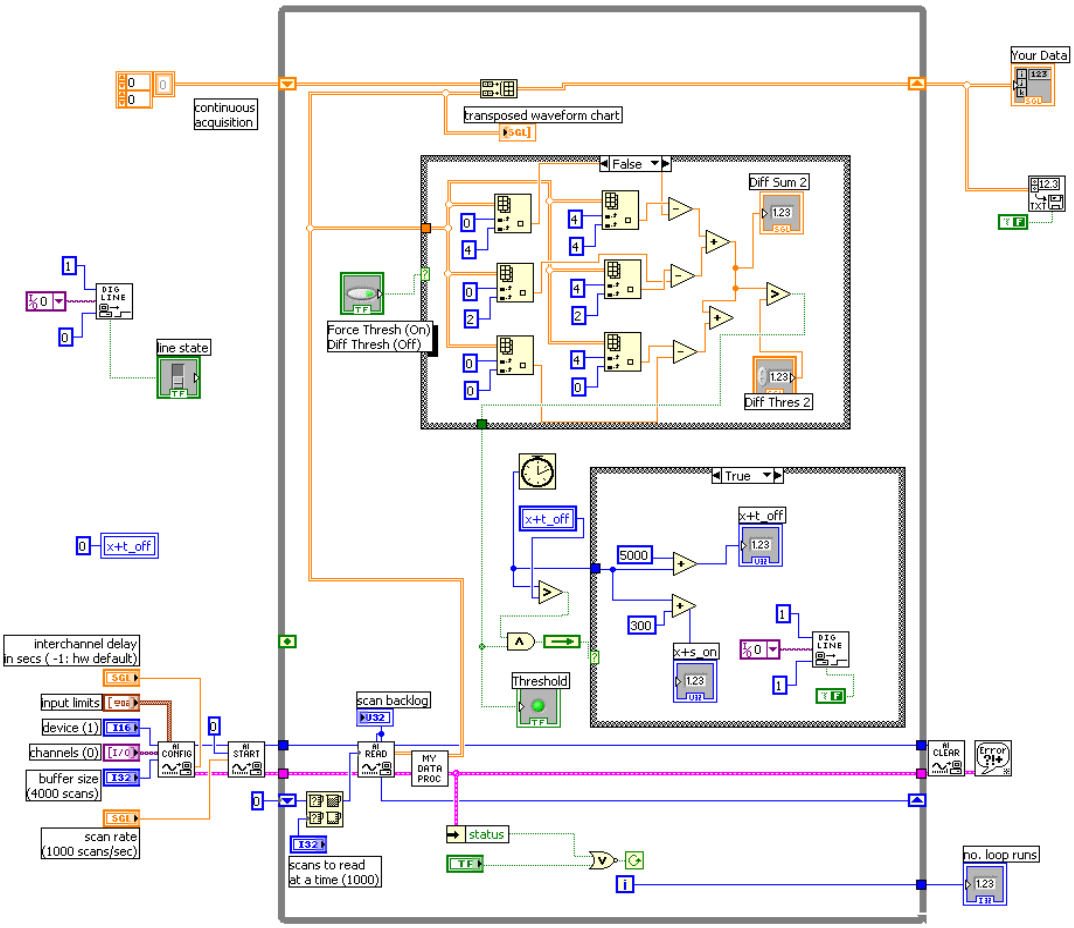

Figure 35: Labview block diagram of DHSS contoller

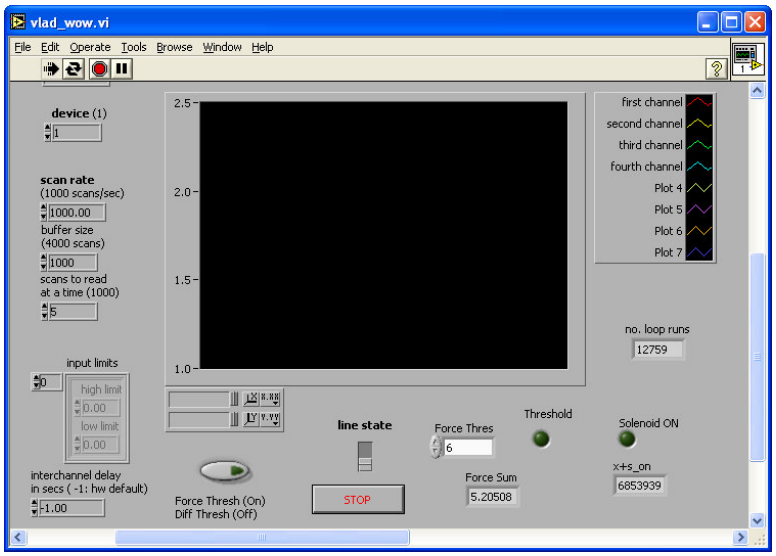

Figure 36: Graphical User Interface of DHSS controller

3.2 Computational Modeling of Dynamic Seating System

The previous chapter provided important insights into extensor thrust behavior. It should be possible to use the torque profiles obtained in the rigid chair simulation to predict the thrust response of a dynamic seating system. This possibility is investigated later in this section. Alternatively, a specified occupant motion can be used to calculate the resulting simulated contact forces between the seating system and the occupant. By simulating the extensor thrust one can avoid the costly implementation of multiple hardware systems for evaluation, as well as prevent potential injury or distress to the subject who would otherwise have to undergo multiple thrusts in unproven experimental systems.

The drawback to an analytical modeling method becomes apparent from the previously presented research in Chapter 2. The mathematical rigor involved in the dynamic modeling is clear, even though the rigid seat modeled is primitive and it only approximates a relatively simple motion. If a simulation-based design approach is to be implemented successfully for dynamic seating systems, then it is necessary to address the issue of modeling complexity. Developing the mathematical models for such complex systems "by hand" would be highly impractical due to large development times and high vulnerability to modeling errors.

Therefore, for the remainder of this thesis a commercially available dynamic modeling package will be used to enable added modeling complexity that can more closely resemble real-life conditions. A MacNeal-Schwendler Corporation (MSC) software package called Working Model 2D was chosen for the simplicity, reliability and interfacing options that it provides.

3.2.1 Working Model Simulation Overview

Working Model 2D is an established dynamics modeling software package that has been used with great success by engineers in industry and academia alike. Creating a model with the package is a matter of drawing the geometries of the rigid bodies in the simulation window, and then mating them with the various joint options provided by the software. Working Model allows the user to set all of the simulation parameters such as the masses of the rigid bodies, the inputs and outputs, the numerical integration scheme, and external application interfaces. These options are easily accessible through well defined GUI windows, as shown in Figure 37.

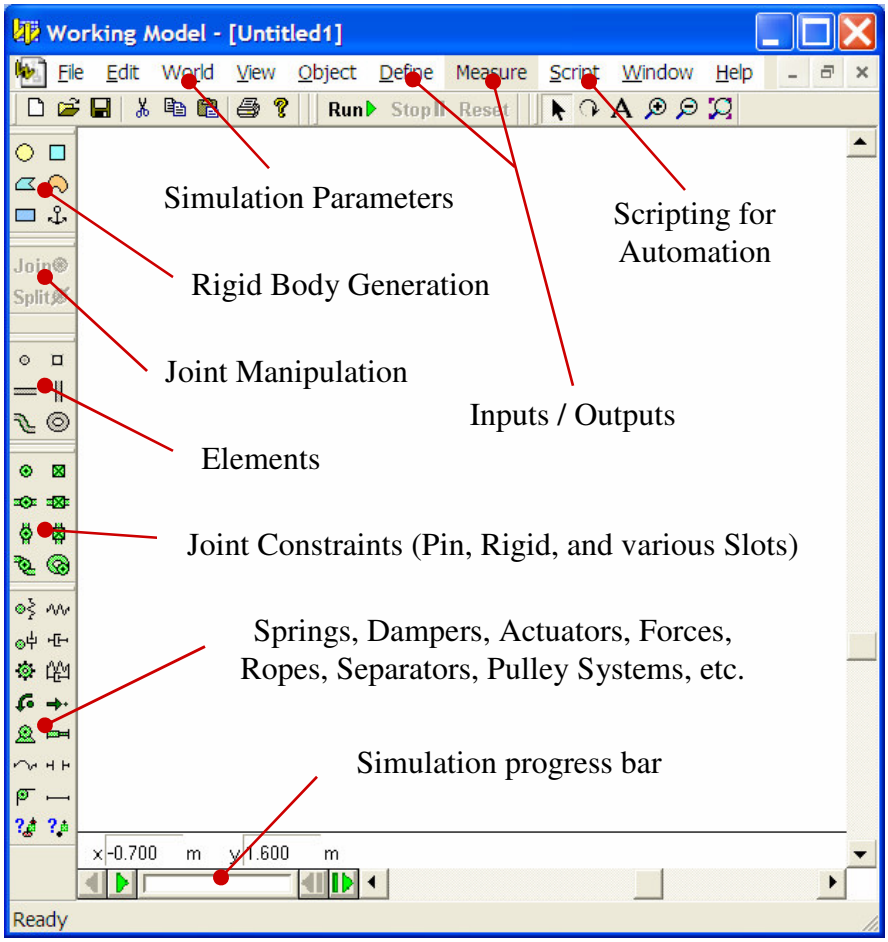

Figure 37: Sample WM2D screenshot detailing GUI functionality

In this thesis the use of Working Model serves three design objectives. The first goal is to visually demonstrate various seating concepts and ensure that the desired seating system and occupant motions are feasible. The second purpose of the model is to test critical subsystem components through rigorous simulation, ensuring their specifications will meet design objectives prior to investing time and money into constructing prototypes. A final, more ambitious goal is to be able to drive design decisions of a proposed system through proper interpretation of simulation results.

For the DHSS model used in this section, all of the critical body and seating system parameters are measured and reflected in the simulation. The complete model schematic illustrating key features is shown in Figure 38. This model captures the geometry of the

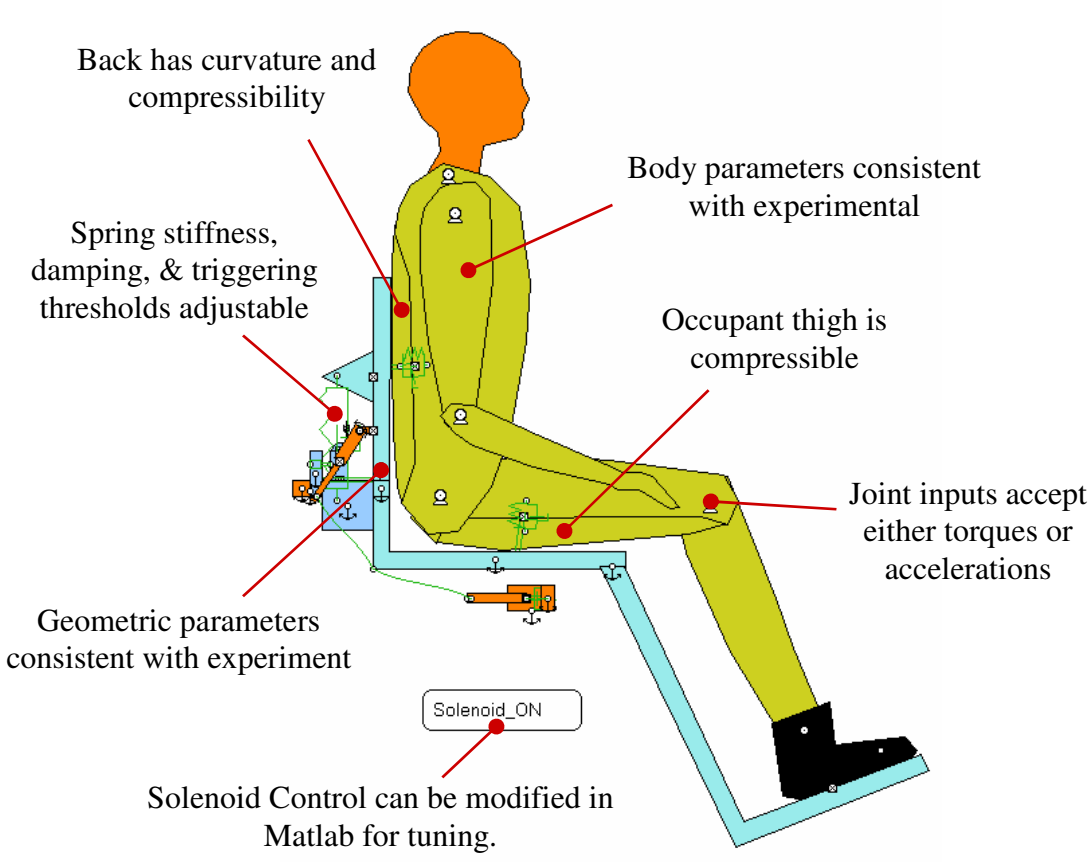

Figure 38: DHSS WM2D simulation model schematic

problem much better than the wireframe model used in Chaper 2, and therefore presents a more accurate representation of the real-life thrust event. By using motors for the ankle, knee and hip joints of the occupant, the input to each joint can be provided as either an angular acceleration or a torque. This allows the user to pick either a forward or an inverse dynamics simulation approach.

While an improvement over the analytic wireframe model, this numerical model is still limited by the rigid-body assumption that prevents it form considering the compressibility of the human body. This limitation is reduced by modeling the thigh and torso of the occupant as two distinct rigid bodies for each of the mentioned human segments. The bottom of the thigh and the back of the occupant are constrained with keyed slot joints such that they can only move in the normal direction to the thigh and torso, respectively. These pairs are then connected with spring dampers that are tuned to mimic realistic human parameters. This important feature allows for a gradual transition in forces and torques when using an inverse dynamics approach to obtain the states of the system. Some of the more subtle tissue compressibility issues, such as variable stiffness over the contact region or nonlinear spring and damping behavior cannot be captured by this model.

The increased modeling complexity, while necessary to accurately capture an extensor thrust, comes at a price. As more bodies and constraints are added to the model, the state matrix becomes very large and complex, and more susceptible to singularities. This becomes a serious problem for the simulation, which in turn demands a lot more processing power and can produce erroneous, noisy results and even modeling instability. Working Model does not provide any insight into the equations it uses to perform time-

marching operations, and it is thus very difficult to determine which parameters or constraints must be altered to improve the simulation speed and accuracy. Therefore, dealing with numerical errors is challenging, and was done by trial and error.

An automation scheme was implemented to improve simulation efficiency and provide a platform that can be used to rapidly study multiple seating system parameters. Working Model 2D can be controlled through a programming language called WMBASIC, which is a variant of the more common BASIC language. A WMBASIC script was written to evoke Working Model commands and to control external applications via a Dynamic Data Exchange (DDE) protocol. The software, however, is not capable of receiving WMBASIC commands from external applications. To overcome this limitation, a core WMBASIC script was written to summon a Matlab program, both shown in Appendix D, to perform all of the necessary calculations and decide what commands must be issued. This Matlab program is able to generate a sequence of WMBASIC commands at predetermined instances. The resulting command sequence is fed back to Working Model, which then proceeds to execute the sequence as if it was part of the original script. This script enables Working Model to be controlled by external applications; a functionality that is not supported by MSC, and enhances Working Model capabilities.

3.2.2 Investigation of Seatback Rigidizer

The seatback rigidizer mechanism is dependent on a high-force solenoid to function properly. After completing the concept design of the subsystem, sizing the solenoid was of particular importance. Multiple considerations such as operating voltage, stroke length, duty cycle and price went into choosing the optimal solenoid for this mechanism;

however the most critical parameter considered was pull force. Working Model was used to determine which solenoids had an acceptable pull force by creating a detailed model of the mechanism and providing worst-case scenario initial conditions, as shown in Figure 39. The force on the top of the seatback was set to 200 lbs and the friction coefficient between the rigidizer bar and L-stop was set purposely high at 0.5. An ON pulse was simulated during which the solenoid was activated for 0.1 seconds with the intent to see whether the burst would be sufficient to pry the rigidizer bar out of the L-stop. Commercially available solenoids with 5, 10, 20 and 50 lbs of pull-force were simulated. The solenoid with 50 lbs of pull was found to be acceptable, while others with 20 lbs of pull or less did not succeed in removing the bar and were thus deemed to be too weak. The 50 lbs version was selected and worked well in the experimental system.

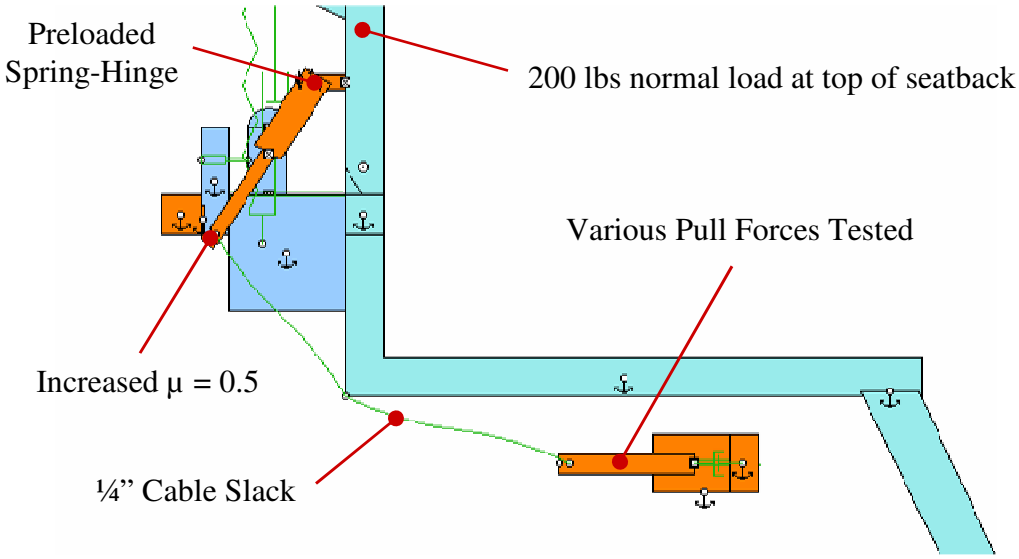

Figure 39: Seatback Rigidizer Simulation Model

The technique used to size the solenoid can also be used in evaluating other dynamic seating system components. The preloaded rotational-spring hinge used to reposition the rigidizer bar into the L-Stop is another example where the simulation model could be used to ensure the spring coefficient is acceptable.

3.2.3 Investigation of Dynamic Seatback and Model Validation

The most challenging aspect of simulating the complete dynamic system under consideration is modeling and simulating the occupant. Consequently, there are several approaches that can be taken to simulate an extensor thrust. One method that could be used is a traditional forward dynamics approach where torque inputs are prescribed to the human body joints. Another approach is estimating the expected motion of the body and extracting the resulting forces and torques with an inverse dynamics approach similar to that used in Chapter 2. Finally, it is also possible to drive occupant position by implementing a feedback controller that adjusts the joint torques such that they track prescribed angular accelerations. These angular accelerations must be appropriately selected such as those based on experimental measurements.

It is reasonable to presume that once torque profiles are obtained for an emulated or an actual extensor thrust, these computed profiles would provide a good approximation for any torque profile that the same individual may undergo during a typical extensor thrust. It can be further assumed that by using a good approximation of the torque profiles of a thrust as joint inputs to a seating system model, a simulated response would also be accurate. Unfortunately, the results obtained from the working model simulation indicate otherwise. By slightly modifying the geometry of the model and using previously obtained torque profiles to drive the body joints, the modeled occupant response can fail to lift off the seat, or may even go unstable. There are two primary reasons that have been identified as causes for this sensitivity.

The first explanation comes from observing that high-tone extensor thrusts have a significant feedback component that can amplify or attenuate thrust intensity and

duration, depending largely on the conditions under which the thrust is triggered and progresses. Some caregivers argue that the body configuration in which a thrust occurs, as well as the external loads acting on the occupant are some of the most critical factors that determine the intensity of an extensor thrust. These parameters will vary significantly between different seating systems, and even within seating systems that are tuned differently. At best, it may be possible to obtain a statistical torque distribution that varies from occupant to occupant.

In simulation, however, the previous explanation does not completely address the discrepancies observed between simulations with very similar conditions. For slower extensor thrust events it turns out that the motion can be modeled with a quasi-static approximation, meaning that the dynamic effects can be effectively ignored. This means that during a thrust, at any given time, the computed torque combination for that time is essentially keeping the body in static equilibrium. The delicate balance can be offset by even a small deviation in one of the joint torques. A small deviation at the beginning of the move will compound over the course of the move, and as the difference between the expected and actual position of the body begin to deviate, so do the expected and actual angular accelerations of the joints. This explanation accounts for the majority of the observed differences between similar simulations. For this model it turns out that the maximum torques are achieved when the thigh separates from the seat bottom. If the simulated occupant configuration is not almost identical at separation, the simulation results will deviate dramatically from the desired motion profiles.

Using an inverse dynamics approach in place of a forward dynamics simulation continues to be a more effective method to obtain the external forces acting on the

occupant throughout a thrust. This requires only predetermined desired motion profiles for different seats, which should already be considered in the development of a dynamic seating system design. Consequently, the inverse dynamics approach will be used for simulations for the remainder of this thesis.

To ensure that the model is acceptable, and can therefore be used for predictive simulations, a model validation procedure is employed. By comparing the predicted and measured footrest forces in the rigid seat, the simulation model can be validated. This technique provides good correlation with experimental results, as shown in Figure 40.

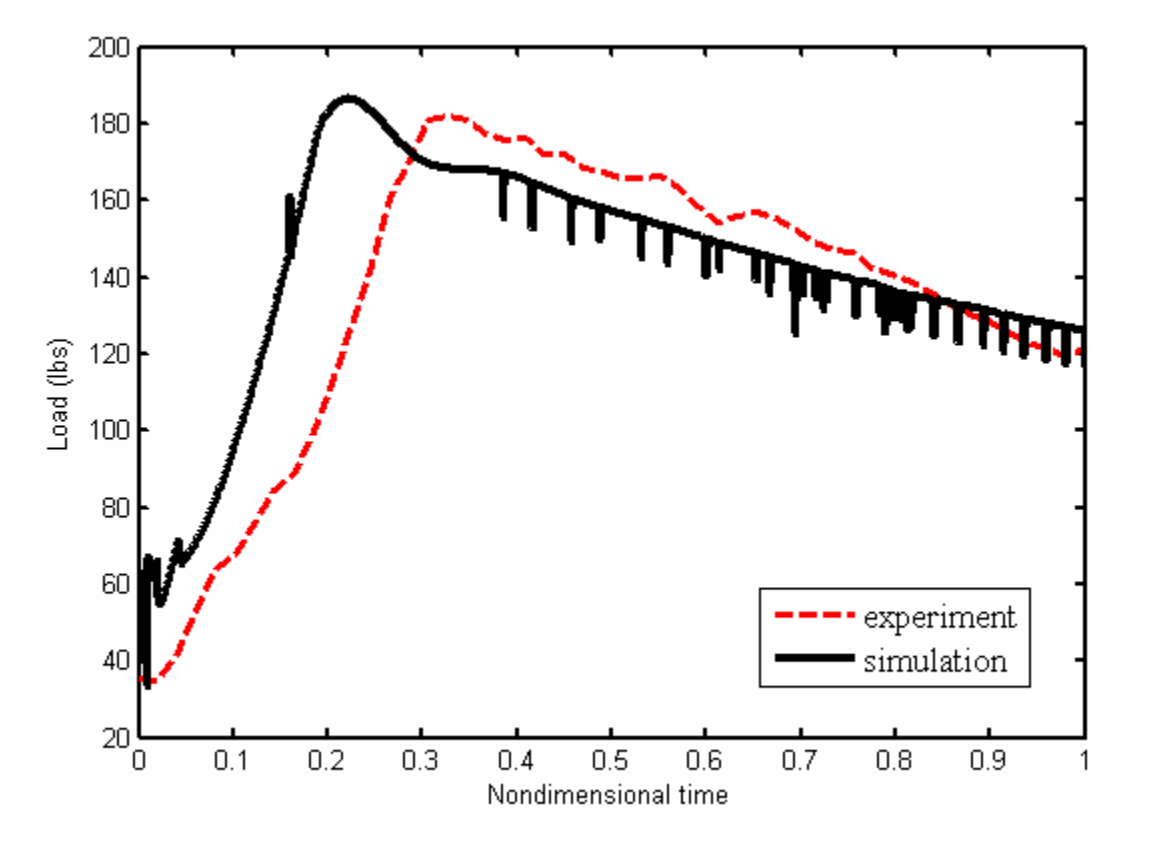

Figure 40: Simulated and experimental footrest force profiles

The simulated response begins to exhibit an "icicle" effect that is clearly noticeable starting after approximately one third of the thrust is completed. This effect, caused by

numerical errors, is extremely difficult to minimize and slows down the simulation dramatically. The simulation response shown was obtained only after extensive manipulation of the simulation and model parameters. While the model validation demonstrates that the model captures the main characteristics of an extensor thrust, it also reveals the main weakness of numerical modeling. Specifically, as model complexity increases, the simulation becomes more susceptible to numerical errors. For this reason it is not feasible to use numerical simulation with this model to personalize seating systems for individual occupants, as originally proposed.

The model can be used, however, to predict the overall improvement achieved between a rigid and a dynamic seat, as shown in Figure 41. The simulation correctly

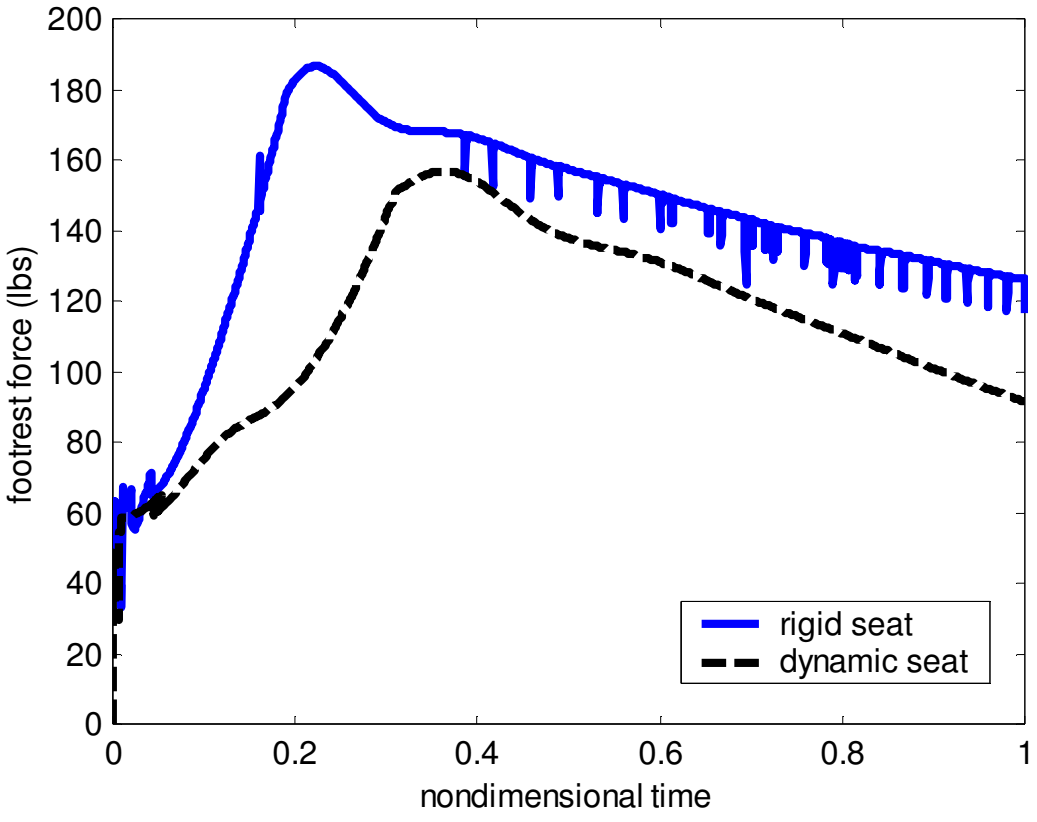

Figure 41: Simulated extensor thrust in a rigid and a dynamic seat

predicts that the peak footrest force will be smaller, and will come later in the extensor thrust. Also, the simulation results indicate that the dynamic seat reduces the forces acting on the footrest throughout the entire thrust, including the end of the thrust where a drop of almost 35 lbs is predicted. In an effort to better understand the relationship between the maximum seatback deflection of the DHSS and the footrest force that is expected at the end of a thrust, a simpler simulation is created. This simulation does not consider compressible occupant body parts, and assumes the occupant has reached the end of the thrust. In this configuration, the occupant is placed on the seatback while the seatback angle is varied between zero and fifty degrees. The resulting footrest force is shown in Figure 42. While this model predicts slightly lower final footrest forces than the compressible model, the estimated 16 lbs force drop between a rigid seat and one that pivots 45º corresponds very well with the observed experimental results that follow. This result indicates that occupant and system alike would undergo less stress in a DHSS.

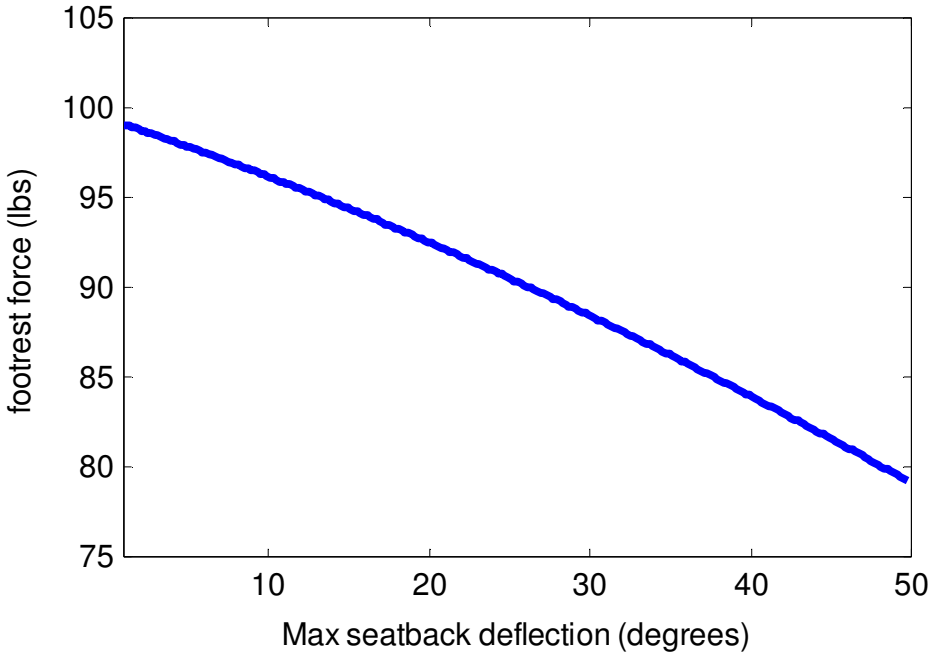

Figure 42: Footrest force at the end of a thrust as a function of seatback deflection

3.3 Experimental Results

The previous section established a number of important trends which indicate that a Dynamic-Hingeback Seating System can improve conditions during an extensor thrust. To gain more confidence in these trends it is necessary to test the validity of the simulation model that was used to obtain them. Multiple extensor thrust experiments were performed with a human subject, where the maximum deflection angle of the seatback was varied from a completely rigid seat to a case with 45º of maximum deflection. These tests were accomplished by adjusting the deflection-limiting hardstop, as shown in Figure 43. Representative motions of the occupant body segments are shown in Figure 44 for similar thrusts that occurred in a rigid and flexible seating system. The results with the flexible seatback are for the case when the maximum seatback angle was set to 45º. Note that the thigh rotates significantly more in a rigid seat. Also, note that a dynamic seat is effective at stabilizing the torso faster. By looking at the various strain gage signals shown in Figure 45, it is possible to observe some of the advantages of a dynamic seatback. Specifically, a reduction of forces and strains is noticeable. A more detailed analysis of these trends will follow later in the section.

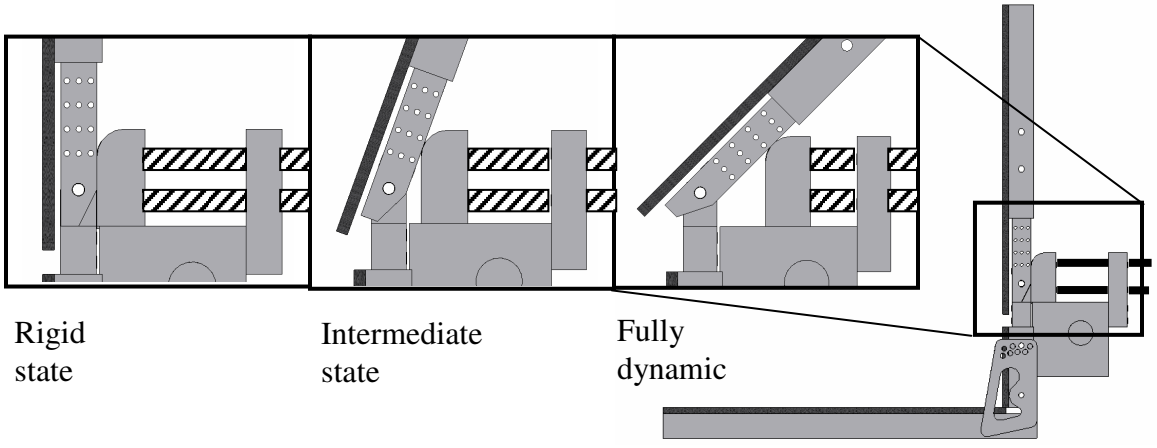

Figure 43: Variability of eflection-limiting hardstop mechanism

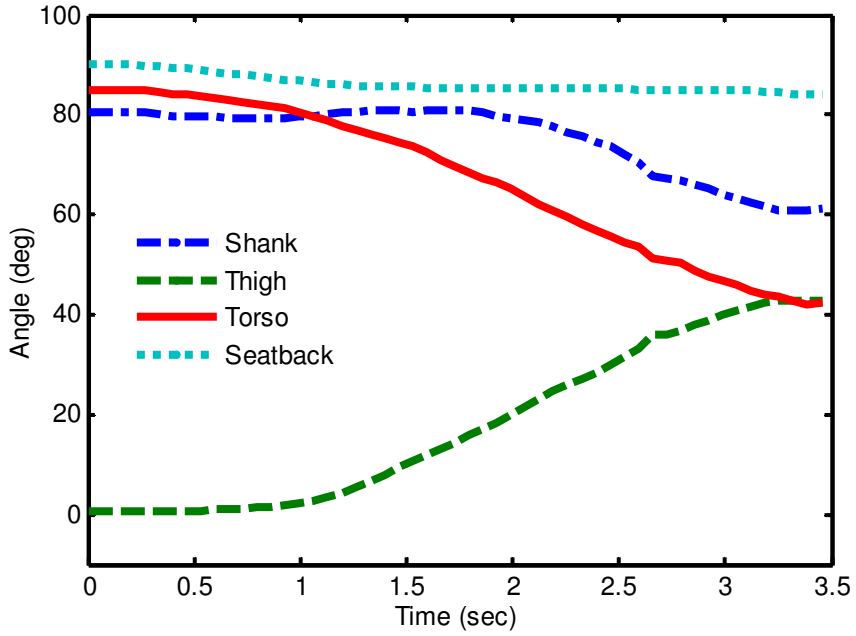

a) Rigid Seat

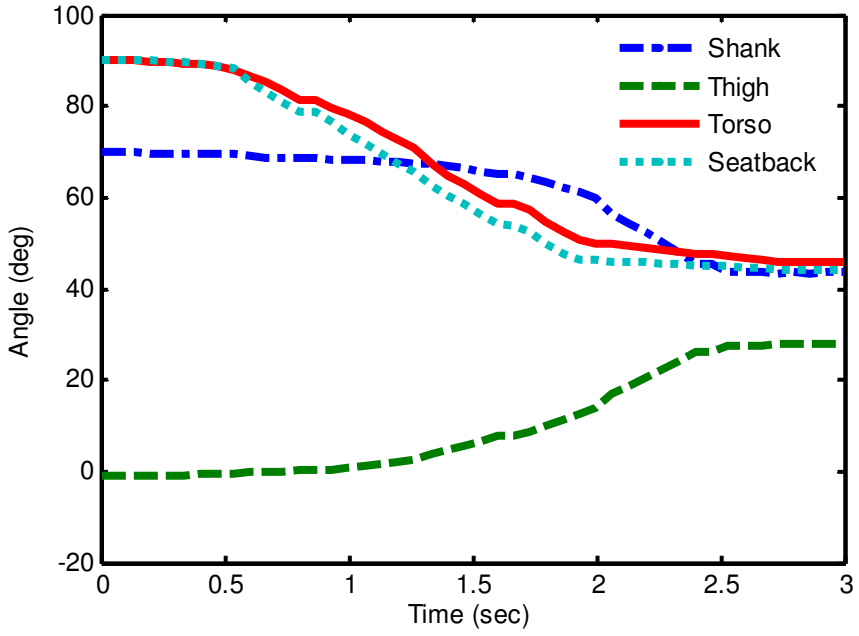

b) Dynamic Seat

Figure 44: Angles of body segments and seatback with horizontal axis during a typical thrust in an a) rigid and b) dynamic seat

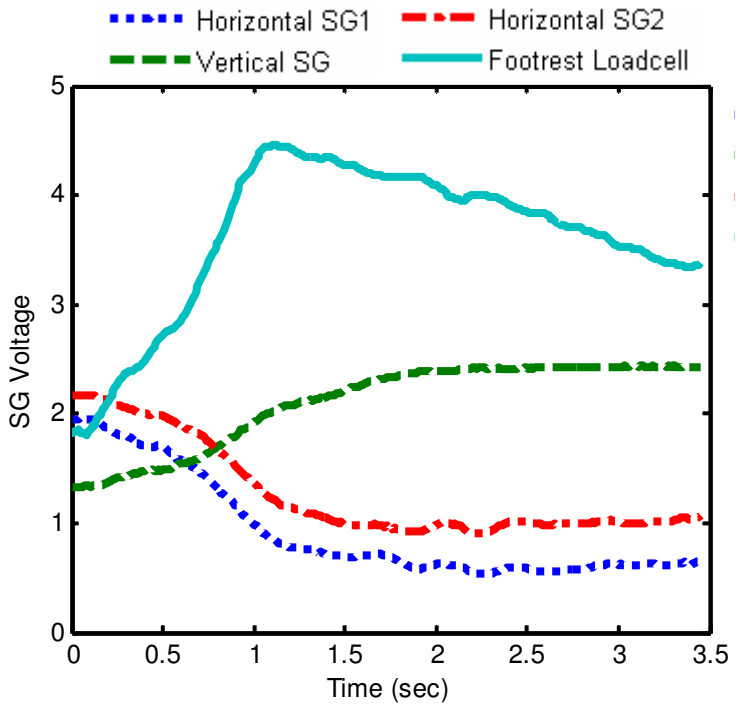

(a) Rigid Seat

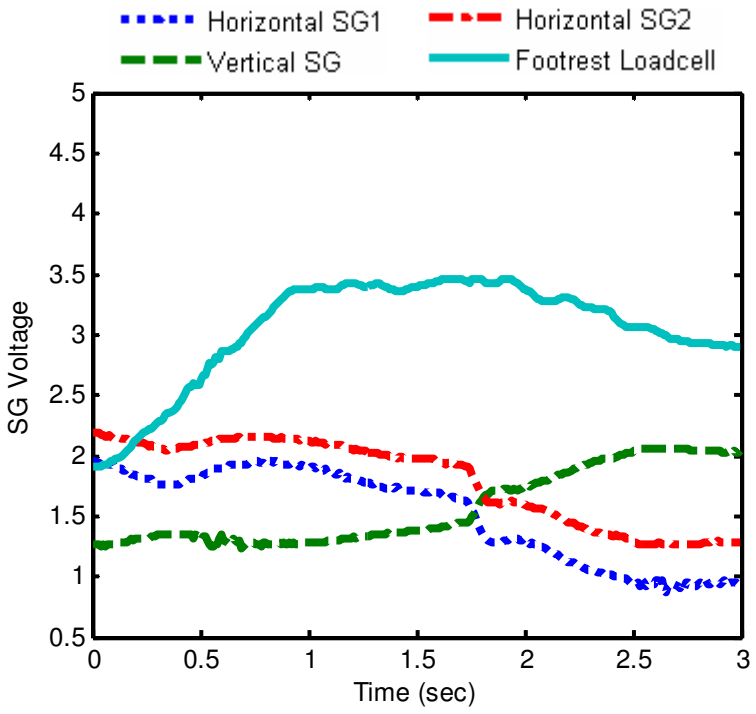

(b) Dynamic Seat

Figure 45: Seatback Strain Gage signals and uncalibrated forceplate signal during a typical thrust in an a) rigid and b) dynamic seat

Figure 46 shows the observed distances between tracking markers on the human subject and seatback as a function of time. This data provides an excellent experiment validation tool. First, notice that the distance between the pivot point of the seatback and the tracking marker placed on the seatback remains relatively constant. This angle varies by at most three percent within all of the experiments performed, indicating that the seatback is observed to be rigid, and therefore that the manual coordinate selection of the pivot point is acceptable. Additionally, a very steady thigh length throughout both experiments indicates that the tracking markers placed on the hip and knee joints were located very close to the anatomical hinge points.

The manual selection of the ankle pivot point appears to be more difficult, as can be deduced from the moderate variability in calf length for both experiments. The most significant change, however, can be observed in the lengthening of the torso. This observation can be attributed to the core differences between the leg and the spine. Each segment of the leg has one primary load-bearing bone that is rigid, whereas the spine is inherently flexible, both axially and in bending. This flexibility can account for some observed elongation of the torso, which is primarily a product of posture change. The torso experiences significantly more elongation during a thrust in the dynamic seatback, indicating a possible reduction of compressive forces acting on the spine, which leads to improved occupant posture.

A thorough investigation of multiple human and system parameters of interest (forces, orientations, etc) was performed to obtain a better understanding of particular trends relating to maximum seatback deflection, and the impact those trends may have on the DHSS system and occupant.

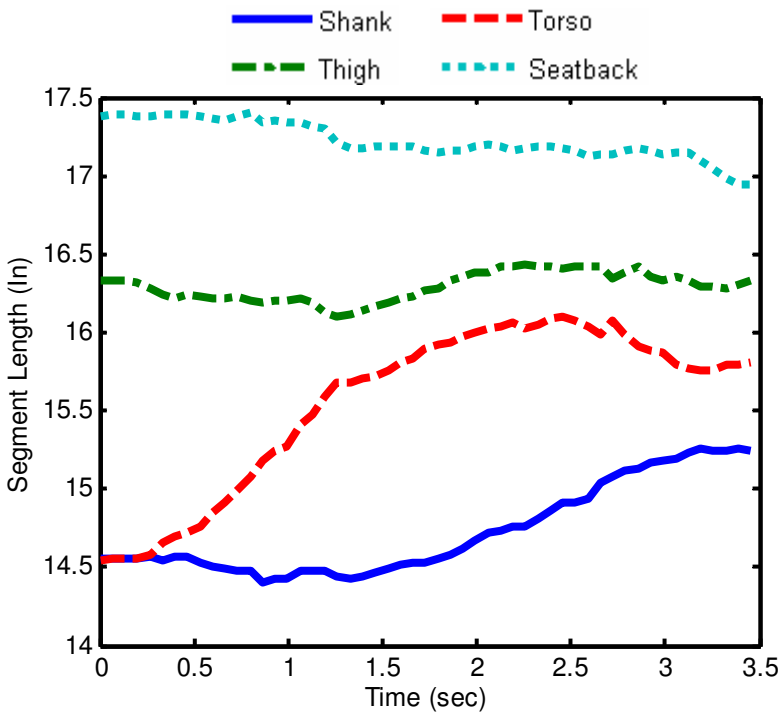

a) Rigid Seat

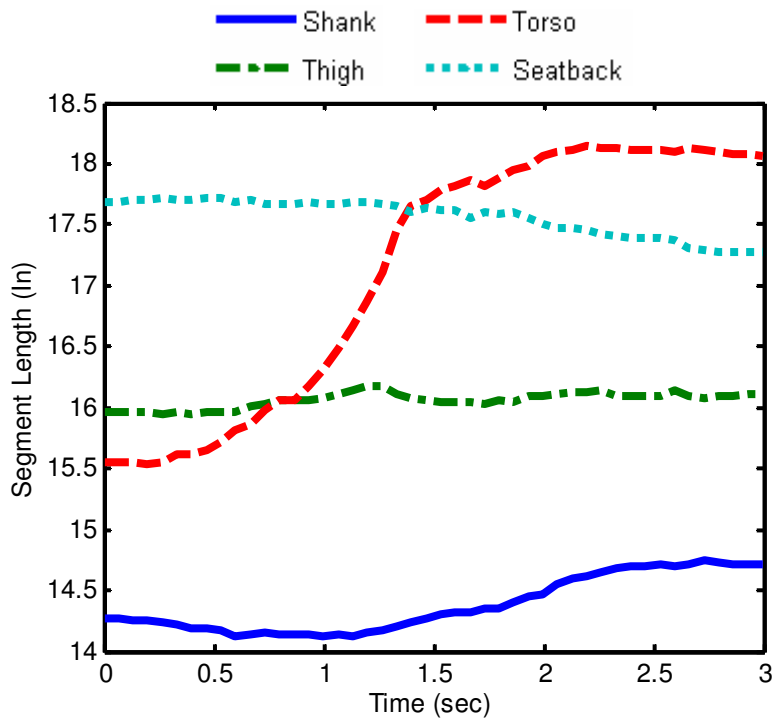

b) Dynamic Seat

Figure 46: Body segments and seatback lengths during a typical thrust in an a) rigid and b) dynamic seat

The first parameter to be examined is the lower leg orientation during an extensor thrust. It is desirable to understand how the added flexibility in the seatback affects the angle of the lower leg throughout the progression of the extensor thrust. To accomplish this comparison, the time vector for each of the experiments performed was nondimensionalized such that t = 0 represents the beginning of the thrust, and t=1 is the completion of the thrust. The angular profiles resulting from various maximum seatback deflection angles are shown in Figure 47. The subplot on the right of the figure shows the trends for the profiles on the left with varying maximum seatback deflection (θ_{back}). In most cases, the starting and ending values will correspond, and thus overlap, with the maximum and minimum value of each profile. This data shows that the addition of the

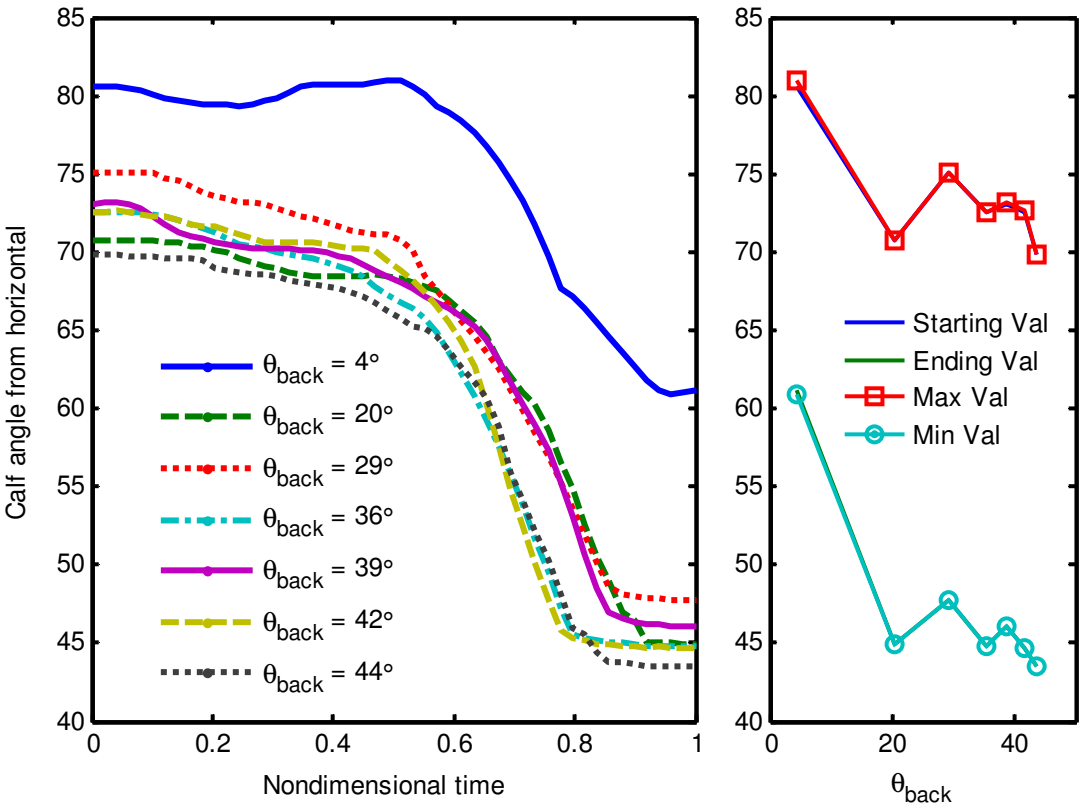

Figure 47: Calf angle measured relative to horizontal for various seatback deflection angles (left) and the corresponding trends (right)

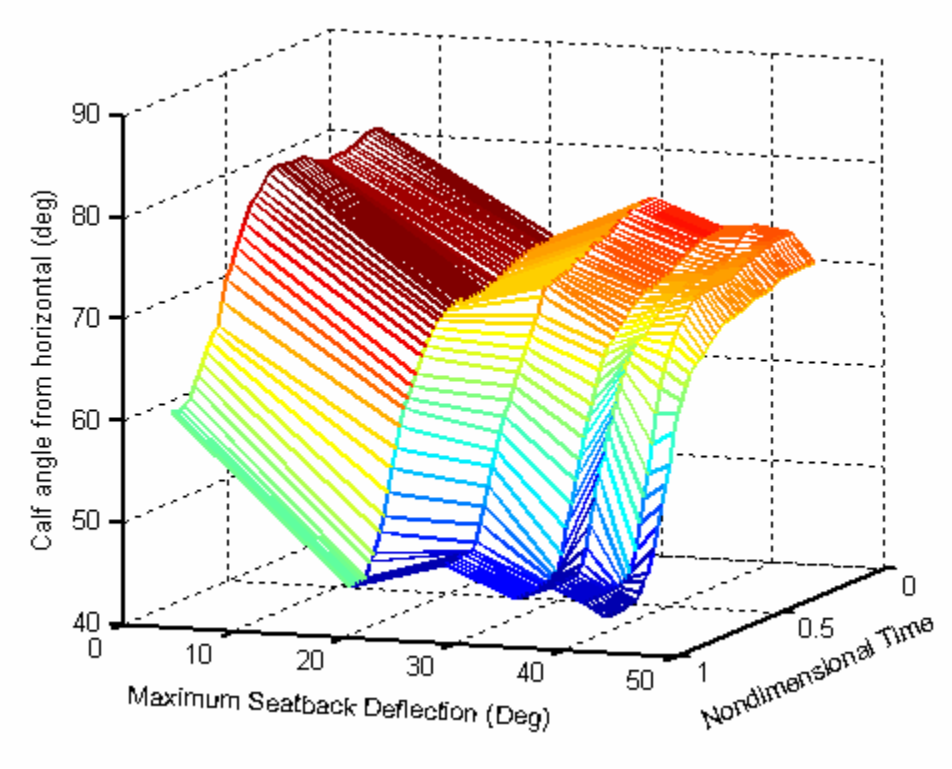

Figure 48: 3D plot showing calf angle trends

dynamic seatback has little impact on the calf angle during an extensor thrust. Note that the data ranging from $\theta_{back} = 20° \rightarrow 44°$ looks very similar. Initial conditions, however, are very important in determining the starting orientation of the calf. The line representing the rigid seatback ($\theta_{back} = 4°$) has a substantial offset to all of the other data sets. This offset is caused by inconsistent positioning of the feet on the forceplate during this experiment, and demonstrates the measurement sensitivity to initial conditions.

Figure 48 holds the same experimental information provided in Figure 47 in 3D form. This gives the added benefit of having a linear interpolation performed between the seven experimental data sets. This interpolation is useful for improving understanding of the trends presented in the corresponding 2D figure, as the experimental data is not obtained for evenly spaced maximum seatback deflection angles.

While the occupant calf motion is not greatly affected by a variable seatback rotation, the thigh segment experiences a stronger correlation with the maximum seatback deflection. This correlation can be seen in Figure 49. The starting angle of the thigh is consistently close to zero degrees for all seven experiments performed. Regardless of whether the occupant is seated in a slouched or upright configuration, the back of the occupants' thigh is firmly contacting the seat bottom due to the weight of the upper body. This provides very consistent initial conditions. When the extensor thrust commences, the thigh begins to accelerate until it has reached a critical nondimensionalized angular velocity of approximately $75°/t_{th}$, where t_{th} is the total thrust time. Once the body has fully extended, the thigh quickly decelerates to a stop. As the maximum seatback

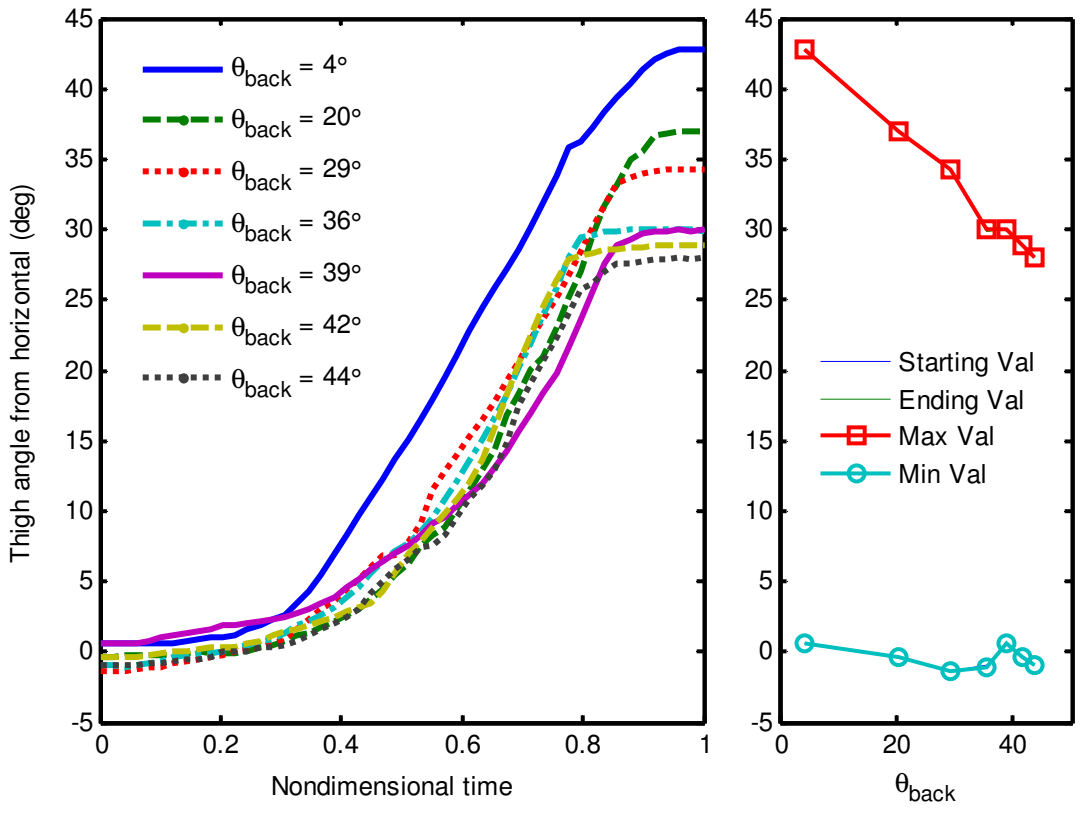

Figure 49: Thigh angle measured relative to horizontal for various seatback deflection angles (left) and the corresponding trends (right)

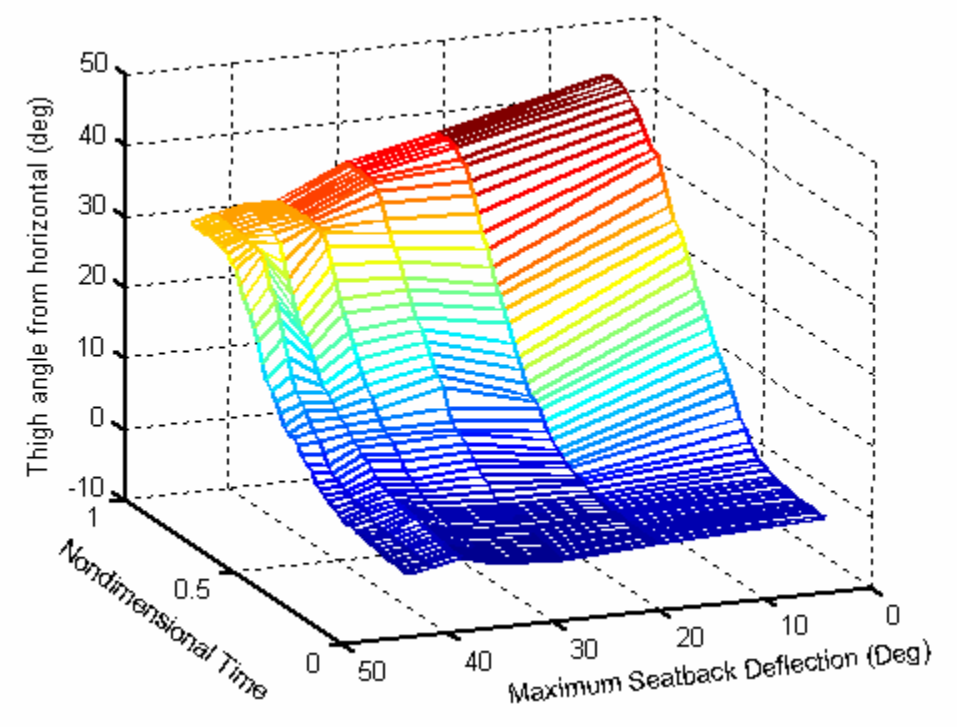

Figure 50: 3D plot showing thigh angle trends

deflection angle increases, the maximum thigh angle decreases at approximately 3/8 thigh degrees per seatback degrees. This decrease is a result of the thigh reaching its final orientation earlier in the thrust. The dynamic seat enables the upper body to rotate back without having to first slide up the seatback and then go backward over the top of the seatback. This translates into a lower hip height at the end of the extensor thrust, explaining the thigh trend which is also shown in Figure 50 in the 3D format. The plot reveals the overall trend where the thigh rotates more as the dynamic seatback is limited in its rotation.

The motion profiles of the occupant torso, shown Figure 51, have more variability between experiments than the thigh motion. Regardless of the maximum allowable seatback deflection, the torso rotates about forty degrees as the body of the occupant is straightening out. The rotation is not always smooth, and it is difficult to pinpoint the

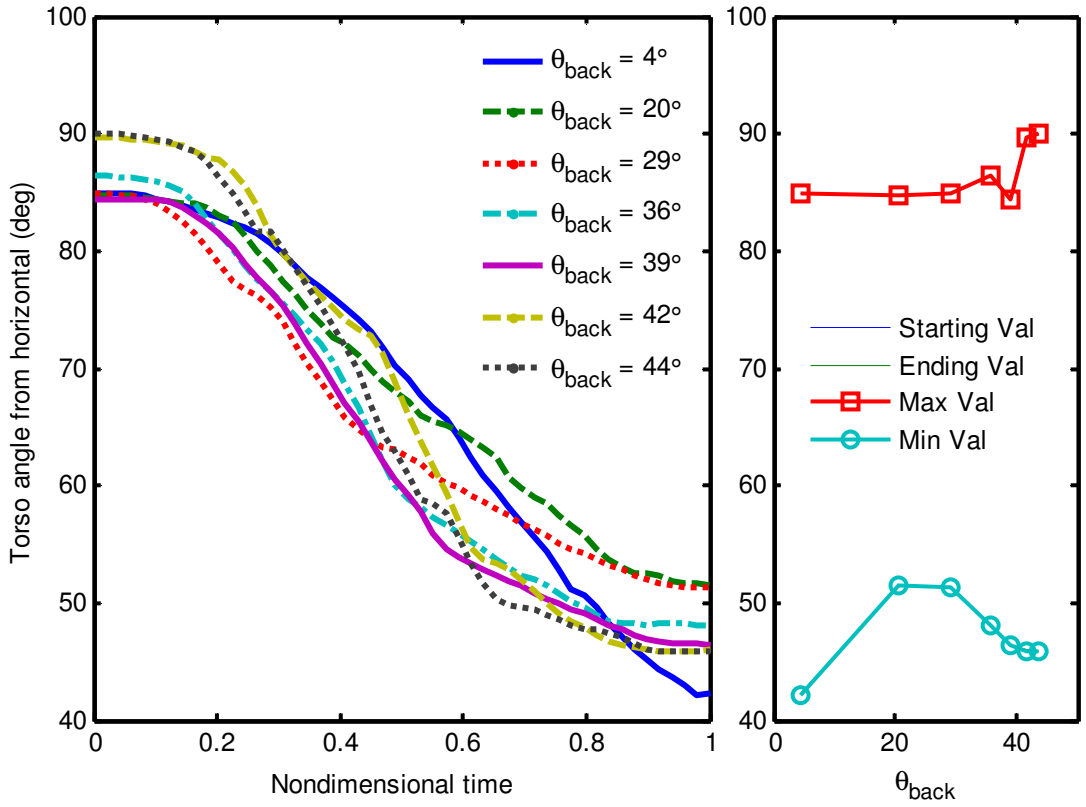

Figure 51: Torso angle measured relative to horizontal for various seatback deflection angles (left) and the corresponding trends (right)

source of the motion variation. One possible source is the presence of stiction occurring as the contact friction between the seat and seatback transitions between static and dynamic friction. Additionally, as the back contour of the occupant changes through the thrust, the motion profile of the torso is affected. Even though the posture of the occupant at the beginning of the thrust significantly affects the initial configuration of the torso, as well as the overall motion of this segment, it appears that seatback deflection does not have a big influence on these torso states. Initially the Studying Figure 52 further reinforces the notion that the torso, as observed in spatial coordinates, while apparently dependent on multiple parameters, is less dependent on maximum seatback

deflection. However, the difference between the maximum and minimum rotation values indicates that a dynamic seatback does lead to an increase in overall torso rotation. The reason this effect is not more pronounced is related to the big difference in thigh angles observed between a rigid and a flexible seat. Since the thigh does not lift as high off the seat bottom in a dynamic seat, the back of the occupant assumes a more parallel orientation relative to the seatback. For large deflection angles, however, the torso angle is expected to decrease more rapidly as the thigh is no longer able to compensate to cancel this effect. For a rigid seat configuration, the geometry of the problem caused the torso to rotate more than it did for a case with a moderate seatback deflection. In a rigid seat, the thigh rotates substantially, lifting the hip high enough to where the torso is able to pivot over the top of the seatback, as previously shown in Figure 32.

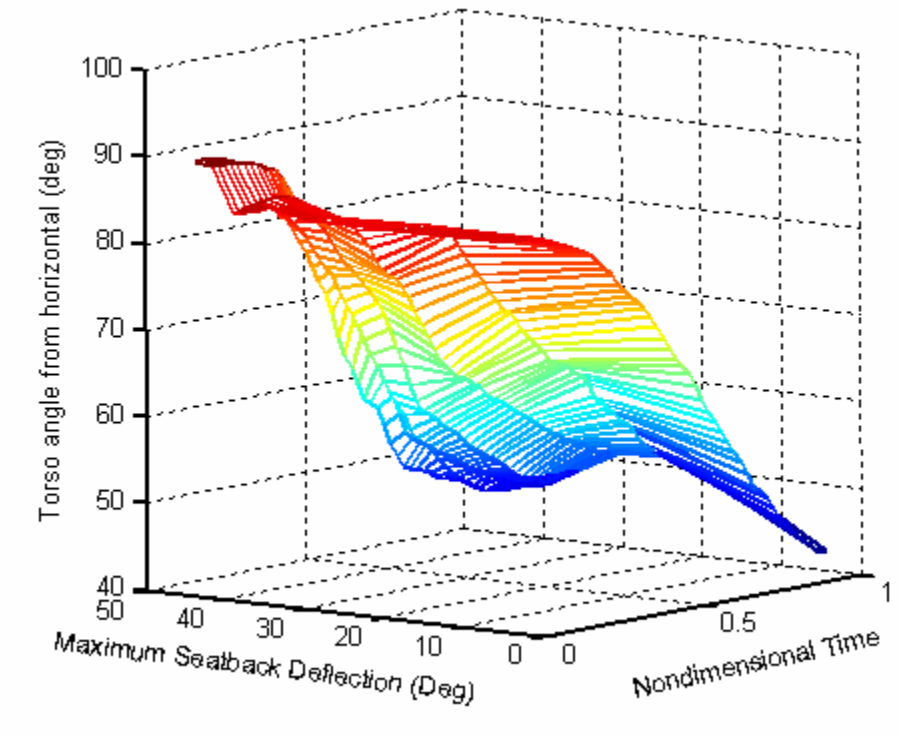

Figure 52: 3D plot showing torso angle trends

A close look at the seatback deflection profiles as a function of maximum seatback deflection is shown in Figure 53. Here, it is important to point out several noticeable trends. First, it should be observed that for all of the experiments the seat starts out at 90º, in an upright seatback configuration. At the beginning of the thrust, as the seatback is loaded it begins to deflect. Interestingly, the deflection rate is almost constant and consistent between experiments. For this experimental system the measured seatback deflection rate is approximately $100º/t_{th}$. Once the seatback makes contact with the adjustable hardstop it comes to a relatively abrupt stop. The experimental data, however, indicates that there is some ongoing deflection for some time after contact. This slight additional deflection is measured even after the seatback has ceased to move because the

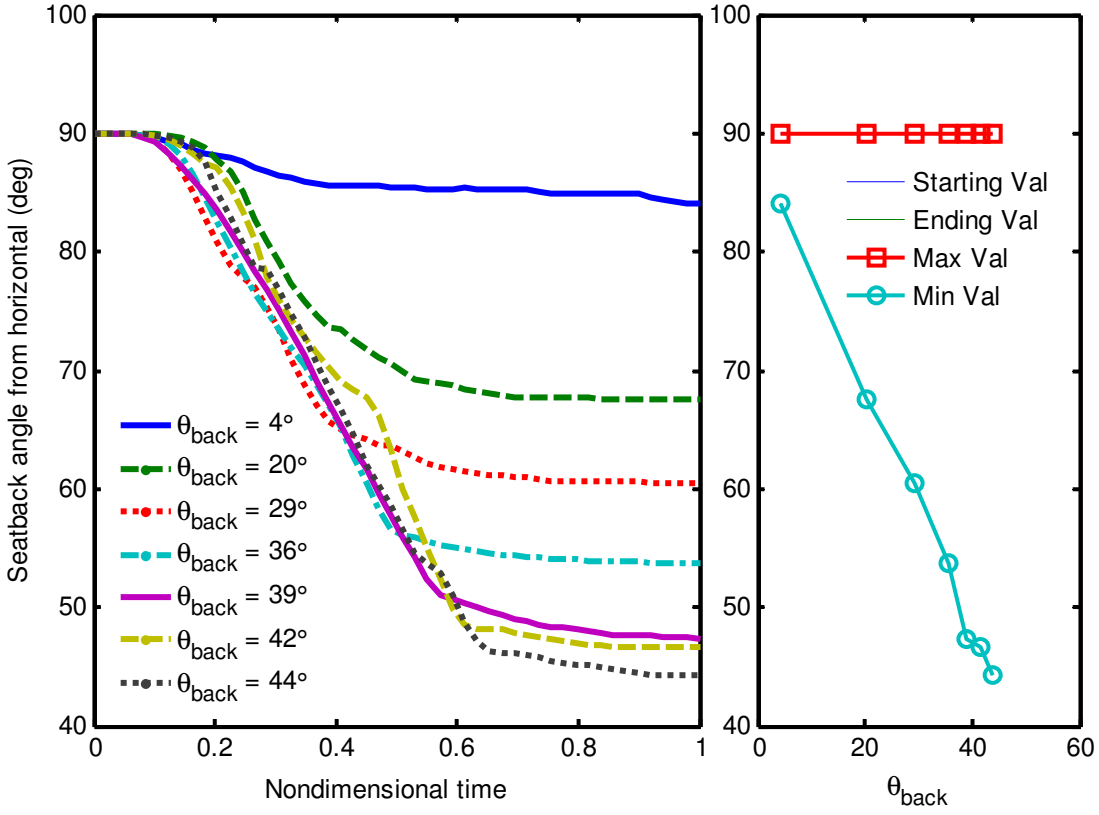

Figure 53: Seatback angle measured relative to horizontal for various seatback deflection angles (left) and the corresponding trends (right)

tracking marker itself is continuing to rotate relative to the chair as the occupant slides against a corner of the marker mount. Regardless, the data shows a very good correlation between the expected maximum deflection and the actual maximum deflection. A 3D view of the data, shown in Figure 54, reveals a crease in the surface topography representing the moment when the seatback hits the hardstop. This figure also indicates that, theoretically, if the seatback deflection was further increased, then the seatback would still hit the hardstop prior to the end of the extensor thrust.

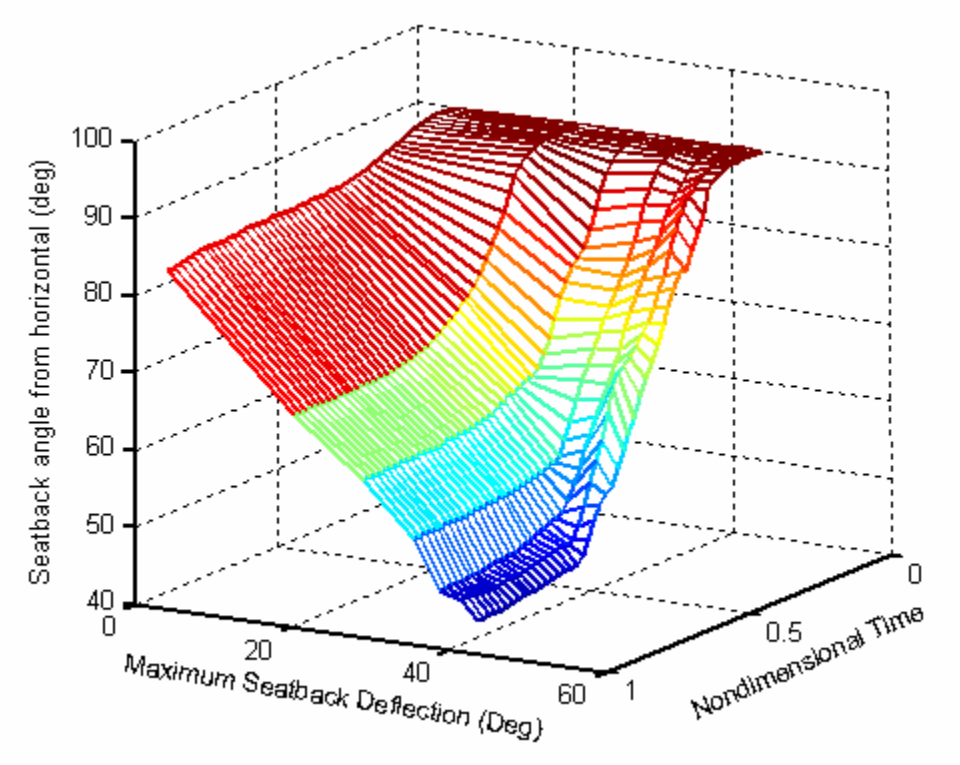

Figure 54: 3D plot showing seatback angle trends

The previous trends were described and accounted for to document the differences between extensor thrusts occurring in rigid and dynamic seating systems. The forceplate data at the footrest, however, also serves an additional purpose as a critical indicator demonstrating the improvement in thrust properties between a rigid and a dynamic seat.

Figure 55 shows forceplate readings for experiments performed with a range of maximum seatback deflection angles. The general time-profile trends are similar in shape, with the footrest being quickly loaded at the beginning of the thrust, a peak force being reached early on, and then a gradual reduction in normal footrest force being sustained during the remainder of the thrust. A comparison between the various thrusts shows that the initial load at the footrest was very consistent between tests, as it should have been for experiments with similar initial conditions. On the other hand, the presence of a dynamic seatback verifiably reduced both the peak and the final footrest forces. This progressive force reduction is an indicator that the occupant is exposed to weaker compressive loads during a thrust in a DHSS than in a rigid seat. Additionally,

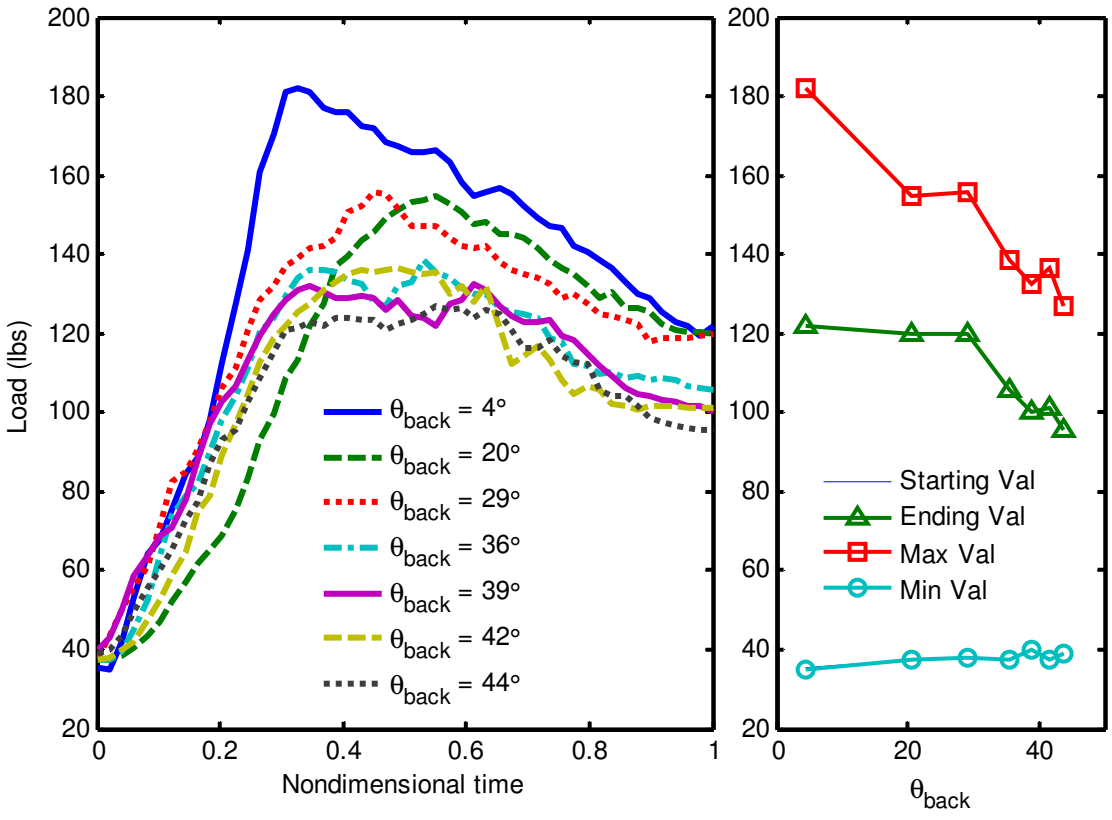

Figure 55: Foot-force progression for measured maximum seatback deflection (left) and corresponding trends (right)

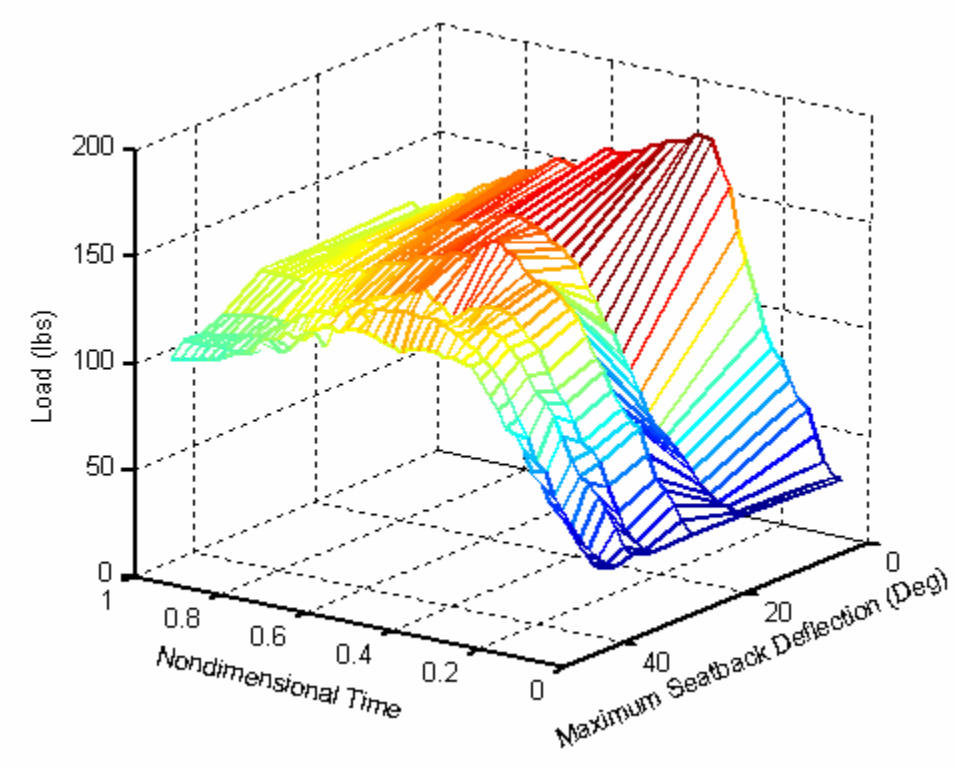

Figure 56: 3D plot showing foot force trends

the data indicates that a DHSS footrest experiences approximately 30% less stress than a footrest on a rigid seat. Figure 56 provides a 3D view of the footrest force trends. This figure clearly demonstrates how the footrest force decreases in magnitude as the seatback angle increases.

Another indication that the dynamic seatback improves conditions during an extensor thrust can be seen by looking at the seatback strain shown in Figure 57. The strain signals at the beginning of each thrust are very close to each other. This indicates that the seatback preload was almost identical for all of the experimental thrusts. The extensor thrust performed in the rigid seat causes the seatback strain to increase from the beginning of the thrust, while all of the thrusts measured in a dynamic system experienced a different strain profile. For these extensor thrusts, the strain profile starts

out with a hump representing the initial loading and subsequent deflection of the seatback. For larger maximum seatback deflection angles the seatback strain increases later in the progression of the thrust and the final strain value is up to 30% smaller than for the rigid seat. This strain reduction translates into an even greater force reduction on the occupant. Seatback strain is primarily caused by normal forces acting on the plastic seatback plate. As the occupant undergoes an extensor thrust in a rigid seat a large component of the contact force between the seatback and the occupant is in the tangential direction. In a dynamic seat the occupant rotates backward with the seatback. Therefore, in this case, the majority of the contact force between the occupant and the seatback occurs in the normal direction, effectively translating into seatback strain. The total

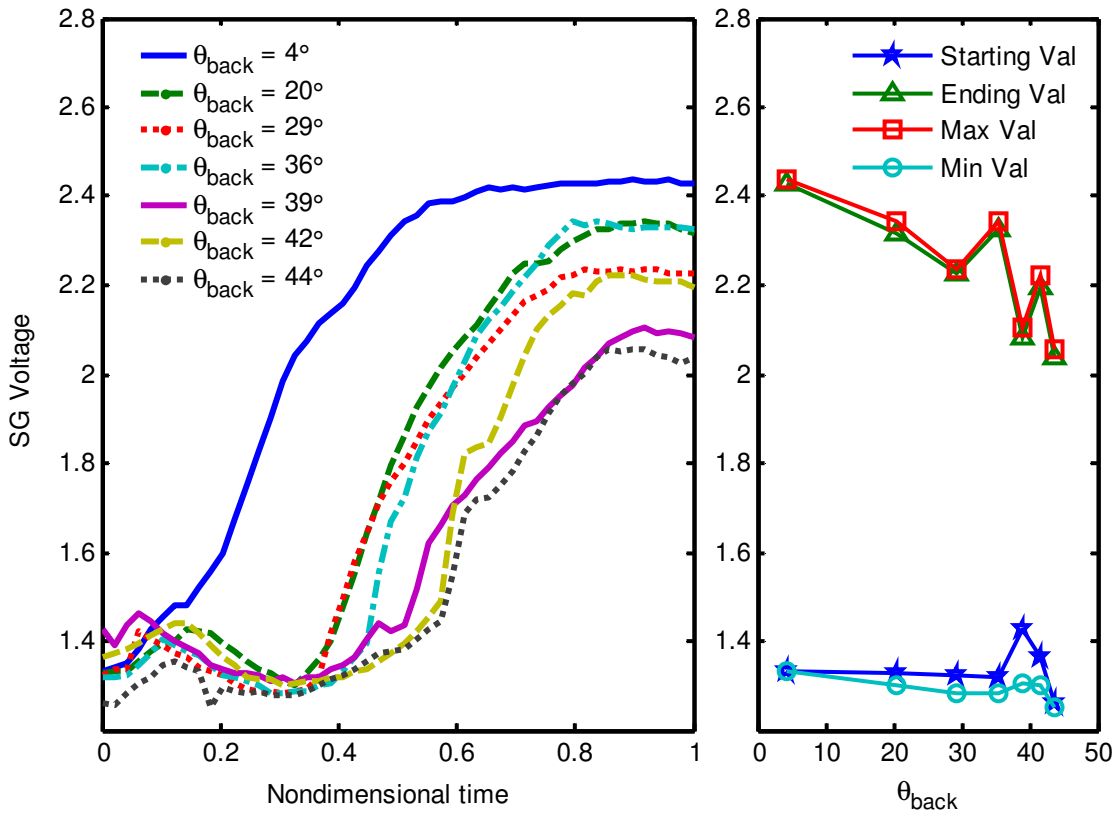

Figure 57: Seatback strain for measured maximum seatback deflection (left) and corresponding trends (right)

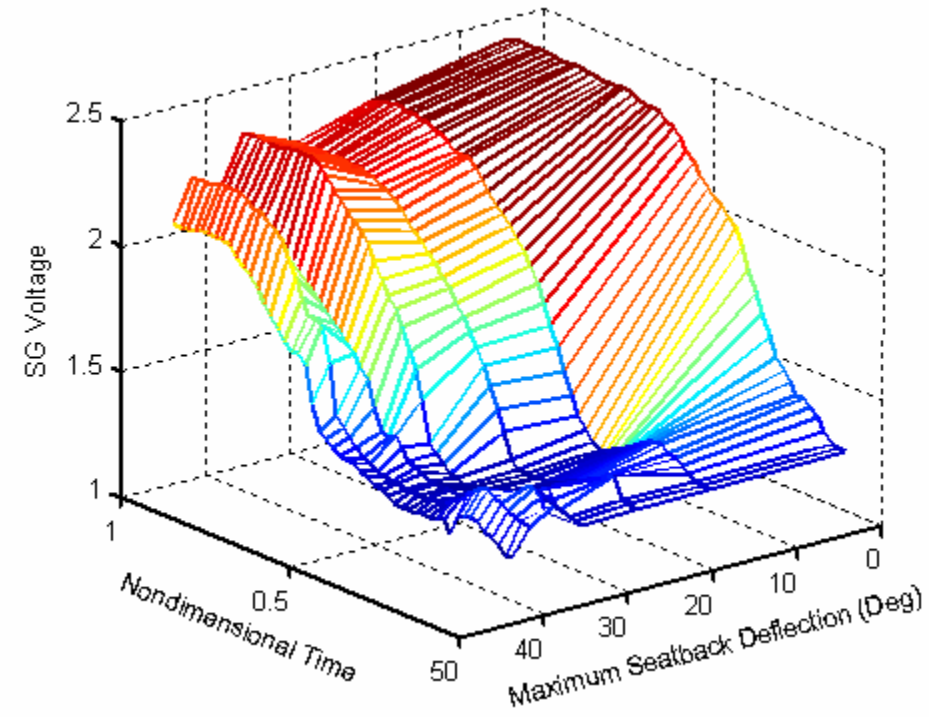

Figure 58: 3D plot showing seatback strain trends

effect is a large reduction in harmful forces on the occupant. Another view of the seatback strain trends is shown Figure 58. Here, the gradual progression in strain reduction and delay is clearly visible as maximum seatback deflection is varied.

Taken together, these experimental results demonstrate that the DHSS improves overall occupant and wheelchair conditions during an extensor thrust. The seating system is able to reduce the forces experienced by occupant and wheelchair alike, as well as increase the range of motion the occupant can undergo during an extensor thrust, translating into increased occupant comfort and system component life.

CHAPTER 4

ALTERNATIVE SEATING SYSTEMS

The previous chapter outlines the development of a simple dynamic seating system that addresses the most basic needs of individuals who exhibit high-tone extensor thrusts. Specifically, the developed DHSS is able to reduce the forces experienced by the occupant and the seat, and increases the range of motion the occupant can comfortably undergo during an extensor thrust. The DHSS design, however, does not address either of these objectives optimally, but rather with a simple, streamlined design. This chapter is meant to introduce more advanced design ideas. These alternative designs[*], have the potential to further improve occupant comfort and safety. Some of these designs are also meant to address additional problems the simple DHSS design did not take into consideration.

4.1 Variable Flexback System

One of the biggest limitations of the DHSS is that it has only one pivot point about which the entire seatback rotates. The human spine resembles more closely a flexible beam than a single point hinge, and therefore cannot easily conform to the shape of the DHSS seatback. In an effort to create a more ergonomic dynamic seating system solution, the Flexback system was developed. As the name implies, the main feature of this system is its flexible seatback. This back is implemented by replacing the rigid seatback with a clamped flexible board made out of fiberglass, or other high-strain material that does not easily yield. The flexible seatback is complemented by a

[*] Most of the designs outlined in this chapter were conceived either by Dr. Sprigle, Dr. Singhose, Dr. S.W. Hong, Jim Kitchen, myself, or a combination thereof. This chapter is meant to test the geometric feasibility of each design, as well as to inform the reader why these designs were considered in the first place.

deflection regulating mechanism to form the Flexback Dynamic Seating System. The deflection regulator is conceptually similar to the seatback rigidizer used in the DHSS, in that it can sustain the seatback in a rigid configuration if necessary, while enabling it to flex otherwise. The deflection regulator, however, is more versatile, and can also be used to help reposition the occupant after an extensor thrust has occured.

Figure 59 shows a schematic operation of the Flexback DSS. Here, the occupant, who is not shown in the figures, gradually loads the seatback (A→B) until it has reached a maximum deflection (C). Once the extensor thrust is over, a roller begins to move up the seatback (D→E) until the occupant has been successfully repositioned in his/her original configuration (F). Inversely, if the controller senses an impending thrust,

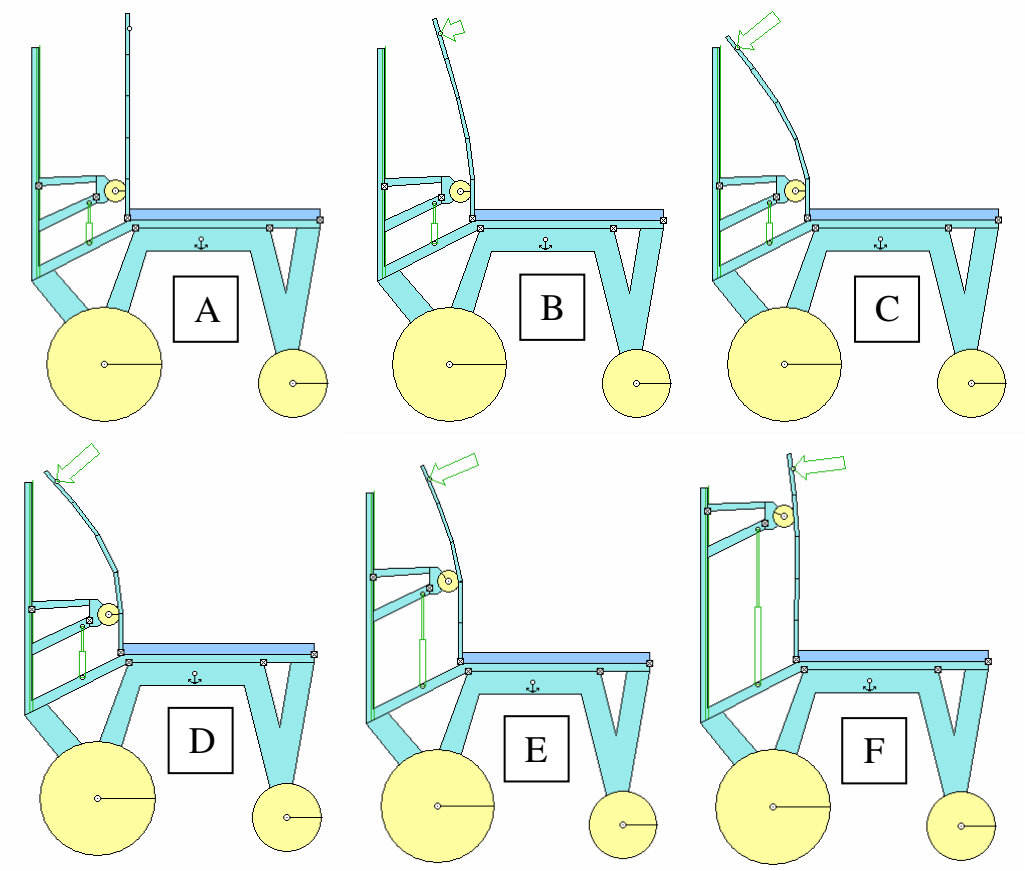

Figure 59: Flexback DSS schematic showing flexing of the seatback under load (A-C), and seatback rigidizing by deflection regulating mechanism (D-F)

then it can quickly reposition the deflection regulator to enable the seatback to flex backwards. If the controller is able to determine the intensity of the imminent thrust, then it could select an optimal seatback flexibility for the thrust, and thus position itself at the appropriate height to achieve the flexibility. This variable-stiffness feature also allows the seat to be adjusted for various individuals.

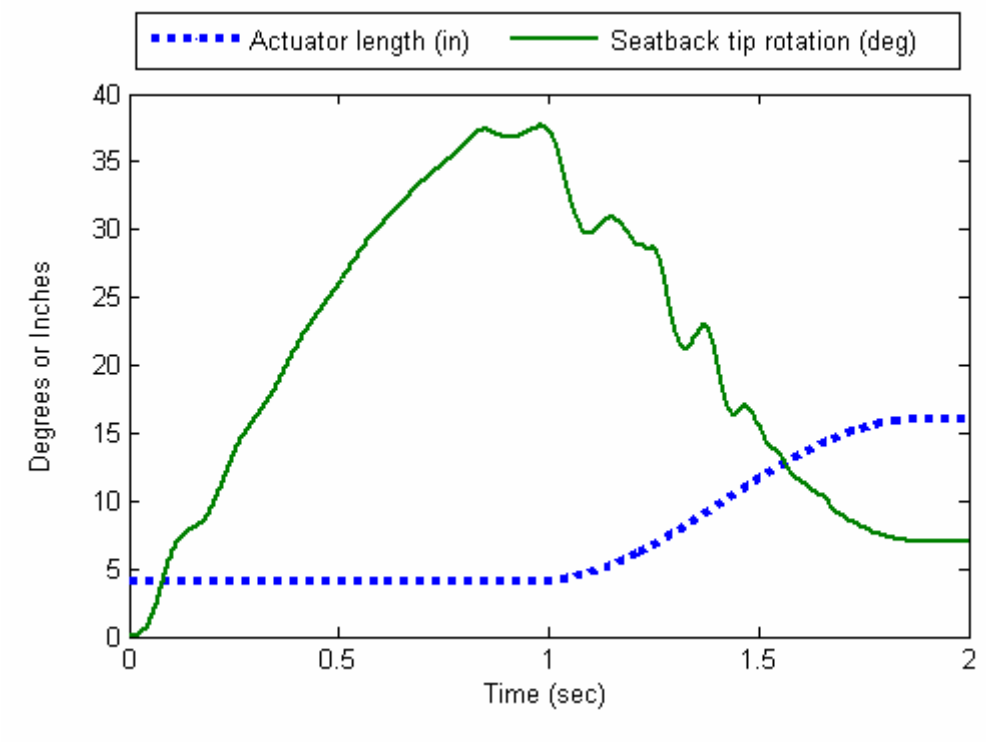

Figure 60: Seatback tip rotation and actuator length as a function of time

4.2 Four-Bar Linkage Coupled-Motion System

The Four-Bar Linkage Coupled-Motion System was developed in an effort to gain more control over the occupant motion, as well as to keep the occupant more upright during an extensor thrust. This system, shown in Figure 61, achieves a coupled motion

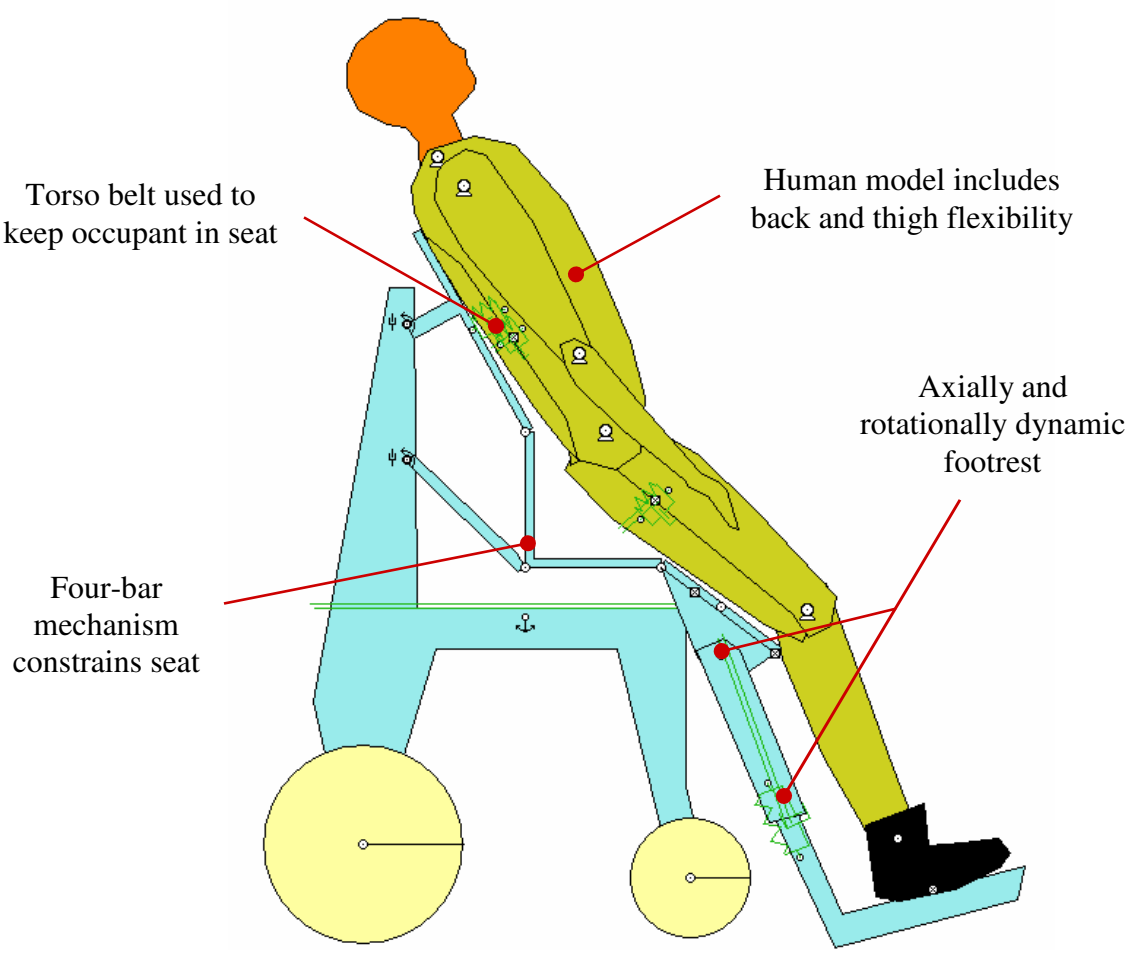

Figure 61: Detailed schematic of Four-Bar Linkage DSS

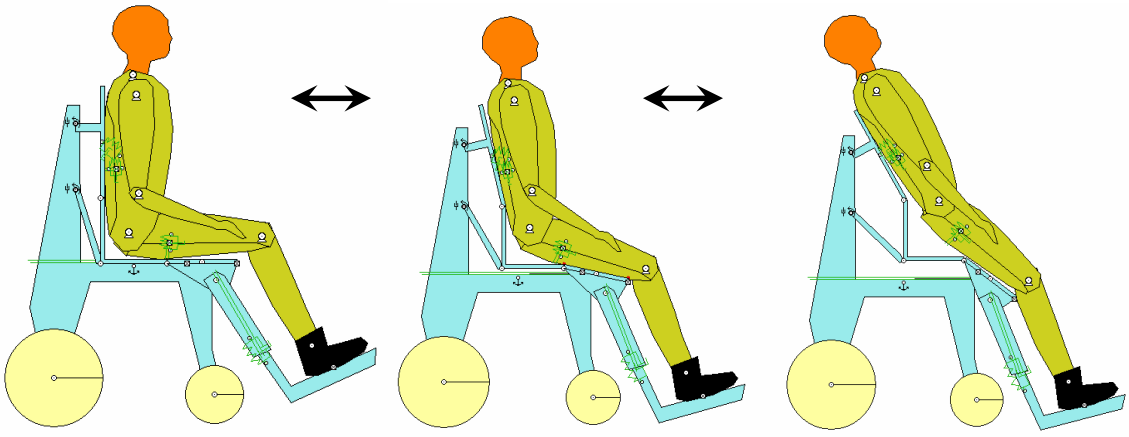

Figure 62: Progression of a simulated extensor thrust in a Four-Bar Linkage DSS

between the seatback and the seat bottom, such that a given orientation of one of these two sections determines the orientation of the other. This coupled motion is beneficial because it can be used to lift the occupant during a thrust, as shown in Figure 62. A similar motion is also achieved by the "Traveling Seat" introduced in Chapter 1. To work properly, this system requires a dynamic footrest that can actuate both rotationally and axially, such that the thigh can slide against the seat bottom as the orientation of the seat is changing. While this system is a potential improvement over a the Dynamic Hingeback Seating System, the occupant still slides against the seating interfaces and completes the thrust tilted backward at approximately 35º, as shown in Figure 63. This figure shows Working Model simulation results for the four-bar linkage system, with the occupant body segment angles shown as a function of time. It should be noticed that the calf barely rotates, while the thigh and torso rotate significantly in this system.

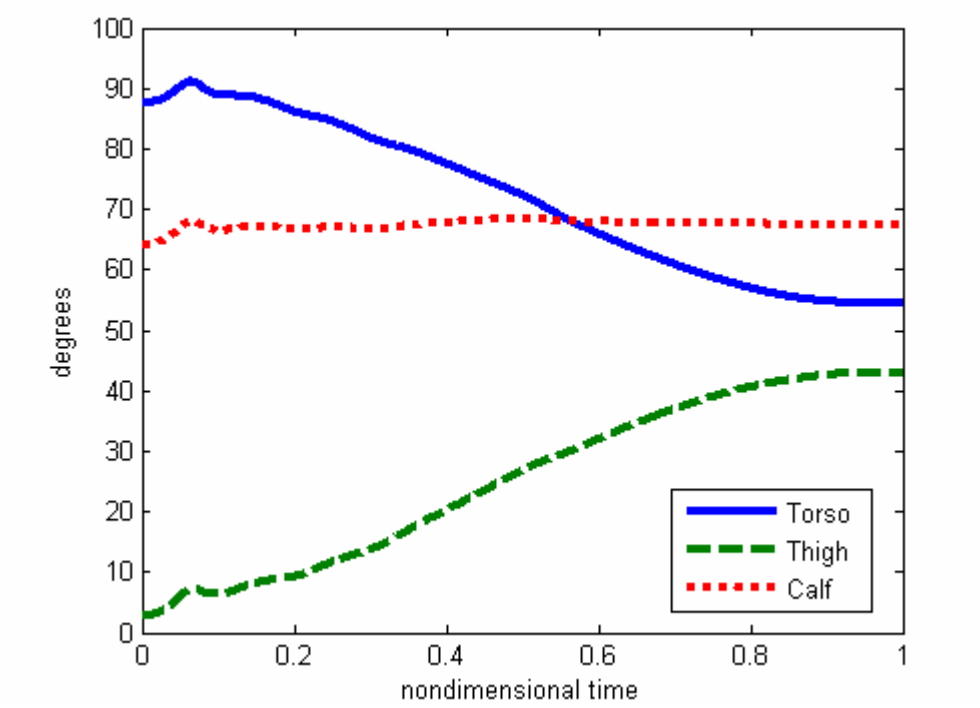

Figure 63: Body segment angles during an extensor thrust in a 4-bar linkage DSS

4.3 Anatomically Hinged Decoupled System

"Skin breakdown" is a serious problem experienced by wheelchair occupants who exhibit high-tone extensor thrusts. Repeated thrusts lead to continuous rubbing of the occupants' back and thighs against the seating elements. At these contact points the occupant often sweats profusely as these areas are not properly ventilated. The sweat causes weakening of the occupant's skin, and the frictional forces during thrusts exacerbates the problem by further irritating the area. Over time this condition can lead to the development of severe rashes and infections.

The Anatomically-Hinged Decoupled DSS, shown in Figure 64, is developed to minimize this effect of the seat on the occupant. This seating system works by using a

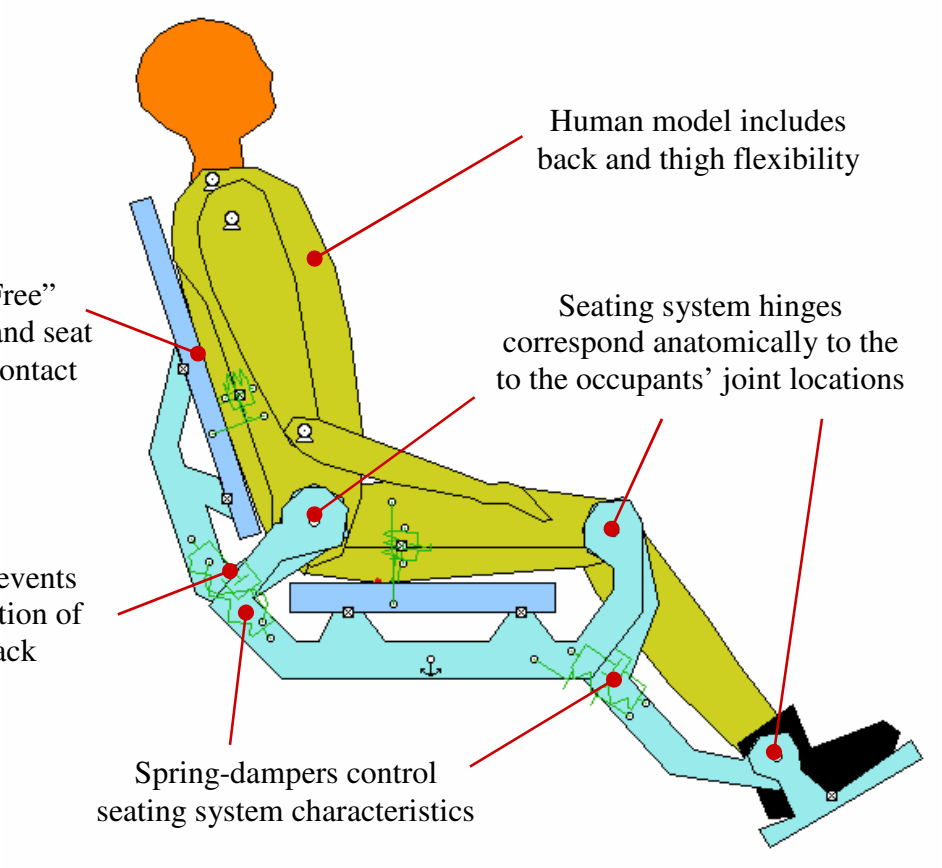

Figure 64: Detailed schematic of Anatomically-Hinged, Decoupled DSS

highly adjustable frame that can be customized such that the hinge points of the dynamic components correspond with the anatomical hinges of the occupant's body. This ensures that, as the occupant undergoes an extensor thrust, the dynamic components of the seating system move along with the occupant, thereby avoiding sliding. Gas shocks can be used to determine the preload and damping of the seatback and the footrest. Cable elements are used to ensure the seatback does not over-rotate due to the built-in compressive preload in the frame. The ankle mechanism is designed to eliminate all transmitted ankle torque by allowing the ankle to rotate freely until the effective torque is nullified. The system is assumed to be fixed onto a wheelchair frame. Wheelchair stability may become an issue because the occupant can lean back significantly during a thrust in this system, as shown in Figure 65.

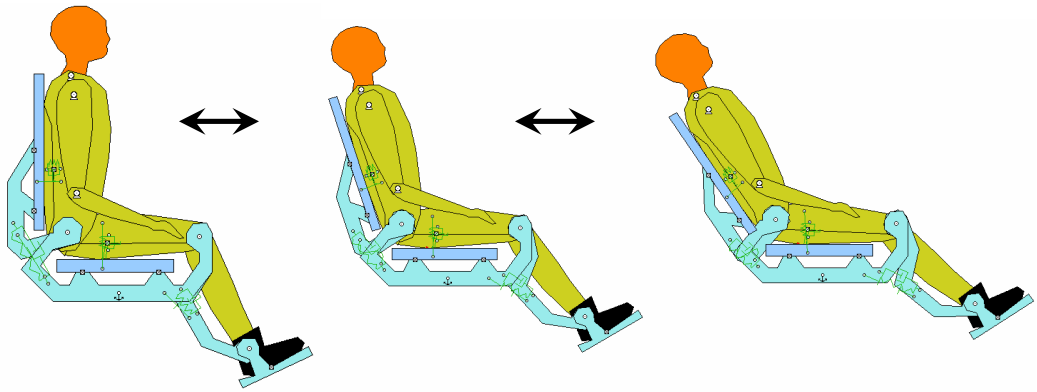

Figure 65: Progression of a simulated extensor thrust in an Anatomically Hinged, Decoupled DSS

The working model simulation results for this system are shown in Figure 66. Here, it can be observed that the thigh does not rotate, while the calf and torso are both rotating towards the horizontal. This results is consistent with the expected motion profiles for this anatomically-hinged DSS.

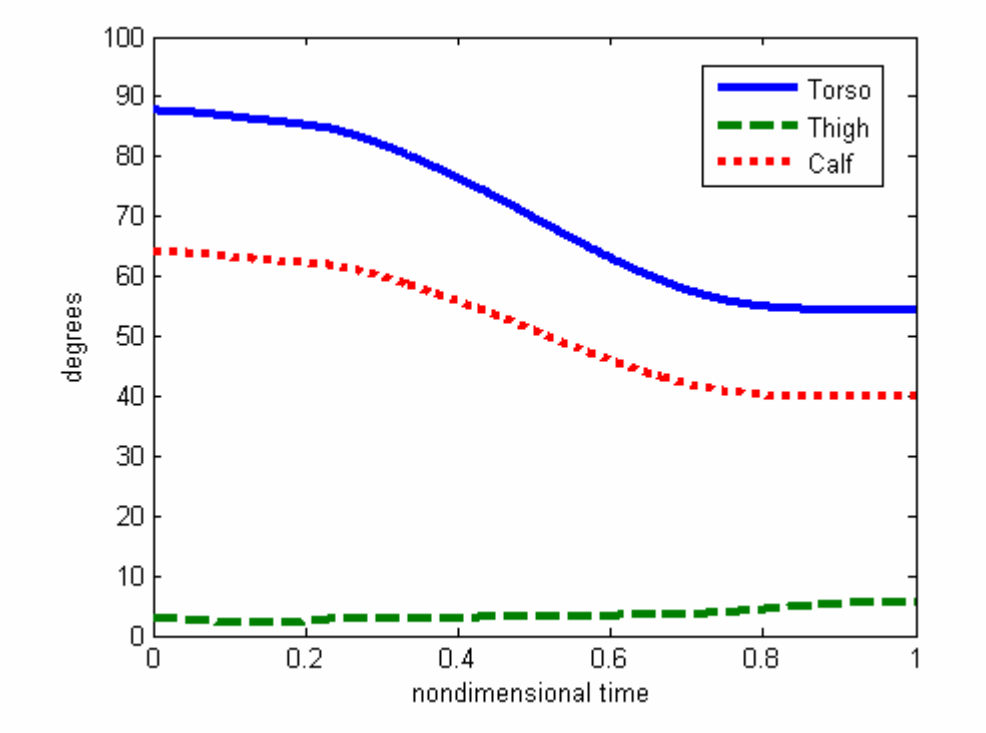

Figure 66: Body segment angles during a thrust in an anatomically-hinged DSS

4.4 Thrust-Induced Vertical Standing System

The Anatomically Hinged Decoupled DSS introduced in the previous section addresses the important issue of "skin breakdown," yet potentially aggravates a different problem. The occupant posture can act as a feedback mechanism which can positively reinforce or attenuate an extensor thrust. If the occupant becomes scared or disoriented during an extensor thrust, it is possible that this will further intensify the thrust. All of the seating systems developed up to this point propose that the occupant be tilted back to some degree due to the motion of the dynamic seatback component. While this may be acceptable for a portion of the affected population, there may be others who will experience an adverse effect due to the sudden change in orientation.

A “Stand-Up” dynamic seating system is proposed to ensure the system will not reinforce an extensor thrust by disorienting the occupant. This system is based on the original Anatomically Hinged frame, but is modified to use the forces generated by the extensor thrust to cause the occupant to extend in the vertical direction, rather than leaning backward as with the previously discussed system. By placing a rigid slot joint on the seatback frame, it is possible to limit its motion to translation in the vertical direction. Next, a pinned slot joint limits the translation of a point on the seat bottom frame to horizontal translation, while enabling the frame to rotate about that point. The resulting motion can be seen in Figure 67. This motion seems especially desirable because it prevents the seating system occupant from becoming disoriented during an extensor thrust and avoids occupant sliding in the seat, in addition to the other discussed benefits of a dynamic seating system. Additionally, this system has the potential to increase occupant functionality by helping occupants to reach for objects and possibly facilitate communication.

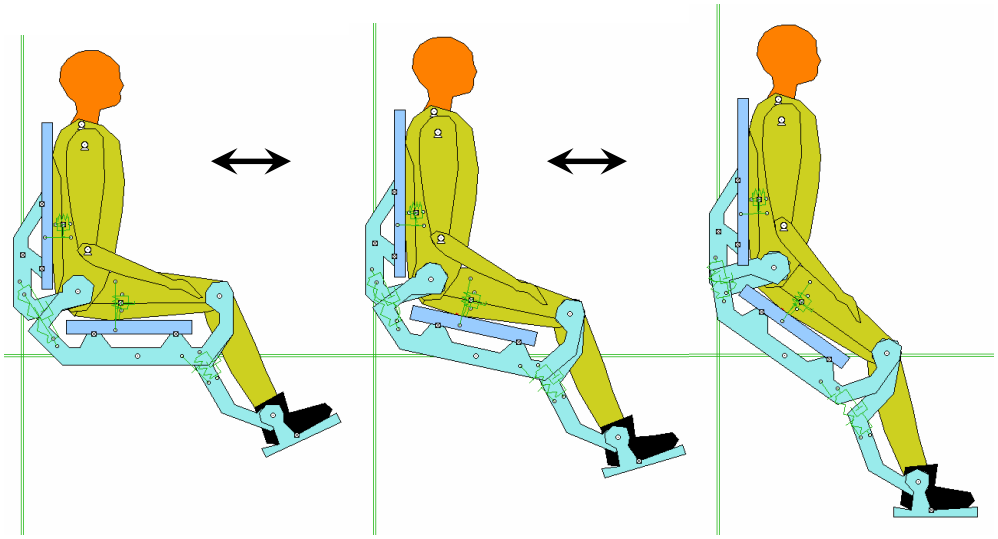

Figure 67: Progression of a simulated extensor thrust in an Anatomically Hinged, Stand-Up DSS

A simulation of the "Stand-Up" DSS reveals that the thigh of the occupant is the only body segment that rotates significantly, as shown in Figure 68. The calf is also rotating slightly upward, and the overall motion of the occupant is a straightening of the body in the vertical direction, which coincides with the original design intent.

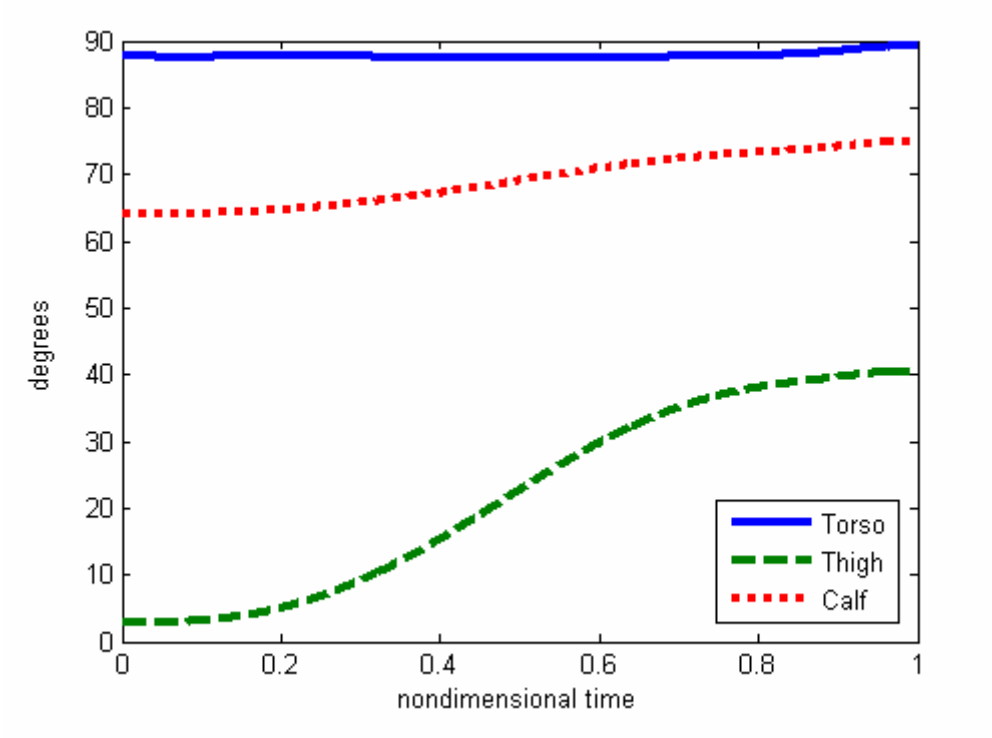

Figure 68: Body segment angles during an extensor thrust in a "stand-up" DSS

Using Working Model it is also possible to obtain the predicted torque profiles for an extensor thrust in an Anatomically-Hinged Stand-Up seating system, as shown in Figure 69. This figure is useful for reaching a number of conclusions. First of all, the zero ankle torque assumption used throughout this thesis appears to hold well in this case, when the ankle torque is backed out with inverse dynamics. The nondimensional time proceeds between t = 0 to 2 because this simulation considered both the extensor thrust and the relaxation period, with t = 1 indicating the completion of the thrust and t = 2

indicating the return to the original configuration. While the numerical errors that have been plaguing Working Model simulations are still present, this result indicates the torques are realistic, and thus the design is feasible.

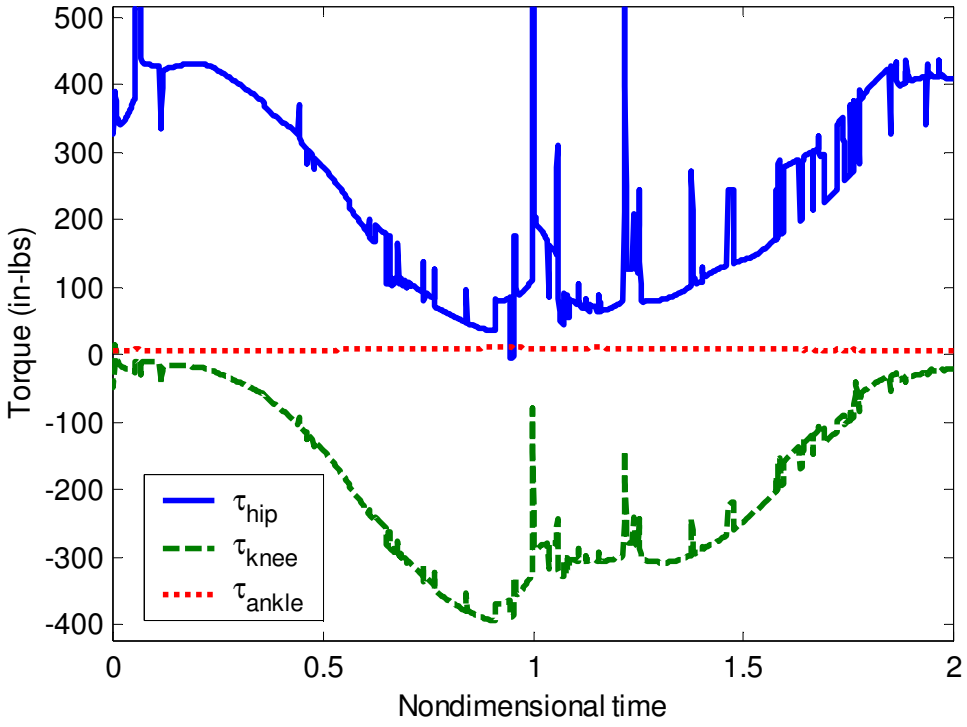

Figure 69: Predicted torque profiles for an extensor thrust in an Anatomically-Hinged, Stand-Up DSS

CHAPTER 5

CONCLUSION

This thesis provides a new and solid foundation for understanding basic design issues of dynamic seating systems for individuals who experience high-tone extensor thrusts. It also proposes several dynamic seating systems that have useful and adjustable features. Contributions of this thesis include:

- Development and validation of an analytical model describing an extensor thrust in a rigid seat
- Simulation-based extensor thrust parameter study used to describe and understand a thrust from a mechanical perspective (motions, torques, forces)
- Design and fabrication of a Dynamic Hingeback Seating System (DHSS)
    - Seatback pivots to allow occupant to extend during a thrust
    - Rigidizer locks seatback in upright position to keep the seat rigid during purposeful thrusts
- Development of a numerical model of the DHSS using Working Model 2D for predicting system performance.
- Experimental verification of predicted loads reductions and of increased range of motion experienced by DHSS occupant
- Proof-of concept simulations for alternative dynamic seating system designs

5.1 Extensor Thrust Characteristics

The thesis presented an inverse dynamics technique that was used to obtain the torque profiles of the occupant, which in turn can be used to compare dynamic seating system performance. This approach was shown to work well when the simulation model was developed both analytically and with Working Model.

A number of important extensor thrust trends were presented. Specifically, it was shown that extensor thrust speed does not have a major impact on the occupant motions

and forces occurring during the thrust. This powerful result enables one to study extensor thrusts in nondimensional time, allowing the researcher to compare thrusts of varying speeds when identifying seating system performance. Also, extensor thrusts were shown to be largely insensitive to occupant-seatback friction.

5.2 Design and Development of Dynamic Seating System

The design of a Dynamic-Hingeback Seating System was outlined in detail in Chapter 3, with all of the subsystem components and control algorithms used being thoroughly documented. A simulation model of the design was created in Working Model, and validated with experimental data. The initial trends predicted by the simulation were later confirmed through further experimentation. These experimental results, obtained with the DHSS were analyzed in detail, and verifiably showed that the DHSS improved occupant and seating system conditions during an extensor thrust.

5.3 Alternative Designs and Future Work

The occupant model was reused to investigate the feasibility of other proposed seating system designs. These designs, outlined in Chapter 4, were found to be feasible through preliminary Working Model simulations. Each of these designs has unique features that could make it a great solution for seating system occupants who exhibit high-tone extensor thrusts. The technique used to develop the Dynamic Hingeback Seating System should be employed to study some of the alternate designs mentioned in this thesis. Additionally, promising designs should be tested with patients and made customizable, such that these seating systems can become commercially viable, and ultimately reach the target population.

APPENDIX A

KINEMATIC RELATIONS

$$\dot{X}_1 = -\ell_1 \sin\theta_1\dot{\theta}_1$$
$$\dot{Y}_1 = \ell_1 \cos\theta_1\dot{\theta}_1$$
$$\dot{X}_2 = -L_1 \sin\theta_1\dot{\theta}_1 - \ell_2 \sin\theta_2\dot{\theta}_2$$
$$\dot{Y}_2 = L_1 \cos\theta_1\dot{\theta}_1 + \ell_2 \cos\theta_2\dot{\theta}_2$$
$$\dot{X}_3 = \dot{X}_2 - (L_2 - \ell_2)\sin\theta_2\dot{\theta}_2 - \ell_3 \sin\theta_3\dot{\theta}_3$$
$$\dot{Y}_3 = \dot{Y}_2 + (L_2 - \ell_2)\cos\theta_2\dot{\theta}_2 + \ell_3 \cos\theta_3\dot{\theta}_3$$
$$\ddot{X}_1 = -\ell_1 \cos\theta_1(\dot{\theta}_1)^2 - \ell_1 \sin\theta_1\ddot{\theta}_1$$
$$\ddot{Y}_1 = -\ell_1 \sin\theta_1(\dot{\theta}_1)^2 + \ell_1 \cos\theta_1\ddot{\theta}_1$$
$$\ddot{X}_2 = -L_1 \cos\theta_1(\dot{\theta}_1)^2 - L_1 \sin\theta_1\ddot{\theta}_1 - \ell_2 \cos\theta_2(\dot{\theta}_2)^2 - \ell_2 \sin\theta_2\ddot{\theta}_2$$
$$\ddot{Y}_2 = -L_1 \sin\theta_1(\dot{\theta}_1)^2 + L_1 \cos\theta_1\ddot{\theta}_1 - \ell_2 \sin\theta_2(\dot{\theta}_2)^2 + \ell_2 \cos\theta_2\ddot{\theta}_2$$
$$\ddot{X}_3 = \ddot{X}_2 - (L_2 - \ell_2)\cos\theta_2(\dot{\theta}_2)^2 - (L_2 - \ell_2)\sin\theta_2\ddot{\theta}_2 - \ell_3 \cos\theta_3(\dot{\theta}_3)^2 - \ell_3 \sin\theta_3\ddot{\theta}_3$$
$$\ddot{Y}_3 = \ddot{Y}_2 - (L_2 - \ell_2)\sin\theta_2(\dot{\theta}_2)^2 + (L_2 - \ell_2)\cos\theta_2\ddot{\theta}_2 - \ell_3 \sin\theta_3(\dot{\theta}_3)^2 + \ell_3 \cos\theta_3\ddot{\theta}_3$$
$$\dot{\theta}_2 = \cos^2\theta_2 \frac{X_2\dot{Y}_2 - \dot{X}_2 Y_2}{X_2^2},\ \dot{\theta}_3 = \cos^2\theta_3 \frac{X_C\dot{Y}_C - \dot{X}_C Y_C}{X_C^2},$$
$$\ddot{\theta}_2 = \frac{\cos^2\theta_2(X_2\ddot{Y}_2 - \ddot{X}_2 Y_2) - \sin 2\theta_2\dot{\theta}_2(X_2\dot{Y}_2 - \dot{X}_2 Y_2) - 2X_2\dot{X}_2\dot{\theta}_2}{X_2^2},$$
$$\ddot{\theta}_3 = \frac{\cos^2\theta_3(X_C\ddot{Y}_C - \ddot{X}_C Y_C) - \sin 2\theta_3\dot{\theta}_3(X_C\dot{Y}_C - \dot{X}_C Y_C) - 2X_C\dot{X}_C\dot{\theta}_3}{X_C^2}$$

where

$$X_C = L_\beta + L_\gamma \cos\theta_r - (L_1 \cos\theta_1 + L_2 \cos\theta_2 - D_1)$$
$$Y_C = L_\gamma \sin\theta_r - (L_1 \sin\theta_1 + L_2 \sin\theta_2 - (L_\alpha - D_2))$$

APPENDIX B

HUMAN SUBJECT PARAMETER CALCULATIONS

Body Segment	Property	B0	B1	B2	B3	B4	x1	x2	x3	x4	**Value**	Std Dev
Leg	M	-6.017	0.0675	0.0145	0.205		41	6.685	31.17		**3.237**	0.121
Leg	C.G.	0.0937	0.396	0.064	-0.041		41	6.685	31.17		**15.48**	1.1
Leg	I1	-1437	28.64	3.202	21.6		41	6.685	31.17		**431.8**	24.3
Leg	I2	-1489	28.97	6.48	21.5		41	6.685	31.17		**412.2**	23.1
Leg	I3	-194.8	0.214	-3.64	8.9		41	6.685	31.17		**67.03**	20.5
Thigh	M	-17.819	0.153	0.23	0.367		37	11.62	47.17		**7.824**	0.572
Thigh	C.G.	-3.655	0.478	-0.07	0.088		37	11.62	47.17		**17.37**	0.99
Thigh	I1	-6729	87.8	50.3	75.3		37	11.62	47.17		**655.7**	206
Thigh	I2	-6774	88.4	38.6	78		37	11.62	47.17		**624.3**	205
Thigh	I3	-1173	4.06	6	26.8		37	11.62	47.17		**311**	52
Forearm	M	-2.04	0.05	-0.0049	0.087		28	9	20.83		**1.128**	0.08
Forearm	C.G.	0.732	0.588	-0.0857	-0.0187		28	9	20.83		**16.04**	0.89
Forearm	I1	-229	7.12	-0.049	5.066		28	9	20.83		**75.46**	6
Forearm	I2	-220	7.06	-0.082	4.544		28	9	20.83		**71.61**	5.1
Forearm	I3	-39.2	0.56	-0.972	1.996		28	9	20.83		**9.315**	2.7
Upper Arm	M	-2.58	0.0471	0.104	0.0651		29	29	6.446		**2.222**	0.144
Upper Arm	C.G.	-2.004	0.566	0.056	-0.016		29	29	6.446		**15.93**	0.618
Upper Arm	I1	-359	10.2	6.4	8.5		29	29	6.446		**177.2**	14.4
Upper Arm	I2	-331	10.3	5.5	5.6		29	29	6.446		**163.3**	13.6
Upper Arm	I3	-106	0.4	3.8	4.5		29	29	6.446		**44.81**	11.2
Head	M	-7.385	0.146	0.071	0.0356	0.199	25.5	58.5	48	18.6	**5.906**	0.245
Head	C.G.	0.21	0.503	0.027	0.043	-0.158	25.5	58.5	48	18.6	**13.74**	0.53
Head	I1	-987	23.74	3.97	3.46	18.58	25.5	58.5	48	18.6	**362.7**	31.1
Head	I2	-983	19.9	8.43	3.22	10.2	25.5	58.5	48	18.6	**362.1**	30.9
Head	I3	-721	7.36	6.14	2.28	18.25	25.5	58.5	48	18.6	**275.1**	31.6
Upper Torso	M	-18.91	0.421	0.199	0.078	0.065	21	91.5	27.37	0.5	**10.31**	0.715
Upper Torso	C.G.	-2.854	0.567	0.0067	0.0321	0.0152	21	91.5	27.37	0.5	**10.55**	0.51
Upper Torso	I1	-5175	105.4	45.8	4.01	8.65	21	91.5	27.37	0.5	**1343**	201
Upper Torso	I2	-2650	65.6	17.12	5.84	9.8	21	91.5	27.37	0.5	**458.8**	96
Upper Torso	I3	-4149	54.8	43.7	8.88	9.63	21	91.5	27.37	0.5	**1248**	184
Middle Torso	M	-13.62	0.444	0.195	-0.017	0.0887	16	78	26.74	0.5	**8.284**	0.694
Middle Torso	C.G.	-0.742	0.485	0.0007	-0.002	0.001	16	78	26.74	0.5	**7.02**	0.44
Middle Torso	I1	-3271	76.7	30.3	10.2	18.3	16	78	26.74	0.5	**601.5**	141
Middle Torso	I2	-2354	65.3	21.5	-2.3	10.57	16	78	26.74	0.5	**311.6**	82
Middle Torso	I3	-2657	43	33.3	1.6	20.6	16	78	26.74	0.5	**681.5**	145
Lower Torso	M	-15.18	0.182	0.243	0.0216		84	36	1.5		**8.888**	0.938
Lower Torso	C.G.	0.205	0.064	0.134	-0.08		84	36	1.5		**10.29**	0.97
Lower Torso	I1	-2354	22.6	34.37	4.41		84	36	1.5		**788.3**	144
Lower Torso	I2	-1816	18	23.6	7.29		84	36	1.5		**556.5**	111
Lower Torso	I3	-2009	20.1	24.9	11.2		84	36	1.5		**592.6**	105

Upper Body C.G. **Upper Body I transverse**
48.3251 **17014.6**

Tot Weight (no hands/feet) **Actual Weight (w/ hands/feet)**
62.21 Kg **65.91 Kg**

APPENDIX C

DSS SURVERY REPORT

Note: This survey was prepared, administered, and summarized by RL Grubbs of the Center for Assistive Technology & Environmental Access (CATEA) at Georgia Tech. His contribution is especially important to dynamic seating system design, and is therefore included in its entirety in this appendix as a reference.

DRAFT Study Report

For

Dynamic Seating System Design Team

(Intended audience—DSS Design team)

*This study and subsequent analysis has not generated ALL design criteria for a dynamic seating system. It has generated MOST of the customer requirements and design criteria that are important to the stakeholders involved. Focus group participants generated many customer requirements that cannot be addressed in the first iteration of a prototype dynamic seating system.

*The follow-up survey and subsequent analysis was done to identify the importance and priorities of customer requirements. Table 1-Design Criteria for DSS (pages 12-14) was derived from analysis of customer requirements from focus group data and from survey data from the follow-up survey.

RL Grubbs, Principle Investigator/Study Moderator
Rehabilitation Engineering Research Center on Wheeled Mobility
Center for Assistive Technology & Environmental Access
Georgia Institute of Technology
December 2004

1.1 Who participated in the study?
1.2 What experience do they have with specialized seating?

		QBK1-Respondents' Demographics					QBK2-Experience with Specialized W/C Seating				
Respondent ID	Count n=	Parent Caregiver	YA w/c user	Therapist	Vendor	Other	Great Deal	Above Average	Average	Not Much	Very Little
1009	1				1			1			
1041	1				1			1			
1042	1				1		1				
103	1	1						1			
1038	1			1				1			
109	1	1					1				
106	1	1					1				
107	1		1				1				
1011	1			1							1
1003	1				1			1			
1010	1			1					1		
1039	1			1						1	
1004	1				1				1		
1043	1			1					1		
1040	1			1				1			
1007	1			1				1			
1006	1			1					1		
105	1	1						1			
1044	1			1						1	
1045	1			1						1	
1002	1			1					1		
108	1	1							1		
102	1	1					1				
Raw Score	23	6	1	11	5	0	5	8	6	3	1
%		26	4	48	22	0	22	35	26	13	4

A group of 23 stakeholders participated in the one of three focus groups and follow-up mail survey (n=23) conducted between April and November 2004. Six families (i.e. parent/caregiver and child/user), one adult user, 11 therapists (i.e. 7 physical therapists, 4 occupational therapists) and 5 vendors participated (see **Figure 1**) in the study.

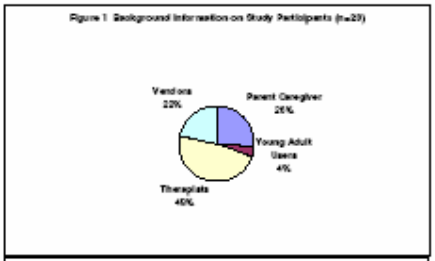

Most participants considered themselves to have at least average or better experience with wheelchair seating systems for users with thrust/high extensor tone. **Figure 2** contains demographic information about study participants.

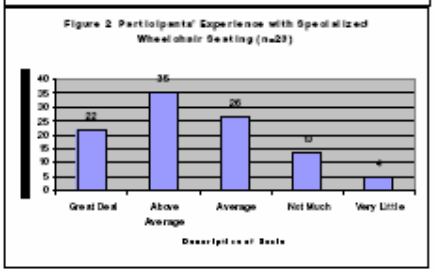

2.1 How do thrusts travel through the body?
2.2 How are purposeful thrusts used?

		QT1-Involuntary thrusts travel from...				QT2-Purposeful thrusts are used to...								
Respondent ID	Count n=	Pelvis out to extremities	Head down to trunk, extremities	Legs up to trunk, arms, head	Initiate in different parts of body	Assist with Transfers	Change Position in W/C	Reach for Objects	Access Switches	Raise Head	Communicate	Drive w/c	Other	Not witnessed
1009	1	1					1	1	1	1	1	1		
1041	1	1						1	1		1			
1042	1				1	1	1	1	1	1	1	1		
103	1				1	1	1		1	1	1			
1038	1			1		1	1	1	1	1	1			
109	1		1			1	1	1	1	1	1	1		
106	1				1	1	1	1	1	1	1	1		
107	1				1	1	1	1	1	1	1	1		
1011	1		1			1			1	1		1		
1003	1			1		1	1		1		1			
1010	1				1	1	1	1	1	1	1	1		
1039	1				1	1		1	1	1	1	1		
1004	1			1					1		1	1		
1043	1				1	1		1	1	1		1		
1040	1				1	1		1	1	1				
100	1				1	1	1	1	1	1	1	1		
1006	1				1	1	1	1	1	1	1			
105	1	1						1			1			
1044	1		1			1		1	1		1			
1045	1				1	1	1	1	1					
1002	1				1	1	1	1	1	1	1	1		
108	1		1			1	1	1	1	1	1			
102	1	1				1		1	1			1		
Raw Score	23	4	4	3	12	19	14	19	22	16	18	13	0	0
% or Rank		17	17	13	52	Rank 2	Rank 5	Rank 2	Rank 1	Rank 4	Rank 3	Rank 6		

Participants were asked to discuss their experience with and knowledge about thrusts. During focus groups, participants identified emotional, physical and environmental triggers for involuntary thrusts and symmetrical and asymmetrical patterns of body movement during involuntary thrusts. When asked where involuntary thrusts (spasms) initiate and how they travel through the body, survey results appear to indicate that a majority of participants (52%) believe that thrusts initiate in different parts of the body (see **Figure 3**).

Figure 3 Where do thrusts initiate and how do they travel through the body? (QT1)

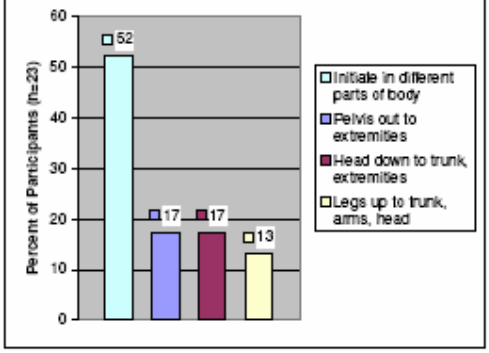

Participants appear to agree that purposeful thrusts are used to accomplish certain tasks. Whereas an involuntary thrust may last a few seconds, purposeful thrusts may last longer depending on the activity or task the person is doing. On the survey, participants were asked to mark a list of activities that children and young adults do using purposeful thrusts. These activities are ranked in **Figure 4**.

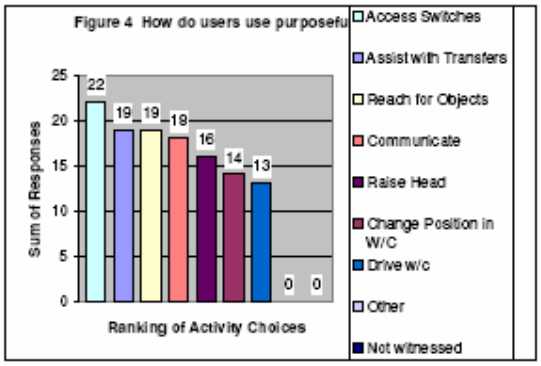

2.3 How do purposeful and involuntary thrusts differ?
2.4 How does the seating system react to user thrust?

		QT3-QT10--About thrusts--How strongly do you agree that...							
Respondent ID	Count n=	Use purposeful thrusts	Involuntary is fast	Purposeful lasts longer	Involuntary stronger	Thrust in upper body	Thrust in lower body	Want static SS	DSS react differently
1009	1	3	1	2	1	0	0	3	1
1041	1	3	2	1	0	0	0	1	3
1042	1	2	2	1	1	1	2	1	2
103	1	3	2	3	0	0	0	0	1
1038	1	3	3	2	1	1	2	0	2
109	1	3	3	3	3	3	1	3	3
106	1	3	3	2	1	1	1	1	2
107	1	3	3	2	1	0	0	1	2
1011	1	3	2	1	1	1	2	2	3
1003	1	2	1	2	2	1	2	1	2
1010	1	3	2	2	1	0	2	1	2
1039	1	2	2	3	2	1	2	1	2
1004	1	3	2	2	2	0	3	2	1
1043	1	3	2	3	1	1	2	1	3
1040	1	2	2	2	1	1	1	1	1
1007	1	3	2	1	3	1	2	2	3
1006	1	3	2	2	0	0	0	0	3
105	1	3	2	3	1	1	2	0	3
1044	1	3	2	3	0	2	2	1	0
1045	1	3	1	1	1	1	2	1	2
1002	1	3	2	2	2	0	0	0	3
108	1	3	3	3	3	3	1	0	3
102	1	3	2	2	2	1	1	2	3
Raw Score	23	65	48	49	30	20	30	25	50

Figure 5 How do purposeful and involuntary thrusts differ and how does the seating system react?

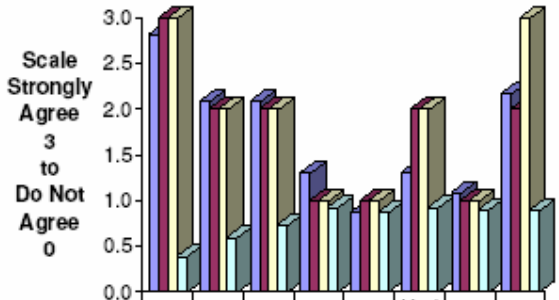

	QT3	QT4	QT5	QT6	QT7	QT8	QT9	QT10
	Yes	Yes	Yes	No	No	Undecid	No	Yes
Mean	2.8	2.1	2.1	1.3	0.9	1.3	1.1	2.2
Median	3	2	2	1	1	2	1	2
Mode	3	2	2	1	1	2	1	3
Standard Deviation	0.4	0.6	0.7	0.9	0.9	0.9	0.9	0.9

As illustrated in **Figure 5**, survey results indicate participants believe that-

- **(QT3)** purposeful thrusts are useful for accomplishing various tasks,
- **(QT4)** involuntary thrusts are faster than purposeful thrusts,
- **(QT5)** purposeful thrusts tend to last longer depending on the task, and
- **(QT10)** a dynamic seating system should react differently to purposeful versus involuntary thrusts.

Participants **do not agree** that-

- **(QT6)** involuntary thrusts are more intense than purposeful thrusts,
- **(QT7)** thrusts occur more frequently in the upper body, and
- **(QT9)** a static seating system is preferred to a dynamic one for accommodating the use of purposeful thrusts.

Participants appear to be **divided** on **(QT8)** whether or not thrusts occur more frequently in the lower body.

There are several important implications for the seating system that can be drawn from this data. First, differences appear to exist between purposeful and involuntary thrusts. Purposeful thrusts tend to be slower than involuntary thrusts, but both types of thrusts are similar in intensity or forces that must be accommodated. This finding supports the idea that the seating system must react differently to purposeful versus involuntary thrusts.

Based on content analysis of focus group data, it appears that when thrusts are used in a purposeful manner, the user depends on a stable or static area, a "stable center of control," to push against to accomplish a desired function. For example, when reaching for an object, the person uses her torso and upper extremity to thrust her arm outward. This is a slower more controlled movement and may last longer. The user appears to benefit from a stable center of control that allows her to push against, while she thrusts her upper extremity outward to accomplish the reaching function. It appears that the seating system needs to offer some rigidity for the user to push against during purposeful thrusts, but at the same time support (or at least not inhibit) the movement of the extremities in accomplishing the intended task. The seating system needs to be designed so a fixed lower back section and velocity sensitive securements maintain pelvic positioning.

In a second example, the user changes position by arching her back and pushing her head against the headrest to shift her torso in the seat. If the headrest gives too quickly during this purposeful thrusting movement, the difficulty may be increased. It appears that, to accommodate purposeful thrusts, the dynamic seating system must provide for a stable center while supporting the desired movement of the extremities in a slow, controlled manner. The seating system "dampens" purposeful thrusts by providing adjustable resistance to the thrust and providing adjustable pressure in the rate-of-return to a neutral position. Participants compared this feature to a car's anti-lock brakes or to the adjustable resistance of exercise machines.

According to survey results, participants believe that involuntary thrusts are explosive and "lightening fast." They indicate that, to be effective, the seating system must react differently to purposeful and involuntary thrusts (see **Figure 5**). The basic difference is that during involuntary thrusts, the system provides less dampening resistance, whereas, during purposeful thrusts, the system provides more dampening resistance. Both types of thrust require adjustable force in the rate-of-return.

Thrusts occur in both upper and lower body. When asked on the survey where thrusts occur more frequently, participants appear to indicate that thrusts occur with about the same frequency in upper and lower body (see **Figure 5**).

Focus group discussions indicated that involuntary thrusts (spasms) are likely to be almost constant in young children with traumatic brain injury. On average, participants indicated that involuntary thrusts occur about 6 to 10 times an hour. In users who are taking Rx Baclofen, the frequency of involuntary thrusts drops to about 3 times an hour. Participants indicated that a child's thrusts are less powerful than teen and young adult thrusts due in part to muscle development and "more rehearsal of the movement."

This has implications for the durability of the seating system and components. For example, this finding appears to indicate that headrest assemblies must be just as durable as footrest and armrest assemblies. Taking the average of 10 thrusts an hour multiplied by 10 hours of seating system use daily, components must withstand approximately 100 thrusts each day or 36,500 thrusts per year for approximately three to five years.

3.1 What assembly and adjustability features are desired?

		QA1-QA10--About Adjustability–How acceptable is it that...									
Respondent	Count	Remove SS from base	SS Folds	Doesn't remove or fold	2" in width depth, no kit	2" depth only, no kit	2" depth kit	2" in depth and or width kit	Adjusts w/o tools	Universal tool Adjust	Adjusts w special tool
1009	1	3	1	0	3	3	2	2	3	3	1
1041	1	3	3	1	3	2	1	2	2	3	0
1042	1	3	0	0	3	2	0	1	2	3	1
103	1	3	2	3	3	1	1	3	2	2	0
1038	1	3	2	0	3	2	2	2	1	3	1
109	1	1	3	3	3	3	3	3	3	3	0
106	1	1	2	3	3	3	2	2	3	3	2
107	1	1	2	3	3	3	2	2	3	3	2
1011	1	3	2	0	2	1	1	2	3	2	0
1003	1	3	2	1	3	2	1	1	3	2	0
1010	1	3	3	1	2	2	2	2	1	3	3
1039	1	3	3	0	3	1	0	0	1	3	2
1004	1				3	3	3	3	0	3	0
1043	1	3	1	0	3	1	1	3	2	2	
1040	1	2	2	0	3	2	1	1	2	3	0
1007	1				3	2	2	2	0	1	3
1006	1	3	3	0	3	3	3	3	3	3	0
105	1	3	2	0	3	2	1	0	3	2	0
1044	1	3	2	0	3	0	0	2	1	2	2
1045	1	3	3	0	3	0	0	3	3	2	0
1002	1	2	1	1	2	1	1	2	3	2	1
108	1	3	3	0	0	0	0	3	3	2	0
102	1	3	3	3	3	2	1	0	3	3	0
Raw Score	23	55	45	19	63	41	30	44	50	58	19

Content analysis of focus group data indicates that participants want a seating system assembly (frame) that is compatible with manual and power bases and components (e.g. backs, seat cushions, securement belts and postural supports) from different manufactures. Participants experience difficulty removing the seating system for transport.

Based on survey results-

- **(QA1)** participants want to remove the seating system from the base, or
- **(QA2)** if the seating system doesn't remove, participants expect it to fold.
- **(QA3)** Stated in a negative manner, they **do not find it acceptable** for the seating system **not** to remove from the base **or** fold for transport (see **Figure 6**).

Figure 6 What are the portability features of the seating system? (QA1-QA3)

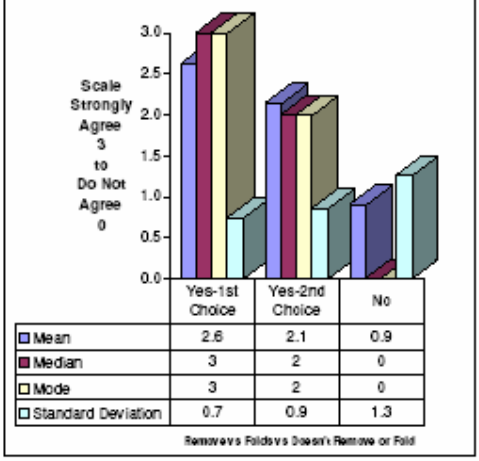

During focus groups, participants were asked about the range of sizes and how much adjustment an ideal seating system should have. Content analysis of focus group data indicates that seating system width ranges are 10″ to 22″ and seat depth ranges are 5″ to 14″. Participants expect the seating system to integrate with current back components for funding purposes.

How will the dynamic seating system address growth? On the survey, participants were asked to choose between two options for addressing growth—**growth adjustments or** the use of **growth kits**.

Figure 7 summarizes survey responses to growth adjustment questions-

- **(QA4)** participants 1st choice is the 2″ growth adjustment option in seat width and depth, without requiring a growth kit,
- **(QA7)** participants 2nd choice appears to be a growth kit that adds 2″ to the seat width and/or seat depth as a one-time increase,
- **(QA5)** participants 3rd choice is a growth adjustment of 2″ in seat depth only with no growth kit required, and
- **(QA6)** participants appeared to dislike the growth kit option that would add 2″ to the seat depth (see Figure 7).

Figure 7 How does the seating system address growth needs of users? (QA4-QA7)

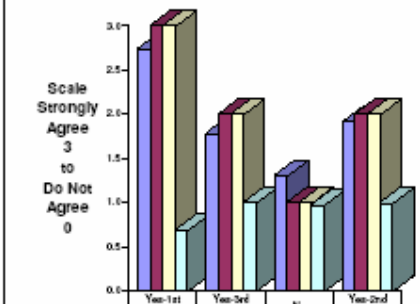

During focus groups, participants described the difficulty they have making seating system adjustments, often several times a day, to accommodate the changing positioning needs of the user. Participants appear to want the seating system to have variable positioning and adjustments that are non-incremental and that telescope for infinite adjustment with a locking mechanism.

On the follow-up survey (see **Figure 8**);

- **(QA9)** participants 1st choice is to make adjustments using a universal tool,
- **(QA8)** participants 2nd choice is to make adjustments without the use of tools.
- **(QA10)** Participants find it unacceptable to require a special tool for making

Figure 8 How are adjustments made to the seating system? QA8-QA10)

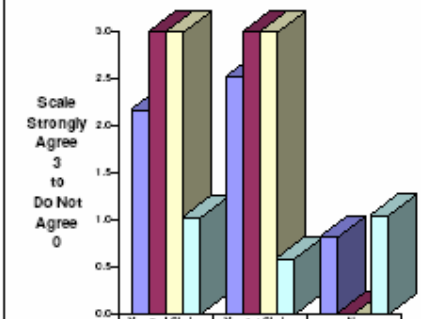

adjustment and that only therapists and vendors could use.

During focus groups, participants identified several mounting issues and solutions. They recommended that the seating system support multiple mounting locations for securements because one mounting location doesn't fit all users needs. They recommended that the seating system use the same (generic) fastener throughout (e.g. 10/32nd or 25/20) to make assembly and adjustment more convenient.

4.1 What are the dynamic features of the seating system?
4.2 What advanced design methods are employed?
4.3 What features do stakeholders want in "rate-of-return"?

		QDM1-QDM7--Dynamic movement of SS--How strongly do you agree that...						
Respondent ID	Count n=	Use electronic sensor, motors	ONLY mechanical devices	Senses amount of force needed	Parent/CG adjust return rate	ONLY Therapists Vendors adjust return rate	Disable w/single action	Features work independently
1009	1	1	1	2	1	3	3	3
1041	1	3	1	3	3	2	3	3
1042*	1	3	3	3	3	0	3	2
103	1	1	2	2	2	0	3	3
1038	1	3	1	3	1	2	3	3
109	1	3	0	3	3	0	3	3
106	1	2	2	3	3	2	3	3
107	1	3	2	3	3	2	3	3
1011	1	2	1	2	1	2	3	1
1003	1	1	2	2	0	3	2	2
1010	1	2	2	2	0	3	1	3
1039	1	1	2	2	3	1	2	1
1004*	1	0	2	2	2	2		3
1043	1	2	1	2	0	2	2	1
1040*	1	2	2		1	2	1	3
1007*	1	3	0	2	1	1	2	0
1006	1	3	1	3	3	1	3	3
105	1	3	1	3	3	0	2	2
1044	1	2	0	2	0	2	3	2
1045	1	3	1	2	1	0	3	3
1002	1	1	1	2	1	2	3	3
108*	1	3	0	3	3	0	3	3
102*	1	1	2	3	3	0	3	2
Raw Score	23	48	30	54	41	32	57	55

Focus group participants discussed several issues surrounding the changing needs of the user throughout the day. At certain times during each day, the user needs variable positions to assist with activities. For example, participants discussed the problems associated with transfers from bed to wheelchair. According to participants, this transfer is best accomplished by getting the user into a "tucked" position to reduce involuntary thrusts. Participants want the seating system to match this "tucked" position, so that the seat-to-back angle is < 90°, in a tilt-in-space configuration. Closing the seat-to-back angle and tilting the user back, makes the transfer easier and helps to work the person's hips back into the seat.

During sit-to-stand transfers, the seat-to-back angle opens up > 90°, thereby putting the person into extension so that she/he can use a purposeful thrust to stand up. Based on content analysis of focus group data, it appears that the ideal seating system permits manual manipulation of seat-to-back angle, seat tilt and back recline so they can be separately and individually configured. It also seems that participants want to be able to set the amount of angle and lock it at "tucked" and "open" and "functional" positions to reduce or facilitate thrusts (e.g. at 70°, 85°, 90°, 110°, 120° and 145°).

It's important to note that participants don't expect the seating system to be dynamic all the time, but rather they expect "dynamic," flexible joints (e.g. at neck, shoulders, lumbar spine, wrists, knees and ankles) that can be set and changed to create the best position for the user at different times, based on changing needs throughout the day.

Participants discussed the need for the seating system to have both tilt-in-space and recline functionality. As stated earlier, tilt-in-space assists with positioning, re-positioning after thrusts and changing positions during the day as task demands change and the need for pressure relief becomes apparent. Recline opens the user's chest up in order to help them breath without putting them into extension. Participants expect the seating system to function in a manner that will support (or at least not inhibit) this development.

Figure 9 What advanced design methods does the seating system use? (QDM1-QDM2)

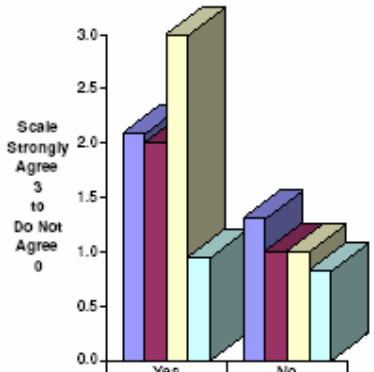

	Yes	No
Mean	2.1	1.3
Median	2	1
Mode	3	1
Standard Deviation	0.9	0.8

Electronic Sensors/Motors vs ONLY Mechanical Devices

Survey data indicates that respondents want electronic sensors and motors to provide advanced sensing and control of the system (see **Figure 9**). During involuntary thrusts, sensors decrease dampening resistance and during purposeful thrusts, sensors increase the amount of dampening resistance. Variable dampening features in the system improve user's switch access, transfers, ability to reach for objects, communication and breathing. Because the system accommodates different types of thrusts, the user will be encouraged to be more active and muscle use will be developed as the user learns to control and use thrust patterns necessary to accomplish self-selected tasks.

Electronic sensors and motors adjust the force necessary in rate-of-return after thrusts, but the rate-of-return can also be adjusted by parents and caregivers (see **Figure 10**).

For added safety, survey respondents indicate that the dynamic features such as variable dampening and adjustable rate-of-return must be enabled and disabled using a single action. They want the dynamic features to work independently and be able to be turned ON or OFF independently (see **Figure 11**). For example, participants want to be able to turn OFF and/or lock out the dynamic functions of footrests in order to reduce self-stimulatory movements in which the user uses the system to do continuous movement or "play" with the dynamic features.

Figure 10 How does "rate-of-return" operate in the seating system? (QDM3-QDM5)

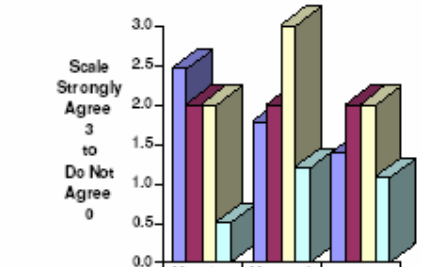

	Yes-1st Choice	Yes-2nd Choice	No
Mean	2.5	1.8	1.4
Median	2	2	2
Mode	2	3	2
Standard Deviation	0.5	1.2	1.1

Senses force needed / Parent/CG adjust rate vs ONLY Therapists/Vendor adjust

During focus groups, participants identified problems with current headrest assemblies and expectations for features in an ideal headrest. The headrest component assembly and cushioning materials must be durable enough to withstand a minimum of 36,500 thrusts per year for a period of 3 to 5 years. Headrests incorporate dynamic features (i.e. dampening resistance and adjustable rate-of-return), flex from 90° to 120° and protect the user from injury during thrusts while maintaining effective positioning.

Figure 11 How do dynamic features of the seating system work? (QDM6-QDM7)

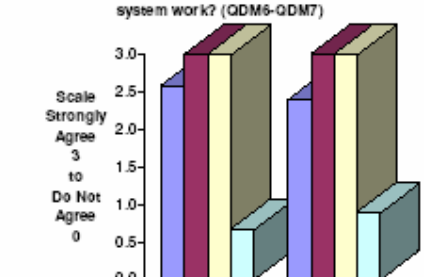

	Yes	Yes
Mean	2.6	2.4
Median	3	3
Mode	3	3
Standard Deviation	0.7	0.9

Disable w/ single action & Features work independently

Participants identified problems with current footrest assemblies and expectations for features in an ideal footrest assembly. The component assembly and materials must be durable enough to withstand a minimum of 36,500 thrusts per year for a period of 3 to 5 years. Footrests incorporate dynamic features (i.e. dampening resistance

and adjustable rate-of-return) and flex 90° at the knee. Footplates incorporate dynamic features (i.e. dampening resistance and adjustable rate-of-return) and flexes 15° plantar to 15° dorsi-flexion. Footrest assemblies protect the user from injury during thrusts while maintaining effective positioning.

Participants identified problems with current armrest assemblies and expectations for features in an ideal armrest. The component assembly and materials must be durable enough to withstand a minimum of 36,500 thrusts per year for a period of 3 to 5 years. Armrests incorporate dynamic features (i.e. dampening resistance and adjustable rate-of-return) and allow for some degree of abduction/adduction and flexion/extension. Armrests prevent user's arms from falling off during thrusts while maintaining effective positioning.

Desirable securements are made from wide, soft yet durable materials (i.e. withstand a minimum of 36,500 thrusts per year) and are available in various sizes to secure the head, pelvis, arms, ankles, etc. Seatbelts are velocity sensitive—in higher velocity (during involuntary thrusts) they minimize user movement, and in lower-velocity (during purposeful thrusts) they permit some movement.

Table 1 lists the design criteria for the dynamic seating system based on content analysis of focus group data and results of the analysis of the follow-up survey.

Table 1: Design Criteria for Dynamic Seating System (DSS)

Category	DSS Design Criteria
Legend/Key	***-Indicates statement from content analysis of focus data +-Indicates statement from survey analysis**
Assembly	• Is compatible with manual and power bases* • Is removable and/or foldable for transport+ • Is a carrier for components (e.g. backs, seat cushions, seat belts, postural supports) from various manufacturers* • Base attachment hardware lasts for 3 years (is durable enough to withstand multiple, daily seat removals/folds and forces that are applied when someone pushes the user in the wheelchair)*
Adjustability	• Seat widths range from 10" to 22" and seat depths from 5" to 14"* • Growth-at least 2 inches in seat width and depth without a growth kit+ • Uses non-incrementally, variable adjustments (e.g. with telescoping tubes and locking mechanism)* • Uses a single, universal tool to make adjustments+
Mounting	• Is integrated into current back components (for funding purposes)* • Is compatible with components (e.g. backs, seat cushions, seat belts, postural supports) from various manufacturers* • Supports multiple mounting locations for securements* • Uses the same (generic) fastener throughout (e.g. 10/32nd or 25/20)* • Mounting hardware withstands approximately 36,500 thrusting movement per year for a minimum of 3 years (10 thrusts per hour on average X 10 hours per day w/c use X 365 days each year = 36,500 thrusts annually)*

Category	DSS Design Criteria
Legend/Key	***-Indicates statement from content analysis of focus data +-Indicates statement from survey analysis**
Variable Positioning	• Permits manual configuration (e.g. can be configured differently based on the needs of the user—amount of seat tilt, back recline, seat height)* • Includes locking pre-sets at specific angles (e.g. 70°, 85°, 90°, 110°, 120°) are used to assist with tasks, for example the seat-to-back angle can be locked at 70° or a "tucked position" during transfers--a "tucked position" minimizes thrusting and assists in bed to w/c transfers* • Includes tilt-in-space and recline functionality*
Dynamic Movement	• Pelvic positioning is maintained by a fixed lower back section • Flexible joints match the joints of the user (e.g. at neck, shoulders, wrists, lumbar spine, knees and ankles)* • System reacts differently to involuntary versus purposeful thrusts+ • System has adjustable dampening capability* • Electronic sensors and/or motors provide advanced sensing and control+ • Sensors adjust the rate-of-return to return user to upright+ • Rate-of-return is adjustable by parents/caregivers+ • Dynamic features are enabled and disabled using a single action+ • Dynamic features work independently from each other and are turned ON and OFF independently (e.g. dynamic footrest function can be turned OFF to reduce self-stimulatory movements of the user)+
Headrests	• Headrest component assemblies and cushioning materials are durable enough to withstand a minimum of 36,500 thrusts per year for 3 years* • Headrests are dynamic (e.g. flexes from 90° to 120°)* • Headrest dampening is adjustable (e.g. based on the force applied by user during thrusting movements)* • Headrest rate-of-return is slow, controlled and can be adjusted* • Headrests protect the user from injury during thrusts while maintaining effective head positioning*
Footrests	• Footrests are durable enough to withstand a minimum of 36,500 thrusts per year for at least 3 years* • Footrest assembly is dynamic (e.g. allows for 90° extension at knee)* • Footrest dampening is adjustable (e.g. based on the force applied by user during thrusting movements)* • Footrest rate-of-return is slow, controlled and can be adjusted* • Footplate is dynamic (e.g. 15° plantar to 15° dorsi-flexion)*
Armrests	• Armrest are durable enough to withstand a minimum of 36,500 thrusts per year for at least 3 years* • Armrests are dynamic (e.g. they allow for some degree of abduction/adduction and flexion/extension)* • Armrests prevent user's arms from falling off during thrusts*

Category	DSS Design Criteria
Legend/Key	***-Indicates statement from content analysis of focus data** **+-Indicates statement from survey analysis**
	• Armrests dampening is adjustable (e.g. based on the force applied by user during thrusting movements)* • Armrests rate-of-return is slow, controlled and can be adjusted*
Securements	• Wide, soft and durable securements are available (e.g. to secure head, pelvis, arms, ankles)* • Seatbelts are velocity sensitive--in higher velocity (e.g. during involuntary thrusts), the seatbelt minimizes user movement, and in lower velocity (e.g. during purposeful thrusts), it permits movement* • Securements are durable enough to withstand a minimum of 36,500 thrusts*

APPENDIX D

MATLAB AND WMBASIC CODE

The following code is included in this appendix because it provides a backdoor solution to a difficult problem. Specifically, it gets around the inability of Working Model to be controlled by other external applications such as MATLAB. Please read the description of how this works in the body of the thesis.

WMBASIC SCRIPT:

```
Sub Main()
    ch% = DDEInitiate("Matlab","engine")
    DDETimeout(60000)
    WMch% = DDEInitiate("WM","WMBasic")
    DDEExecute ch%, "cd 'C:\Wheelchair project\WM\scripts'"
    DDEExecute ch%, "Initialize"
    COMList$ = "New"
    WHILE COMList$ <> "Empty"
        DDEExecute ch%,"COM_Cycle"
        A$ = DDERequest(ch%,"Command")
        DDEExecute WMch%,A$
        COMList$ = DDERequest(ch%,"is_empty")
    WEND
    Status$ = "Going"
    WHILE Status$ <> "Done"
        DDEExecute ch%, "Master_Updt"
        Frames$ = DDERequest(ch%,"Frames")
        Frame% = Val(Frames$)
      | Status$ = DDERequest(ch%,"Status")
        COMList$ = "New"
        WHILE COMList$ <> "Empty"
            DDEExecute ch%,"COM_Cycle"
            A$ = DDERequest(ch%,"Command")
            DDEExecute WMch%,A$
            COMList$ = DDERequest(ch%,"is_empty")
        WEND
        WM.ActiveDocument.Run Frame%
        WM.ActiveDocument.Reset
        DDEExecute ch%,"Process_Data"
    WEND
    WM.ActiveDocument.Close
    DDETerminateAll
End Sub
```

MATLAB CODE:

Initialize.m – Used to establish link with Working Model and begin data automation process

```
close all
clear all

samp_freq = 1000;

%Initializing variables
cur_COM = 0;
Status = 'Going';
cur_sim = 1;
last_sim = 1;

%Choose from the following: \n');
%   1. Inverse Dynamics\n');
%   2. Forward Dynamics\n');
dyn_type = 1;

if dyn_type == 1
%Choose from the following: \n');
%   1. No rigidizer - variable hardstop');
%   2. Other options');
%   3. Even more unavailable options');

inv_type = 1;


if inv_type == 1
   load '..\results\hardstop_results_v6'
   %last_sim = length(A.list);
   p_coeff = [-0.00000000166119 0.00000009011004 -0.00000507039498 ...
         -0.00010860582951 -0.01767434205949 2.75053977745729];

   COM_List{1} = 'Dim WM1 as WMDocument';
   COM_List{2} = 'Set WM1 = WM.Open("Inverse_Dynamics_nostop.wm2d")';
   COM_List{3} = ['WM1.AnimationStep = ' num2str(1/samp_freq)];

end

elseif dyn_type == 2

   load '..\results\hardstop_results_v6'

   thetas = eval(['A.' A.list{cur_sim} '.thetas']);
   time = eval(['A.' A.list{cur_sim} '.c_time']);

   %omegas2 = diff(thetas)/(time(2)-time(1))
   %time2 = time(1:(end-1))';
```

```
   %time = time2(1:5:end,:);
   %omegas = omegas2(1:5:end,:);

   %time_interp = linspace(0,time(end),round(samp_freq*time(end)))';
   %for i = 1:3
   %   omegas_interp(:,i) = spline(time,[0;omegas(:,i);0],time_interp);
   %end



   n_poly = 10;   %polynomial order used for fit
   for count = 1:3
      thetas_interp(:,count) =
polyval(polyfit(time',thetas(:,count),n_poly),time_interp);
   end

   for i = 1:3
      thetas_interp(:,i) = thetas_interp(:,i) - thetas_interp(1,i);
   end

   alphas_interp = diff(thetas_interp,2,1)/(1/samp_freq)^2;
   alphas_interp = [alphas_interp(1,:) ; alphas_interp ;
alphas_interp(end,:)];

   Frames = length(time_interp);

   k_gain = 100;

   tau_knee = -450;
   tau_hip = 1150;
   tau_ankle = 0;

   e_hip_old = 0;
   e_knee_old = 0;
   e_ankle_old = 0;

   d_gain = 1;

   dtlim = 1;

   COM_List{1} = 'Dim WM1 as WMDocument';
   COM_List{2} = 'Set WM1 = WM.Open("Forward Dynamics_nostop.wm2d")';
   COM_List{3} = ['WM1.AnimationStep = ' num2str(1/samp_freq)];


end
```

Master_Updt.m - Used to perform iterative simulations and prepare necessary Working Model commands for iterations

```
if dyn_type == 1
   if inv_type == 1
      tht_back = eval(['A.' A.list{cur_sim} '.info.tht_back']);
      hs_dist = p_coeff(1)*tht_back.^5 + p_coeff(2)*tht_back.^4 + ...
         p_coeff(3)*tht_back.^3 + p_coeff(4)*tht_back.^2 + ...
         p_coeff(5)*tht_back + p_coeff(6);

      clear alphas thetas alphas_interp thetas_interp time time_interp;

      thetas = eval(['A.' A.list{cur_sim} '.thetas']);
      time = eval(['A.' A.list{cur_sim} '.c_time']);

      thetas(:,3) = thetas(:,3) - thetas(:,2);
      thetas(:,2) = thetas(:,1) - thetas(:,2);

      d_thetas = thetas(1,:) - thetas(end,:);


      alphas(1,:) = (2*thetas(1,:) - 5*thetas(2,:) + 4*thetas(3,:) ...
         - thetas(4,:));
      alphas(length(thetas),:) = (-thetas(end,:) + 4*thetas(end-1,:)
...
         - 5*thetas(end-2,:) + 2*thetas(end-3,:));
      for i = 2:(length(thetas)-1)
         alphas(i,:) = thetas(i+1,:) - 2*thetas(i,:) + thetas(i-1,:);
      end
      alphas = alphas./(1/(eval(['A.' A.list{cur_sim}
'.info.fps']))^2);

      time_interp = linspace(0,time(end),round(samp_freq*time(end)))';

      %alphas_interp = interp1(time,alphas,time_interp,'cubic');

      n_poly = 8;   %polynomial order used for fit
      for count = 1:3
         thetas_interp(:,count) =
polyval(polyfit(time',thetas(:,count),n_poly),time_interp);
      end

      alphas_interp = diff(thetas_interp,2,1)/(1/samp_freq)^2;
      alphas_interp = [alphas_interp(1,:) ; alphas_interp ;
alphas_interp(end,:)];

      %remove coments below and change joint inputs to rotational for
position control ...
      %alphas(:,2) = (thetas_poly(:,2) -
thetas_poly(1,2)*ones(size(thetas_poly(:,2))));
      %alphas(:,3) = (thetas_poly(:,3) -
thetas_poly(1,3)*ones(size(thetas_poly(:,3))));
```

```
      %plot(time,thetas,time_poly,thetas_poly); pause
      %plot(time,alphas(:,1),time_interp,alphas_interp(:,1));

      Frames = length(time_interp);

      Ivect = 0;

      i = 1;

      COM_List{1} = 'WM.ActiveDocument.Reset';
      COM_List{2} = ['WM.ActiveDocument.Constraint(42).Field.Formula =
' num2str(hs_dist)];

   end
else
   i = 1;
end

if cur_sim == last_sim
   Status = 'Done';
   cur_sim = 1;
else
   cur_sim = cur_sim + 1;
   clear outputs
end
```

COM_Cycle.m - Used to transmit commands to Working Model

```
if not(exist('COM_List'))
   Command = 'Work% = 0'
   is_empty = 'Empty'
elseif cur_COM == 0;
   is_empty = 'No';
   last_COM = length(COM_List);
   Command = '$wmstart$';
   cur_COM = 0.5;
elseif cur_COM == 0.5
   Command = 'Sub Main()';
   cur_COM = 1;
elseif cur_COM == last_COM + 1
   Command = 'End Sub';
   cur_COM = last_COM + 2;
elseif cur_COM == last_COM + 2
   is_empty = 'Empty';
   Command = '$wmend$';
   cur_COM = 0;
   clear COM_List
else
   Command = COM_List{cur_COM};
   cur_COM = cur_COM + 1;
end
```

REFERENCES

[1] Cooper, R.A., 2001. Advances in wheelchair and related technologies. Medical Engineering & Physics, Vol.23, 3-4, 2001.

[2] Zeltwanger A..P., Brown D., Bertocci G., June 2001. Utilizing computer modeling in the development of a dynamic seating system. Proceedings of the 24th RESNA, Reno, NV, USA.

[3] InterCo GmbH website, http://www.interco-reha.de

[4] Miller's Adaptive Technologies, Product Catalog, 2004

[5] Pandyan, A.D., Price, CI.I.M., Rodgers, H., Barnes, M.P., Johnson, G.R., 2001. Biomechanical examination of a commonly used measure of spasticity. Clinical Biomechanics, Vol.16, 859-865.

[6] Lebiedowska, M.K. and Fisk, J.R., 1999. Passive dynamics of the knee joint in healthy children and children affected by spastic paresis. Clinical Biomechanics, Vol. 14, 653-660.

[7] Simon, D. and Foulds, R., 2004. Developing a quantitative measure of muscle spasticity. Proceedings of the IEEE 30th Annual Northeast Bioengineering Conference, Springfield, MA, USA.

[8] Hutchinson, E.B., Riley, P.O. and Krebs, D.E., 1994. A dynamic analysis of the joint forces and torques during rising from a chair. IEEE Trans. Rehabilitation Eng., Vol.2, No.2, 49-56.

[9] Sibella, F., Galli, M., Romei, M., Montesano, Crivellini, A., M., 2003. Biomechanical analysis of sit-to-stand movement in normal and obese subjects. Clinical Biomechanics Vol.18, 745-750.

[10] Mak, M.K.Y., Levin, O., Mizrahi, J., Hui-Chan, C.W.Y., 2003. Joint torques during sit-to-stand in healthy subjects and people with Parkinson's disease. Clinical Biomechanics Vol.18, 197-206.

[11] Mak, M.K.Y., Levin, O., Mizrahi, J., Hui-Chan, C.W.Y., 2004. Reduction of lower limb model indeterminacy by force redundancy in sit-to-stand motion. Journal of Applied Biomechanics, Vol.20, 95-102.

[12] Goossens, R.H.M. and Snijders, C.J., 1995. Design Criteria for the Reduction of Shear Forces in Beds and Seats. Journal of Biomechanics, Vol.28, No.5, 225-230.

[13] Yamaguchi,G.T., Moran, D.W. and Si, J., 1995. A computationally efficient method for solving the redundant problem in biomechanics. Journal of Biomechanics, Vol.28, No.8, 999-1005.

[14] Van den Bogert, A.J., Read, L. and Nigg, B.M., 1996. A method for inverse dynamic analysis using accelerometry. Journal of Biomechanics, Vol.29, No.7, 949-954.

[15] Cahouet, V., Luc, M. and David, A., 2002. Static optimal estimation of joint accelerations for inverse dynamics problem solution. Journal of Biomechanics, Vol.35, 1507-1513.

[16] Runge, C.F., Zajac, F.E., III, Allum, J.H.J., Risher, D.W., Bryson, A.E., Jr., and Honegger, F., 1995. Estimating net joint torques from kinesiological data using optimal linear system theory. IEEE Trans. On Biomedical Engineering, Vol.42, No.12, 1158-1164.

[17] Nigg, B.M. and Herzog, W., 1995. Biomechanics of the Musculo-skeletal System, John Wiley & Sons, Inc.

[18] Pataky, T.C., Zatsiorsky, V.M. and Challis, J.H., 2003. A simple method to determine body segment masses in vivo: reliability, accuracy and sensitivity analysis. Clinical Biomechanics, Vol.18, 364-368.

[19] Zatsiorsky, V. and Seluyanov, V., 1985, Estimation of the mass and inertia characteristics of the human body by means of the best predictive regression equations. International Series on Biomechanics, Vol. 5B, 233-239.

[20] de Lava, P., 1995. Adjustments to Zatsiorsky-Seluyanov's segment inertia properties," Journal of Biomechanics, Vol.29, 1223-1230.

[21] Markwald, M. (1998). Traveling seat. U. S. P. Office. USA, Eitorf, DE. **6,488,332**.

[22] Farricielli, S. (1997). Ergonomically designed seat assembly for portable wheelchair. U. S. P. Office. USA. **5,904,398**

[23] Klooster, S. J. (2004). Vibration Suppression and Safety Seat Motion Design of a Hyper-Active Seat. G.W. Woodruff School of Mechanical Engineering. Atlanta, Georgia Institute of Technology. **MS:** 119.

[24] Vaughan, J. E. (2004). Active and Semi-Active Control to Counter Vehicle Payload Variation. G.W. Woodruff School of Mechanical Engineering. Atlanta, Georgia Institute of Technology. **MS:** 91.

[25] S.W. Hong, V. P., William Singhose, Stephen Sprigle (2005). Motion Measurement and Force Determination During Unconstrained Extensor Thrust. 28th Annual RESNA Conference, Atlanta, GA.

[26] S.-W. Hong, H. Seomoon, V. Patrangenaru, W. Singhose, and S. Sprigle (2005). An Efficient Method for Identification of Human-Generated Forces During Extensor Thrust. IASTED International Conference on Biomedical Engineering, Innsbruck, Austria, 2005.